Title
Increasing fuel utilization of breed and burn reactors

Author
Di Sanzo, Christian Diego

Publication Date
2014

Peer reviewed|Thesis/dissertation

Increasing Fuel Utilization of Breed and Burn Reactors

by

Christian Diego Di Sanzo

A dissertation submitted in partial satisfaction of the

requirements for the degree of

Doctor of Philosophy

in

Engineering - Nuclear Engineering

and the Designated Emphasis

in

Energy Science and Technology

in the

Graduate Division

of the

University of California, Berkeley

Committee in charge:

Professor Ehud Greenspan, Co-chair
Professor Jasmina Vujic, Co-chair
Professor Joonhong Ahn
Professor Van P. Carey

Spring 2014

Increasing Fuel Utilization of Breed and Burn Reactors

by
Christian Diego Di Sanzo

Abstract

Increasing Fuel Utilization of Breed and Burn Reactors

by

Christian Diego Di Sanzo

Doctor of Philosophy in Engineering - Nuclear Engineering

and the Designated Emphasis in Energy Science and Technology

University of California, Berkeley

Professor Ehud Greenspan, Co-Chair

Professor Jasmina Vujic, Co-Chair

Breed and Burn reactors (B&B), also referred to Traveling Wave Reactors, are fast spectrum reactors that can be fed indefinitely with depleted uranium only, once criticality is achieved without the need for fuel reprocessing.

Radiation damage to the fuel cladding limits the fuel utilization of B&B reactors to $\sim$ 18-20% FIMA (Fissions of Initial Metal Atoms) – the minimum burnup required for sustaining the B&B mode of operation. The fuel discharged from this type of cores contain $\sim$ 10% fissile plutonium. Such a high plutonium content poses environmental and proliferation concerns, but makes it possible to utilize the fuel for further energy production.

The objectives of the research reported in this dissertation are to analyze the fuel cycle of B&B reactors and study new strategies to extend the fuel utilization beyond $\sim$ 18-20% FIMA.

First, the B&B reactor physics is examined while recycling the fuel every 20% FIMA via a limited separation processing, using either the melt refining or AIROX dry processes. It was found that the maximum attainable burnup varies from 54% to 58% FIMA – depending on the recycling process and on the fraction of neutrons lost via leakage and reactivity control. In Chapter 3 the discharge fuel characteristics of B&B reactors operating at 20% FIMA

and 55% FIMA is analyzed and compared. It is found that the 20% FIMA reactor discharges a fuel with about $\sim 80\%$ fissile plutonium over total plutonium content. Subsequently a new strategy of minimal reconditioning, called *double cladding* is proposed to extend the fuel utilization in specifically designed second-tier reactors. It is found that with this strategy it is possible to increase fuel utilization to 30% in a sodium fast reactor and up to 40% when a subcritical B&B core is driven by an accelerator-driven spallation neutron source. Lastly, a fuel cycle using Pressurized Water Reactors (PWR) to reduce the plutonium content of discharged B&B reactors is analyzed. It was found that it is possible to burn the B&B discharged fuel up to an additional 105.6 $\mathrm{GWd/MT_{IHM}}$ and 66.1 $\mathrm{GWd/MT_{IHM}}$, for melt refining and AIROX, respectively.

Contents

List of Figures

List of Tables

Acknowledgments

I would like to thank the three professors who made this work possible.

I would like to thank Prof. Greenspan for supporting and guiding my work during these years and for his constant support, even during hard moments.

I would like to thank Prof. Vujic for her constant support to my research, even at hard times, and her continuous encouragements.

I would like to thank Prof. Ahn for believing in me when I started my Ph.D., and being supportive during all my years in graduate school.

Chapter 1

Introduction and Motivations

The world's energy demand is constantly increasing, driven by growing needs of emerging economies. Countries, such China and India, and non-OECD [1] countries in general, will drive a continuous increase in energy demand in the next decades [1], as shown in Figure 1.1. Energy generation is the main producer of Greenhouse Gases (GHG) emissions, accounting for two-thirds of global greenhouse-emissions [2]. Fossil fuels, coal in particular, are responsible for most of world energy related carbon dioxide emissions, as shown in Figure 1.2. In 2014, the Intergovernmental Panel for Climate Change recommended to lower global GHG emissions in 2050 to levels 40% to 70% lower than in 2010, in order to keep temperature change of the earth below 2 °C [3]. As energy production is such a strong contributor to GHG emissions, it is a fundamental part of any climate change mitigation policy. Therefore to prevent climate change and its disastrous effects, a reliable carbon-free source of energy must be found.

Increasing attention has focused in recent years on emission-free renewable energies such as solar and wind. However, it poses a significant challenge to satisfy base load demand with renewable energies, given their intermittent nature. Nuclear Power is therefore an attractive alternative, given its GHG-free nature and its ability to produce large amount of electrical energy per unit mass of fuel. However, governments and environmentalists have put nuclear power under scrutiny due to concerns about nuclear waste disposal, safety, proliferation and short-term availability of uranium reserves. This has created a renewed attention from the scientific community with the goal of

[1] Organization for Economic Co-operation Development

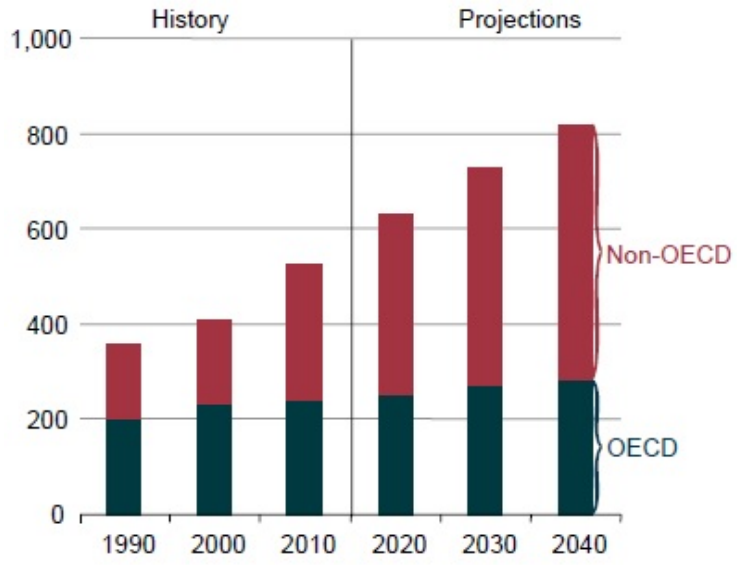

Figure 1.1: World energy consumption, 1990-2040 (quadrillion Btu) [1]

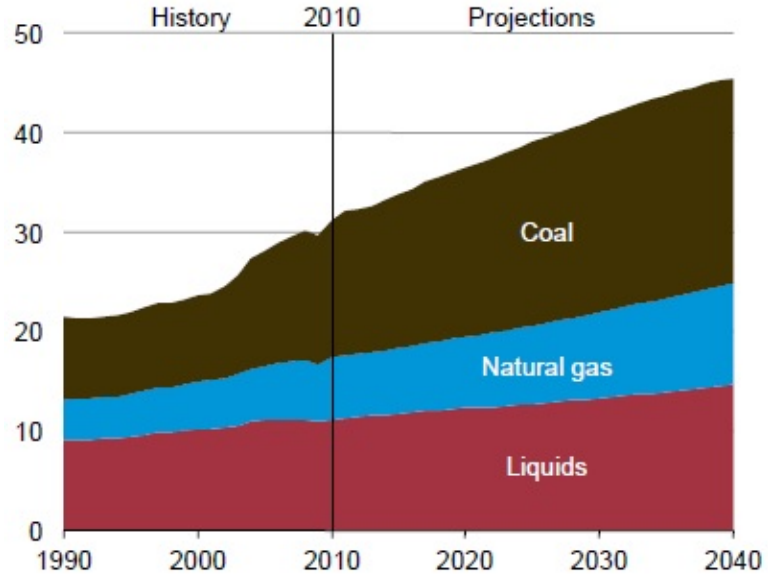

Figure 1.2: World energy-related carbon dioxide emissions by fuel type, 1990-2040 (billion metric tons) [1]

finding a solution to these problems, evolving from the current system based on Light Water Reactors (LWR) to more advanced nuclear reactor designs, as shown in Figure 1.3. In July 2001, the Generation IV International Forum (GIF) was born. The goal of this Forum was to select future nuclear reactor designs based on the following criteria [4]:

- sustainability;
- economics;
- safety & reliability;
- proliferation resistance.

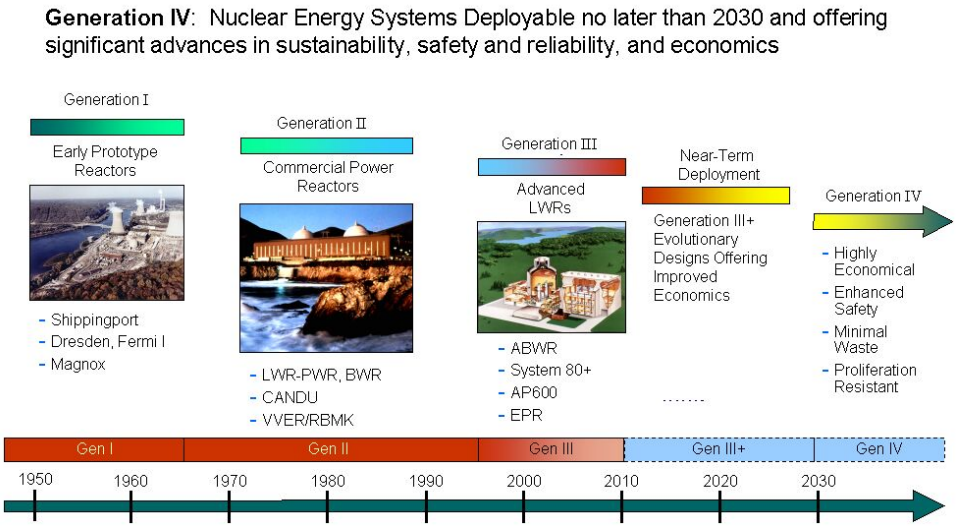

Figure 1.3: Evolution of Nuclear Reactor Designs, according to Gen. IV International Forum [4].

As a result, six designs were chosen: the very high temperature reactor, the sodium-cooled fast reactor, the supercritical water-cooled reactor, the gas-cooled fast reactor, the lead-cooled fast reactor and the molten salt reactor. With the goal of sustainability in mind, the best choice for energy needs would be the use of fast breeder reactors, such as the sodium-cooled fast reactor. The current LWR once-through cycle uses only 0.6% of the

energy value of uranium resources, as it is not able to efficiently utilize fertile isotopes. Fast reactors are able to breed fissile isotopes from fertile isotopes such as ^{238}U, which makes 99.28% of natural uranium and thereby to utilize nearly 100% of the energy value of natural uranium.

For achieving this high fuel utilization, the fuel has to be reprocessed when the peak radiation damage approaches $\sim$ 200 dpa — the upper bound cladding materials have been qualified to withstand. This corresponds to an average fuel burnup of, approximately, 10% FIMA (Fissions of Initial Metal Atoms). The reprocessing involves removal of all fission products and separation of the plutonium or trans-uranium (TRU) elements from the uranium, though partial separation of fission products has also been examined [5]. The reprocessing phase is of greatest concern when keeping in mind proliferation issues. In fact, the separation of plutonium (of which $\sim$ 80% is fissile) or even TRU poses a significant proliferation concern, since governments or terrorists could use this material to fabricate nuclear weapons instead of using it for energy production. However, with reprocessing, the fuel utilization factor of breeder reactors can be as high as 99%, a gargantuan gain from the 0.6% of current LWRs. If fast reactors and their fuel cycle could be designed to avoid or minimize the need of separating TRU elements from the used nuclear fuel (UNF), a sustainable and proliferation resistant nuclear energy system could be envisioned.

In 1958, Feinburg proposed [6], for the first time, a fast reactor that could sustain a fission reaction when fueled directly with natural uranium without need of reprocessing. This type of reactor, called Breed-and-Burn (B&B), is able to breed the fissile material and burn it *in situ*, without the need for reprocessing, though at the expense of a lower overall fuel utilization (down to $\sim$ 20% for strictly no-reprocessing B&B). After Feinburg's proposal, a few studies on this concept were done, such as the Fast Mixed Spectrum Reactor at MIT [7]. A good review of these earlier B&B designs can be found in Ref. [8]. In 1995, the idea was redeveloped by Teller who envisioned a new fast reactor design where breed and burn waves could travel through a stack of fuel [9].

1.1 Breed and Burn reactors

Breed and Burn (B&B) reactors can be fueled with depleted uranium only, once initial criticality is established, removing the need for fuel reprocess-

ing. Depleted uranium is the by-product of the uranium enrichment process, which is used to enrich the fuel of current nuclear reactors. It consists mostly of fertile ^{238}U, with a small fraction ($\sim 0.2\%$) of ^{235}U. As of today, there are more than 700,000 MT of depleted uranium in the United States [10]. This is a huge reserve that, with B&B reactor technology, can be directly used for energy production.

After Teller′s design, several studies were performed on conceptual designs of the Breed and Burn reactors. Sekimoto [11] at the Tokyo Institute of Technology developed several conceptual designs of the B&B reactors, called CANDLE. The CANDLE reactor uses an axial fuel reload scheme and needs a high requirement of fuel burn-up ($\sim 40\%$). In 2008, a private company, TerraPower LLC [12] was founded with the goal of commercializing B&B technology and building a prototype by 2020. Later, Greenspan et al. [13] at University of California, Berkeley, developed several designs of the Breed and Burn reactors where the fuel is shuffled radially with a cylindrical arrangement of hexagonal fuel assemblies.

For a reactor to be able to operate in a B&B mode, a minimum burnup is needed, since the fuel needs to produce a large enough amount of excess fission neutrons sufficient to breed enough fissile material for the fission reaction to be sustained. This minimum burnup has been found to be in the proximity of 18-20% FIMA [14] (see Section 2.3). To achieve such a high burn-up, a fuel cladding material able to withstand such a high irradiation needs to be developed. At $\sim 20\%$ average FIMA, the cladding will need to withstand a radiation damage of about 500 dpa (displacements per atom) [15]. However, current data for HT-9, a good and well studied candidate for fast reactor cladding, are available only up to ~ 200 dpa [16]. Knowledge about high irradiation performance of other cladding materials is even further behind. The development of cladding materials able to withstand high irradiation damage is likely to be the biggest challenge for the B&B reactor commercialization [15]. However, if B&B reactor technology is to achieve commercial success, at least in their first stage, B&B reactors will work with the minimum burn-up required for B&B operations $\sim$ 18%-20% FIMA. The fuel discharge at this burn-up still contains a considerable amount of fissile materials, approximately 10%, which in a once-through B&B cycle will be disposed as waste. This waste poses a significant proliferation risk, due to its high content of fissile material ^{239}Pu, and it could be used for further en-

ergy production, instead of being disposed of. Moreover, such a considerable quantity of ^{239}Pu poses waste concerns, in regards of environmental impact and criticality accident in repository.

The objective of this study is to find alternative ways to further increase the fuel utilization of the Breed and Burn reactors, without chemical separation of plutonium and minor actinides from the uranium and of all the actinides from most of the solid fission products. At the same time we also want to reduce the fissile plutonium content in the B&B discharged fuel. This study is organized as follows:

Chapter 1: Introduction and motivations.

Chapter 2: A description of the physics of the Breed and Burn reactors with a focus on various parametric studies is provided. The synergy of limited separation fuel cycles with B&B reactors is analyzed.

Chapter 3: The performances of B&B fuel cycles using limited separation reprocessing are analyzed for various recycling scenarios and compared to other fast reactor designs

Chapter 4: A new process consisting of re-cladding nuclear fuel over the previous clad is described and evaluated. This process is more proliferation resistant than the other options previously analyzed by Heidet [17]. This process is applied to the design of second-tier Breed and Burn reactors, i.e. the B&B reactors that are fueled with the discharged fuel from first tier B&B ($\sim$ 20% FIMA) with the goal of increasing fuel utilization and reducing amount of waste per unit of electricity generated.

Chapter 5: A new option is analyzed where the discharged fuel from B&B is used in current Pressurized Water Reactors (PWRs). The fuel is processed without actinides separation, re-fabricated into oxide fuel and used in PWRs to generate additional energy and minimize the fissile nuclides content.

Chapter 6: This chapter assesses the characteristics of the spent fuel produced in B&B reactors in comparison to the options studied in Chapter 4 and 5. This final chapter also draws conclusions and provides ideas for future work.

Chapter 2

Breed and Burn Reactor Physics

2.1 Physics of breeding

A Breed and Burn mode of operation is based on breeding of enough fissile materials and fission part of it *in-situ* using a once-through fuel cycle. A nucleus that can fission after the absorption of a zero-kinetic energy neutron is called *fissile*. Fissile nuclei are, for example, ^{235}U, ^{239}Pu, ^{241}Pu. On the other side, a nucleus that after neutron absorption generates a fissile nucleus is called *fertile*. The systems under study in this thesis are ^{238}U/^{239}Pu systems, where the burning of ^{239}Pu generates enough neutrons to be absorbed in ^{238}U, such that produces an equal or higher fissile nuclei concentration. The reaction can be illustrated as:

$$^{238}\mathrm{U} \xrightarrow{n,\gamma} {}^{239}U \xrightarrow[23.5\ \mathrm{min}]{\beta-} {}^{239}\mathrm{Np} \xrightarrow[2.3565\ \mathrm{d}]{\beta-} {}^{239}\mathrm{Pu} \tag{2.1}$$

^{239}Pu can undergo fission or neutron capture again, generating higher atomic number nuclides. The entire ^{238}U/^{239}Pu conversion chain is shown in Figure 2.1.

For a B&B reactor the breeding gain needs to be considerable so as to minimize the burnup required for sustaining the B&B mode of operation. A high breeding gain can be obtained only with a fast neutron spectrum.

The average number of neutrons generated per neutron absorbed in the

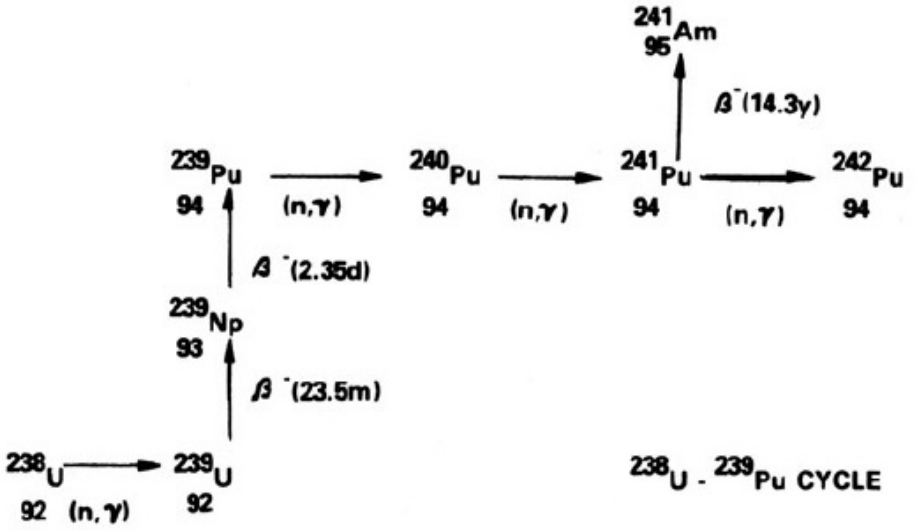

Figure 2.1: U-Pu conversion chain [18]

fuel, $\overline{\eta}$, averaged over the neutron flux spectrum, can be written as [18]:

$$\overline{\eta} = \overline{\nu}_f \frac{\overline{\sigma}_f}{\overline{\sigma}_f + \overline{\sigma}_c} = \overline{\nu}_f \frac{1}{1 + \overline{\alpha}} \tag{2.2}$$

where $\overline{\nu}_f$ is the average number of neutrons generated per fission, $\overline{\sigma}_f$ is the spectrum averaged microscopic fission cross-section, $\overline{\sigma}_c$ is the spectrum averaged microscopic capture cross-section and $\overline{\alpha} = \frac{\overline{\sigma}_c}{\overline{\sigma}_f}$.

To maintain reactor criticality, at least one neutron from each fission should be used for the next fission. When breeding is wanted, at least another neutron needs to be absorbed in fertile material, and therefore the total number of neutrons generated for each absorption must be at least 2. However, accounting for leakage and neutron absorption in non-fuel components, it is clear that the number of neutrons generated for one neutron absorbed in fuel must be higher than 2.

For each of the primary fissile isotopes, $\overline{\nu}_f$ is fairly constant for neutron energies up to about 1 MeV (about 2.9 for ^{239}Pu and about 2.5 for ^{233}U and ^{235}U) and slowly rises at higher energy. On the other hand, $\overline{\alpha}$ varies considerably with energy and between isotopes. For ^{239}Pu, $\overline{\alpha}$ rises sharply

in the intermediate energy range between 1 eV and 10 keV and then drops again at high energy [18]. This behavior of $\overline{\nu}_f$ and $\overline{\alpha}$ leads to the variations of $\overline{\eta}$ with energy, as shown in Figure 2.2.

From Figure 2.2 it is evident that the ^{239}Pu is the fissile isotope that can produce the highest breeding gain, since its $\overline{\eta}$ is consistently greater than 2 at energies above 100 keV. To further assess the use of fissile isotopes, Table 2.1 reports values of $\overline{\eta}$ for typical LWR and fast reactor spectrum. It is evident that the highest breeding gain is obtained by the ^{238}U/^{239}Pu cycle. Since B&B reactors are particular type of fast reactors where the breeding gain needs to be high enough so that the reactor can breed enough fissile isotopes to sustain criticality, the best choice for this reactors is ^{238}U/^{239}Pu cycle.

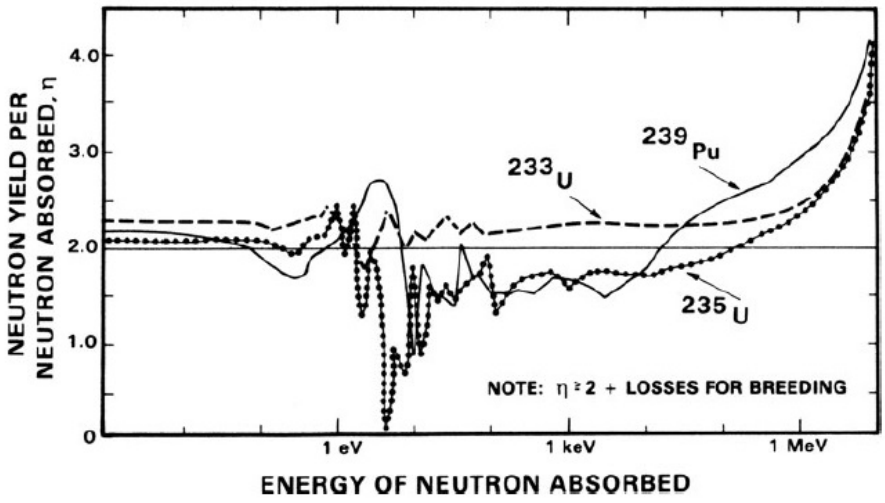

Figure 2.2: $\overline{\eta}$, neutrons produced per neutron absorbed vs. energy for various fissile isotopes [18].

It was demonstrated that the B&B mode of operation could not be established with liquid metal coolant for thorium reactors [14], therefore ^{232}Th/^{233}U systems will not be part of this work.

Table 2.1: Value for $\overline{\eta}$ averaged over fast and thermal spectra [18]

$\overline{\eta}$-averaging spectrum type	^{239}Pu	^{233}U	^{235}U
Average over an LWR spectrum (0.025 eV)	2.04	2.06	2.26
Average over a typical oxide-fueled fast reactor spectrum	2.45	2.10	2.31

2.2 Breed and Burn Reactor Designs

Traditional fast reactors have two different regions: one for burning fissile materials (seed) and one for breeding (blanket). However, in general the blanket/seed are not necessarily two separate regions. A reactor can used blanket assemblies dispersed in the core, or even different axial fuel zones for blanket and seed. Other fast reactor core designs do use a blanket at all. However, all fast reactors need fuel reprocessing for replacing the cladding and removing fission products. The unique feature of B&B reactors is that they can sustain criticality indefinitely without the need for reprocessing, when fueled with depleted uranium, i.e. essentially fertile material only. An illustration of a breed-and-burn core design of the travelling wave type is shown in Figure 2.3.

Here the word *wave* refers to the spatial fission density profile. Since plutonium is the primary fissile material in B&B reactors, its concentration is higher in the burning region and approaching zero in the fresh fuel region. As the burning region moves through the reactor, the concentration wave moves with it.

2.2.1 CANDLE Designs

In this section, the most important B&B reactor designs that have been developed so far are described.

Edward Teller *et al.* [9] were the first to revive the interest in B&B reactors. Their original Traveling Wave Reactor (TWR) concept is, in principle, similar to the CANDLE reactor concept for which there is more illustrations available in the literature and will therefore be used to describe the TWR principles.

Starting from the early 2000s, Sekimoto *et al.* at Tokyo Institute of

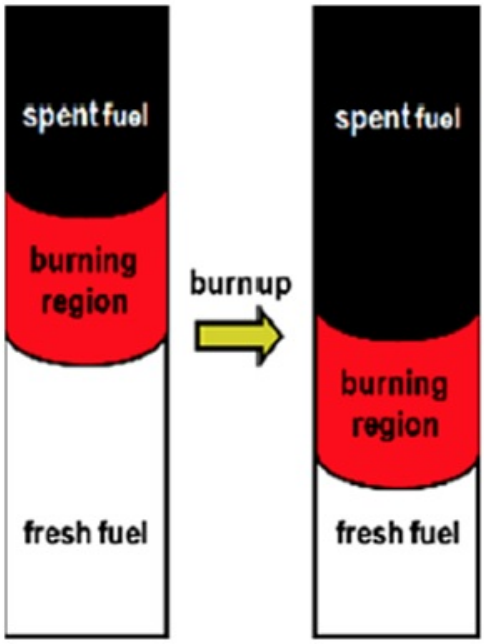

Figure 2.3: Burn-up process along the core axis of Breed and Burn reactor [19]

Technology has developed the concept of CANDLE reactor. CANDLE stands for *Constant Axial shape of Neutron flux, nuclide densities and power shape During Life of Energy production*. The CANDLE reactor is a type of Breed and Burn reactor where the propagation of plutonium concentration waves happens axially, as shown in Figure 2.4. This scheme of fuel management requires high discharge burnups, of the order of 40% FIMA; the corresponding peak radiation damage is close to $\sim$ 1,000 dpa. To withstand such a high burnup a cladding replacement is needed, since current materials, such as HT9, are not able to withstand burnup higher than 200 dpa (see Section 2.4). The strategy suggested for refueling the CANDLE core is illustrated in Figure 2.5. It consists in chopping the spent part of the fuel and replacing it with fresh fuel. This process has been theorized by Nagata *et al.* [20, 21], but no specific feasibility studies on this concept have been performed. Sekimoto *et al.* have studied the CANDLE concepts with various coolant (sodium, lead, lead-bismuth) and various fuels (metallic alloy, nitride, uranium and

thorium); CANDLE research is still ongoing [19, 22–24].

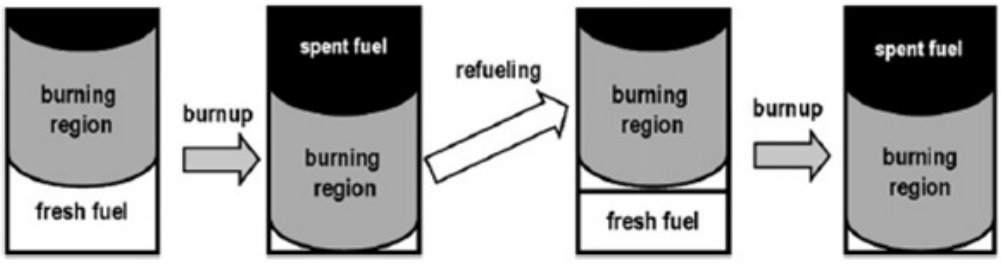

Figure 2.4: CANDLE reactor mode of operation. The fresh fuel is reloaded from the bottom of the reactor and the top spent fuel is discharged at the end of cycle [19].

2.2.2 Terrapower Designs

In 2008 a private company, TerraPower LLC, was founded with the goal of commercializing a Breed and Burn Reactor. TerraPower has been referring to its reactor as the Traveling Wave Reactor (TWR). The company is a spin-off of Intellectual Ventures, an intellectual property corporation. The initial studies of TerraPower were based on the Traveling Wave type reactor, similar to concept proposed by Edward Teller *et al.* [9]. At a further analysis this was proven to be an unfeasible design and the most recent designs implemented a shuffling scheme of the type described later in Chapter 3. A schematic of the new design, using a core with fuel assemblies arranged in a cylindrical way is described in Ref. [25] and shown in Figure 2.6. TerraPower aims to build a prototype of such a reactor, to produce a power level of 1200 MW thermal (th), and in a later stage to introduce a larger model of 3000 MW_{th}. The minimum discharge of such a reactor is supposed to be in the 18-20% FIMA range. However, TerraPower is still researching a wide range of design parameters and the designs are in continuous evolution [12, 26].

2.2.3 UC Berkeley Designs

At UC Berkeley, Heidet and Greenspan have studied the feasibility of various versions of B&B core designs [13, 14, 27–30], all based on a cylindrical

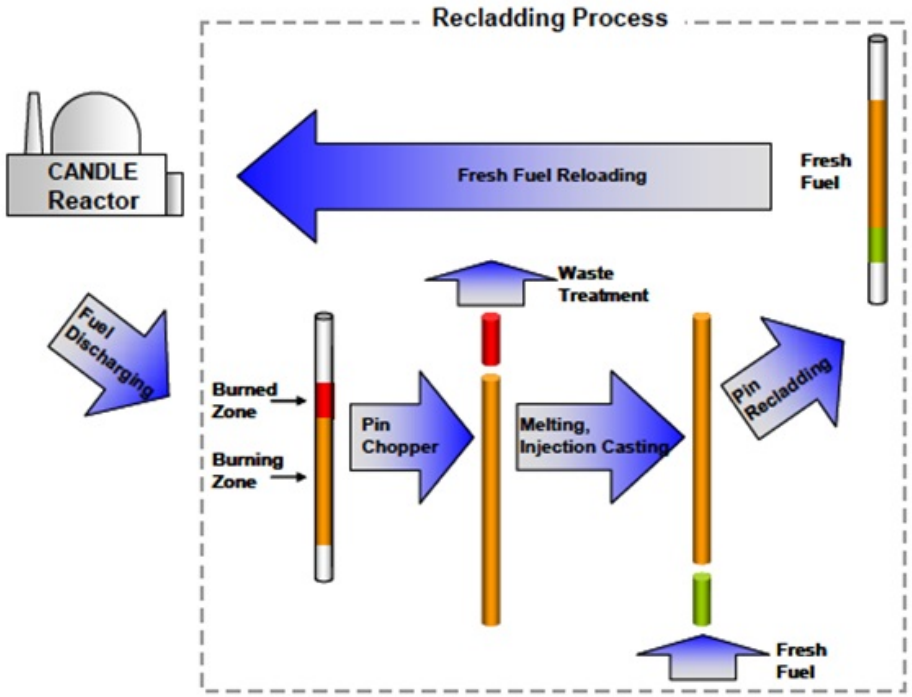

Figure 2.5: CANDLE fuel cycle scheme. The cycle scheme includes a reprocessing to overcome material damage limits [19].

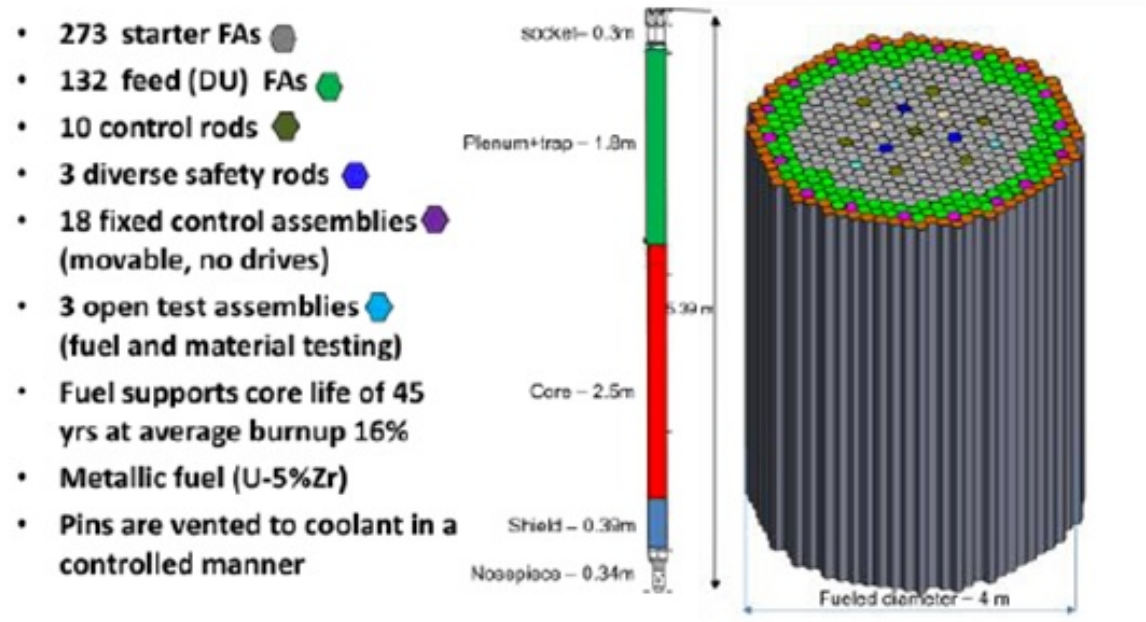

Figure 2.6: Schematic representation of the prototype core of TWR by Terrapower [25].

arrangement of hexagonal assemblies. The two main designs studied are: 1) a large sodium cooled B&B reactor of 3000 MW_{th} [13]; and 2) a medium size B&B reactor [27] of 1200 MW_{th} that has radial dimensions similar to S-PRISM fast reactor, developed by General Electric[31, 32]. The studies were summarized in Heidet thesis at UC Berkeley [17]. These designs are the starting point of this work and are described in details in Chapter 3.

2.3 Neutron balance

To understand the performance of a B&B reactor, it is useful to follow the evolution of k_∞ of a unit cell, representative of the material composition of a B&B reactor. As the mean free path of neutrons in fast reactors is much longer than a fuel pin, it is possible to homogenize assembly materials. Therefore, the reactor core material can be represented as a mixture of coolant, clad and fuel. Using the same fuel assembly dimensions as used in Heidet & Greenspan study of large B&B reactors [13], the volume fractions of fuel constituents can be derived and are reported in Table 2.2. The fuel is U-10%Zr alloy, the cladding material is HT9 and the coolant is sodium. The fuel density is 11.94 g/cm^3, and the fuel smear density is 75%. HT9 is a ferritic martensitic steel, which composition is given in Table 2.3. The fuel used is a metallic alloy of uranium and zirconium, with zirconium being 10% of the fuel by weight. This unit cell is a $10 \times 10 \times 10$ cm homogenized cube with reflective boundary conditions applied to all sides. The unit cell is depleted at constant power, using the neutron-transport code MCNP5 [33] and depletion code ORIGEN 2.2 [34], coupled by the coupling utility MOCUP 2.1 [35]. These codes and the coupling method are accurately described at the end of this chapter in Section 2.6. The depletion is performed with a power density of 112.5 W/cm^3 which is representative of the average power density in a B&B reactor [13]. The evolution of k_∞, obtained by the simulation, is plotted in Figure 2.7.

The burnup is reported in units of FIMA (Fission of Initial Metal Atoms), FIMA is defined as the fraction of initial metal atoms that are fissioned at time t it can be written as:

$$FIMA(\%)_t = \frac{N_0 - N_t}{N_0} \times 100 \tag{2.3}$$

where N_0 is the number of metal atoms at t=0, while N_t is the number of

Table 2.2: Volume fractions used for homogenized unit cell.

Volume fractions	
coolant	28%
fuel+gap	50%
clad	22%

Table 2.3: HT-9 Composition by weight percent used in simulations.

HT-9	wt %
Fe	85 %
Cr	11.5 %
Ni	0.5 %
Mo	1.5 %
Mn	0.9 %
Si	0.6 %
Density(g/cc)	7.522

metal atoms present at time t. Therefore at t=0, FIMA is 0% while at the end of the depletion, when all metal atoms have fissioned, FIMA is 100%. Since the number of atoms is directly proportional to the number of moles, it is possible to write FIMA in terms of moles of metal atoms:

$$FIMA(\%)_t = \frac{M_0 - M_t}{M_0} \times 100 \tag{2.4}$$

For fresh fuel, the only metal that can fission is uranium (^{238}U and ^{235}U atoms). However, as the fuel is burned part of the uranium is transmuted into other actinides, and part is fissioned. When counting the metal atoms present at time t, all actinides need to be accounted for, as these represent metal atoms that can fission but have not fissioned yet; therefore, all elements with atomic number $N > 89$ are accounted for.

As shown in Figure 2.7, at the beginning of burnup k_∞ is much less than 1; and it is equal to 0.23, due, primarily, to fissions in ^{238}U. As the fuel is burned, the amount of fissile content (in particular ^{239}Pu) increases and k_∞ increases up to a value of 1.2. After the peak value is reached accumulation

of fission products along with the depletion of ^{238}U are causing k_∞ to drop, eventually down to zero if all actinides could be fissioned. At the beginning, k_∞ is much lower than 1, implying that the fuel is at this point a neutron sink. However when it becomes >1, the fuel is a net neutron producer. For a Breed and Burn reactor to work, the fuel needs to produce at least as many neutrons as the neutrons absorbed and lost in the entire system. This concept is mathematically represented by balancing neutron absorptions and production.

The neutron balance technique has been clearly illustrated by Heidet [14] and Petroski [36]. In this study, we report the formulation by Heidet & Greenspan. In section 2.5, we apply it for the determination of minimum and maximum burnup of B&B using limited separation fuel cycles.

The neutron balance consists in relating the production and absorption to k_∞ evolution. The number of neutrons produced in a small interval of burn-up, let us say $d(BU)$, expressed in FIMA, can be written as:

$$neutrons\,produced\,in\,d(BU) = \overline{\nu}(BU) N_{HM} d(BU) \tag{2.5}$$

where $\overline{\nu}$ is the number of neutron produced in each fission and it is dependent on the burnup and N_{HM} is the number of heavy metal nuclei present in the fuel at t=0. By definition k_∞ can be thought as:

$$k_\infty = \frac{neutron\,production}{neutron\,absorption} \tag{2.6}$$

However, for our uses k_∞ is calculated by neutron transport codes and it is therefore given. It is possible to calculate the neutron absorbed as:

$$neutron\,absorbed\,in\,d(BU) = \frac{\overline{\nu}(BU) N_{HM} d(BU)}{k_\infty} \tag{2.7}$$

For a more realistic account and to relate k_∞ to a real 3-D reactor core, neutron losses should be accounted for as well. The main mechanisms of neutron losses are Leakage (L) and absorption in Reacivity Control (RC) systems. Therefore, accounting for losses, the neutron production is:

$$neutron\,produced\,in\,d(BU) = \overline{\nu}(BU)\, N_{HM} d(BU) P_{NL} P_{RC} \tag{2.8}$$

where P_{NL} is the non-leakage probability of neutrons and with P_{RC} is the fraction of neutrons not captured in the Reactivity Control systems. The net

neutron production (production minus absorption) can be derived integrating Eq. (2.8), while subtracting Eq. (2.7) from it:

$$net\,production = \int_0^{BU} (\overline{\nu}(BU) N_{HM} P_{NL} P_{RC} - \frac{\overline{\nu}(BU) N_{HM}}{k_\infty}) d(BU) \quad (2.9)$$

then, (2.9) can be re-written as:

$$net\,production = N_{HM} \int_0^{BU} \overline{\nu}(BU)(P_{NL} P_{RC} - \frac{1}{k_\infty})\, d(BU) \quad (2.10)$$

Knowing k_∞ evolution and $\overline{\nu}$ through neutron transport calculations it is possible to plot Eq. (2.10), when making assumptions on the values of P_{NL} and P_{RC}. When Eq. (2.10), i.e. the net neutron production is positive, a B&B mode of operation can be sustained, therefore the equation that defines a B&B reactor can be written as:

$$N_{HM} \int_0^{BU} \overline{\nu}(BU)(P_{NL} P_{RC} - \frac{1}{k_\infty})\, d(BU) \geq 0 \quad (2.11)$$

For fast reactors loaded with metallic fuel at high volume fraction the calculated $\overline{\nu}$ is $\sim$2.9, valid in general for BU$>$ 5% FIMA. In following calculations, the value of $\overline{\nu}$ derived by simulations will be used. Using the k_∞ evolution of Figure 2.7 it is possible to plot Eq. (2.10), as in Figure 2.8.

From Figure 2.8, it is observed that when the net neutron balance is greater than zero the B&B mode of operation can be sustained and this happens at a burn-up higher than 10.2%, in case of no leakage or reactivity control losses. The B&B mode of operation can theoretically be sustained up to 59% FIMA, since the neutron balance is positive up to that value, though this high burnup is unrealistic for material damage.

For a more realistic assessment, because of leakage and reactivity control systems, losses need to be taken into account. For a control management strategy 2% can be assumed as a typical value of Reactivity Control losses (RC) [14].

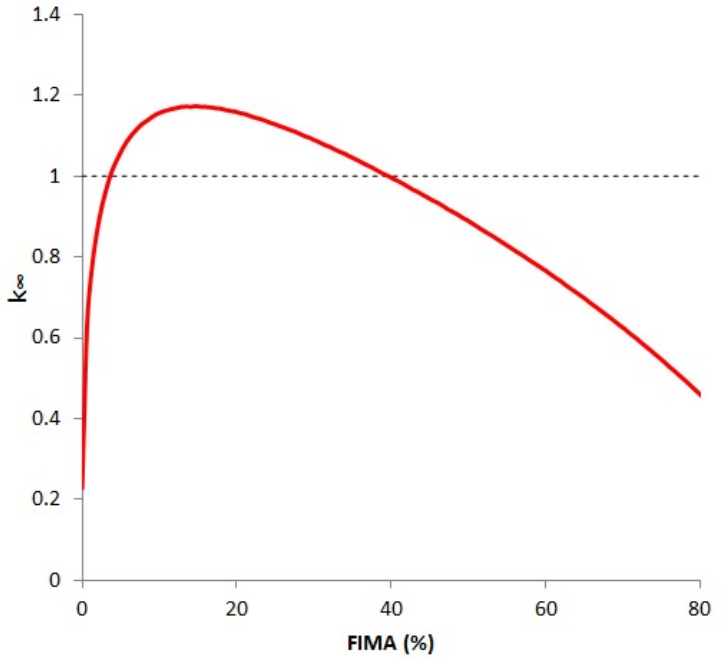

Figure 2.7: k_∞ evolution for U-10%Zr alloy fuel.

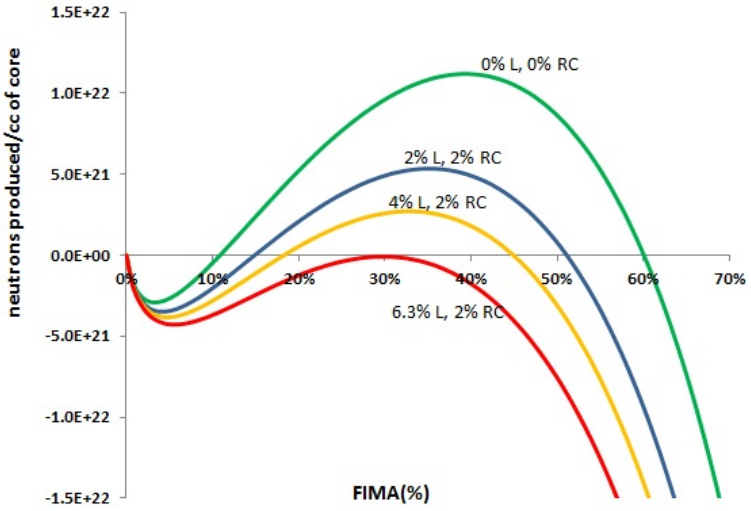

Figure 2.8: Net neutron production for cm^3 of core for U-10%Zr fuel for various value of leakage (L) and Reactivity Control (RC) losses.

Figure 2.8 shows the net neutron production for various values of leakage (L). It is observed that the neutron leakage heavily affects the minimum burnup requirement. A higher value of L shifts the point of zero balance towards higher burnups. It is also observed that when assuming RC=2% and L=6.3% the neutron balance is never positive, meaning that B&B mode of operation cannot be sustained. Traditional fast reactors have leakage that is about 20% it is therefore imperative to design B&B reactor with a small leakage and tight neutron economy. If leakage is too high, the B&B mode of operation cannot be sustained. Various B&B reactor designs [13, 27] have reduced the average leakage to a value of about 4% to 6% and therefore can operate with a minimum burnup of $\sim$ 18%-20% FIMA. Table 2.4 reports the value of minimum and maximum burnup for all cases of Figure 2.8.

It is important to remind that the predictions of the neutron balance method are only an approximation that can be used to restrict the parameter space of full core design studies. In fact, the main difference between the unit cell model and a full B&B core are in the neutron spectrum, since the unit cell has an infinite medium spectrum, while the B&B core neutron spectrum is space-dependent and affected by leakage and absorptions in surrounding

areas. Moreover, the leakage L does not have a fixed value when the reactor is run, and the precise leakage value is also hard to predict.

Table 2.4: Minimum and maximum burnups in % FIMA for various values of L and RC for U-10%Zr alloy fuel.

Leakage	Reactivity Control losses	minimum burnup	maximum burnup
0%	0%	10.2	59%
2%	2%	15	50%
4%	2%	18.2	45%
6.3%	2%	-	-

2.4 Minimum burn-up and material damage requirements for U-Zr alloy fuel

The neutron balance method can be applied to study the minimum burn-up requirements for different fuels. As the fuel of choice in this work, is the U-Zr alloy, it is important to study the impact of Zr content on the minimum burnup requirement.

Figure 2.9 shows the k_∞ evolution for various Zr content (0% , 5% and 10% by weight). Fig. 2.9 shows that the variation in the maximum value of k_∞ is 4.4% from 0% Zr to 10% Zr. This affects the minimum required burn-up, as shown in Fig. 2.10.

In Figure 2.9, together with the k_∞ evolution, the dpa accumulation in the cladding is also plotted. The dpa, displacement per atom, is the measure by which an atom is displaced from its original lattice position and it is a measure of radiation damage. As mentioned in Section 1.1, current data on HT-9 behavior with radiation are only available up to about 200 dpa [16]. Therefore it is important to correlate the minimum burnup found from the neutron balance to the radiation damage in dpa.

The dpa accumulation can be calculated using the appropriate MCNP

tally. The MCNP tally gives a dpa cross-section integrated over the flux :

$$\sigma_{MCNP}[barns - MeV] = \int_0^{E_max} E_{PKA}\sigma_{dpa}\,\Phi dE \tag{2.12}$$

This represents a reaction rate and it is given in units of MeV-barn, since it includes the integrated average value of the energy of Primary Knock-on Atoms (PKA) E_{PKA}, so to scale the damage proportionally to the PKA energy. The dpa accumulation over a time step T can be found using the Kinchin-Pease model [37]:

$$DPA = \eta\frac{\sigma_{MCNP}}{2E_d}\,T\,S \times 10^{-24} \tag{2.13}$$

where E_d is the atom displacement energy, i.e. the energy required to displace an atom from its lattice position; η is the atom displacement efficiency which is assumed to be 0.8 [37]; S is the neutron fission source strenght, since the MCNP dpa reaction rate is calculated per fission neutron.

To simplify calculations, E_d for HT-9 will be approximated with E_d of iron, its main constituent, which is 40 eV. This methodology for dpa calculation has been used in Fig. 2.9.

From Eq. (2.9), it is observed that the dpa accumulation is higher in metallic uranium (0% Zr) compared to fuel with zirconium as it is expected, since pure uranium has a harder spectrum and therefore each neutron can displace more atoms, thanks to the higher incident energy. At 20% burn-up, the dpa accumulation is 405 dpa for U-10%Zr and 480 for U. It is important to observe that the unit-cell depletion overestimates the dpa accumulation in the first few percent FIMA, due to an overestimation of the flux of high energy neutrons. In a 3-D reactor, the fuel will actually run in a softer flux, when introduced in the reactor.

The k_∞ can be used, as outlined in Section 2.3, to calculate the minimum burnup requirement. Fig. 2.10 shows the neutron balance for the U-Zr alloy fuels in case of L = 4% and RC = 2%, while Table 2.5 shows the minimum and maximum burnups for the U-Zr fuels, depending on Zr content.

From Table 2.5, it is possible to understand the need of new material testing and development for the realization of B&B reactors. For typical case with L = 4% and RC = 2% the dpa that the cladding experiences are in the around of 350. However, it is important to realize that the neutron balance represents a core-average of the neutronic properties. In a reactor, though the discharge batch will have a burnup close to the one found by the

neutron balance method, the peak burnup, and consequently the radiation damage, will be in the highest flux point of the fuel rod, usually in the center of the reactor. At a first approximation, this peak dpa can be represented as a 50% increase on the averaged dpa, e.g. if the averaged discharge fuel is at 20% FIMA, the peak burnup is 30% FIMA. Consequently the minimum burnup for a U-5%Zr fuel corresponds to approximately 520 dpa. The 500 dpa limit is what is considered to be the objective to be able to realize a B&B reactor that works without reprocessing [15].

Table 2.5 also reports the maximum burnup. Theoretically such high burnups could be achieved. However to reach such high burnups, the fuel will definitely need some sort of reprocessing. In the next section, B&B reactors with limited reprocessing, and reprocessing effects on burnup are analyzed.

Table 2.5: Average minimum and maximum burnup in % FIMA for various U-Zr fuels; dpa to materials are given at average minimum burnup.

	Zr (w/o)	minimum burnup	dpa at min. bu	peak dpa (dpa×1.5)	maximum burnup
no losses	0%	8	240	360	67%
	5%	9.1%	245	368	64%
	10%	10.3%	245	368	60%
L=4% RC=2%	0%	12.2 %	325	488	57%
	5%	15%	347	521	51%
	10%	18.2%	370	555	45%

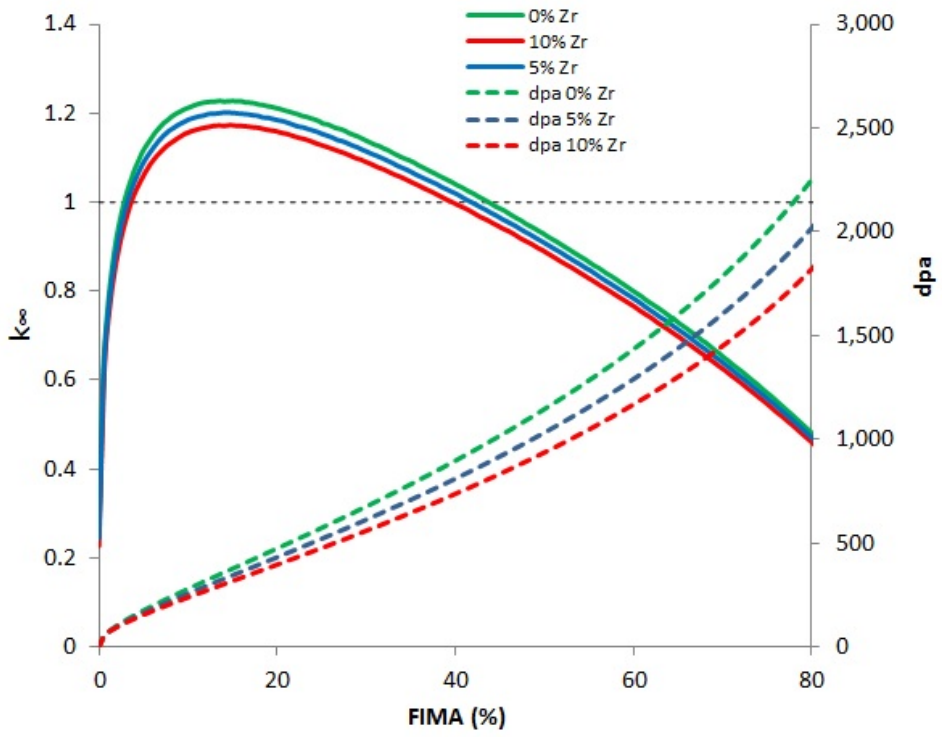

Figure 2.9: k_∞ evolution for U-Zr alloy fuel with 5% and 10% Zr and for metallic uranium (0% Zr); dpa accumulation in HT-9 is also plotted for the various fuels.

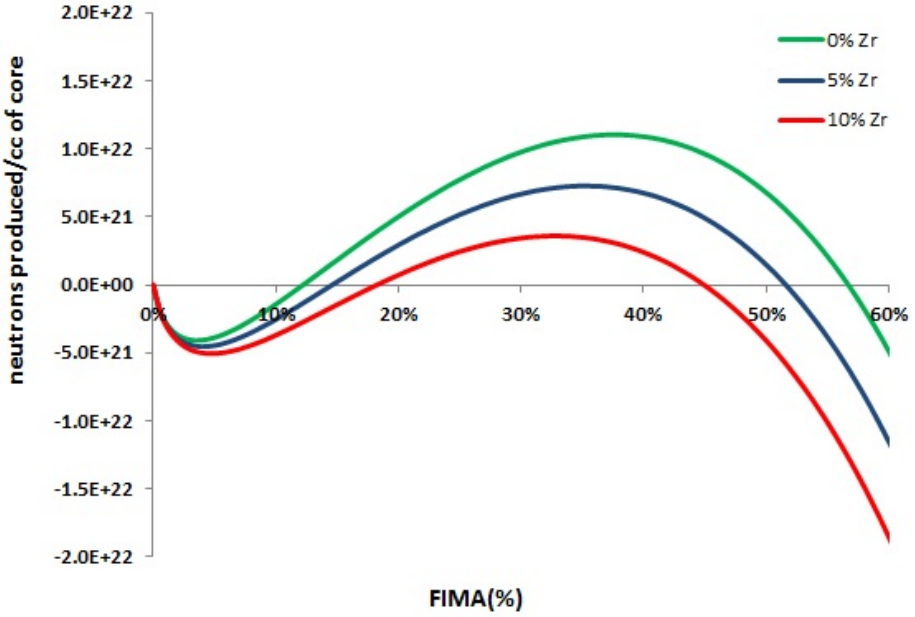

Figure 2.10: Neutron balance for U-Zr with 0%-5%-10% Zr for P_{NL}=96% and P_{RC} = 98%.

2.5 Maximum burnup with limited separation fuel cycles

As B&B reactors are neutronically able to reach high burnups, it is of particular interest to study fuel cycles that combine proliferation resistant reprocessing technology with B&B reactors. In fact, as it becomes necessary to replace the cladding and reprocess the fuel when the cladding radiation damage limit is reached, the entire fuel does not need to be fully reprocessed by neutronic performance. However, the fuel will need to be recladded and therefore will need to undergo some sort of reprocessing. The ideal recycling process is a proliferation resistant process that removes as little material as possible from the fuel, since fission products removal is not necessary for neutronics performance. Two processes have been developed in the past, which both separate a minimal amount of fission products, leaving most of actinides in fuel: 1) the AIROX process applied to oxide fuels and extensively studied during the DUPIC project [38] and 2) the melt-refining process, developed to reprocess EBR-II fuel [5].

2.5.1 AIROX

AIROX process was developed as a dry procedure to re-utilize LWR spent fuel in CANDU. The procedure is highly proliferation resistant, since it could not separate actinides from Fission Products (FP). The operations of AIROX process are summarized in Fig. 2.11. This process has been developed only for oxide-fuels. In this work, we will assume that an AIROX-like process could be applied to metallic fuel. AIROX removes only specific FPs with reduction-oxidation reactions. At the end of the process 100% of T, C, Kr, Xe and I, 90% of Cs and Ru and 75% of Te and Cd are removed in gaseous form. In addition, gaseous FPs that are present in gaseous form during reactor operations and accumulate in the fuel rod plenum are assumed to be removed at 100% efficiency. Table 2.6 summarizes the removal fractions for AIROX.

2.5.2 Melt-refining

In the melt refining process, the metallic fuel is first chopped and removed from the cladding. The fuel is then melted in a furnace at 1300 °C -1400 °C

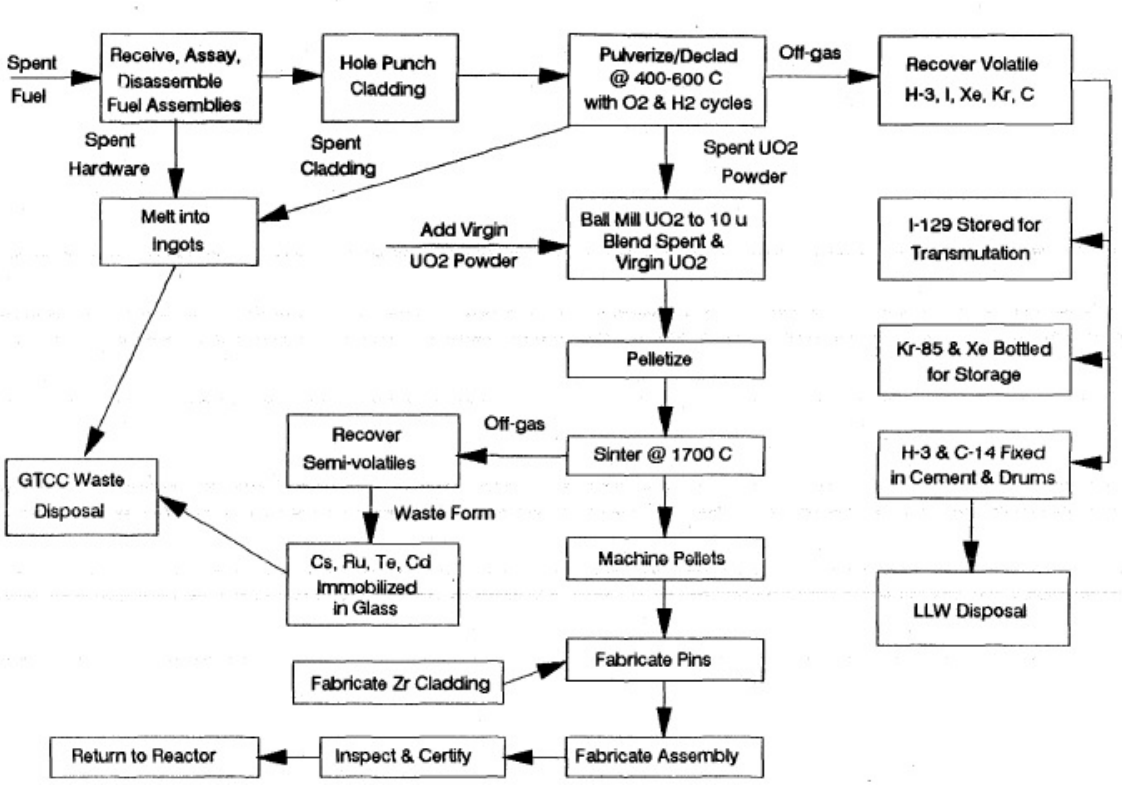

Figure 2.11: Unit operations in the AIROX process [38]

for about one to three hours in argon atmosphere. Figure 2.12 shows the original furnace of the EBR-II project [5]. In the melting process, some FPs are removed by volatization, while others are partially removed by oxidation with the zirconia of the crucible. It was found that this process can remove nearly 100% of volatile FPs Br, Kr, Rb, Cd, I, and Cs, and 95% of Sr, Y, Te, Ba and rare earths (lanthanides). Moreover, 95% of Th and Am are also oxidized with zirconia and removed from the fuel. These materials accumulate in the crucible and need to be removed from the crucible and properly disposed in a suitable waste form. In the reference case for melt refining, the only actinides that oxide and remain in the reaction layer on the crucible surfaces are Th and Am at a fraction of 95%. However, it is important to note that, during operations, some actinides might remain in the crucible. Since this process has been performed only at a laboratory scale, the fraction of actinides that might remain in the crucible has not being explored sufficiently to reach optimization. In Section 2.5.3 we will explore the case of 1% and 10% of all actinides lost in the crucible, during melt refining.

Lastly, as for the AIROX process, gaseous FPs that are present in gaseous form during reactor operations and accumulate in the fuel rod plenum are assumed to be removed at 100% efficiency. Table 2.6 summarizes the removal fractions for melt refining.

Table 2.6: Summary of removal fractions in AIROX and melt-refining

	AIROX	melt-refining
Actinides	0%	95 % Th, Am 0% others
Fission Products	100% H,C,Kr,Xe,I 90% Cs,Ru 75% Te,Cd	100% Br,Kr,Rb,Cd,I,Cs 95% Sr,Y,Te,Ba, La-Lu
Gaseous Fission Products	100% H,He,N,O,F,Ne,Cl,Ar,Kr,Xe,Rn	

2.5.3 Neutron balance with AIROX and melt-refining

The effects of limited separation fuel-cycles can be studied, applying the processes in exam to the unit cell depletion. As we explained in Section 2.4

Figure 2.12: Melt refining furnace [5]

the minimum burnup for B&B mode of operation will be at $\sim$ 18%-20%, implying a peak dpa of about 500. If we assume that further material testing will provide data that enable utilization of steel cladding up to 500 dpa, to further increase the fuel utilization, a reprocessing will be needed at $\sim$ 18%-20% FIMA.

Figure 2.13 shows unit cell depletion for U-10%Zr fuel that undergoes reprocessing through AIROX or melt refining, at every 20% FIMA. It is observed that there is an increase in k_∞ every time the fuel is reprocessed, due to the removal of FPs. The increase is about 4% for melt refining and 2% for AIROX, since the latter removes less FPs than melt refining. The radiation damage to the cladding is also plotted in the same figure. As the material is reprocessed, the cladding is replaced; this is shown by the discontinuities in the figure. Excluding the first step that suffers of the usual spectrum hardness overestimation for fresh fuel, the average radiation damage, in the second and third step, does not exceed 350 dpa, corresponding to an estimated peak of 525 dpa. Therefore with the use of such a process, the cladding limits are preserved in the around of 500 dpa. Moreover, the fuel utilization is expanded beyond the maximum burn-up of 45% found in the case of no-reprocessing (Table 2.5).

For L = 4% and RC = 2%, the neutron balance is shown in Figure 2.14. It is evident how the discontinuities are reflected in the balance with a change of the net production slope at 20% and 40% FIMA. Before 20% FIMA, as no reprocessing has occurred, all the curves are identical.

Table 2.7 summarizes the results for maximum burn-up for the various cases. It is found that the use of melt-refining can extend the maximum burn-up from 45% up to 58%.

Table 2.7: Maximum burnup for different fuel cycles

reprocessing type	maximum burnup
none	45%
AIROX	54%
melt-refining	58%

Next, we analyze the effect of using AIROX at different burnup intervals. Figure 2.15 shows the k_∞ evolution for various cases of AIROX reprocess-

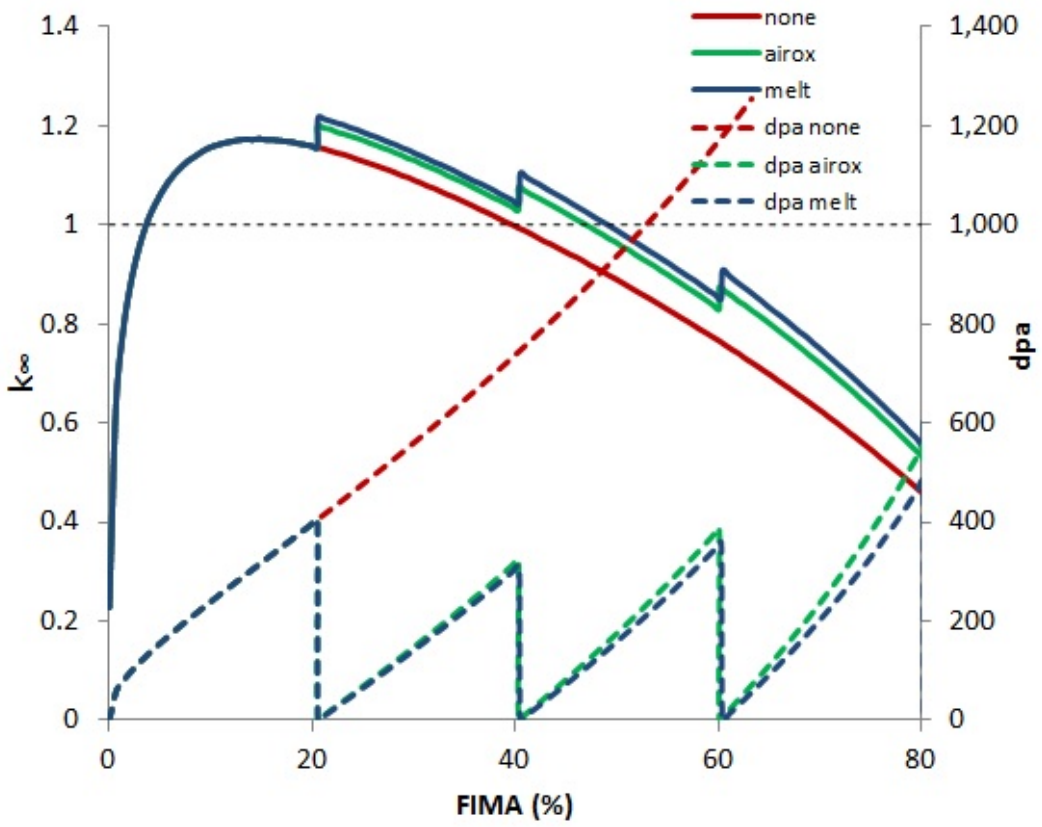

Figure 2.13: k_∞ evolution for U-10%Zr alloy fuel with no reprocessing and with AIROX and melt-refining every 20% FIMA; dpa accumulation in HT-9 is also plotted.

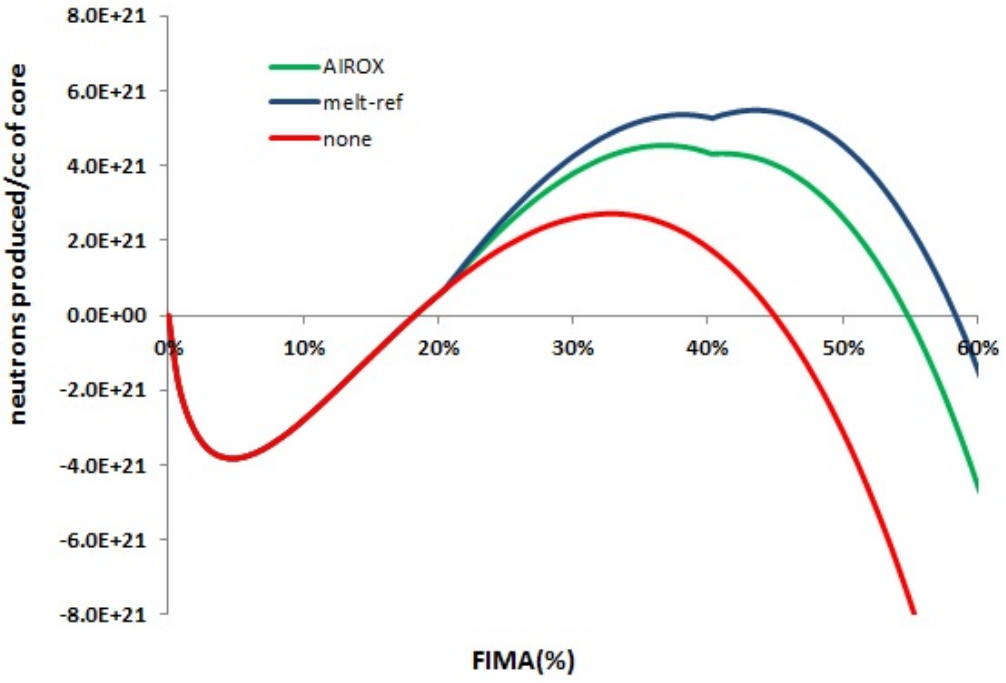

Figure 2.14: Neutron balance for U-10%Zr with P_{NL}=96% and P_{RC}=98% with no reprocessing and with AIROX and melt-refining every 20% FIMA.

ing. The interval at which the recycling is done is varied and three cases are studied: AIROX every 5% FIMA, every 10% FIMA and every 20% FIMA. Figure 2.15 shows the evolution of k_∞ along the burnup with AIROX recycling at different intervals. As observed, discontinuities are present whenever recycling is performed. Performing AIROX more often is a way to limit the radiation damage to the cladding.

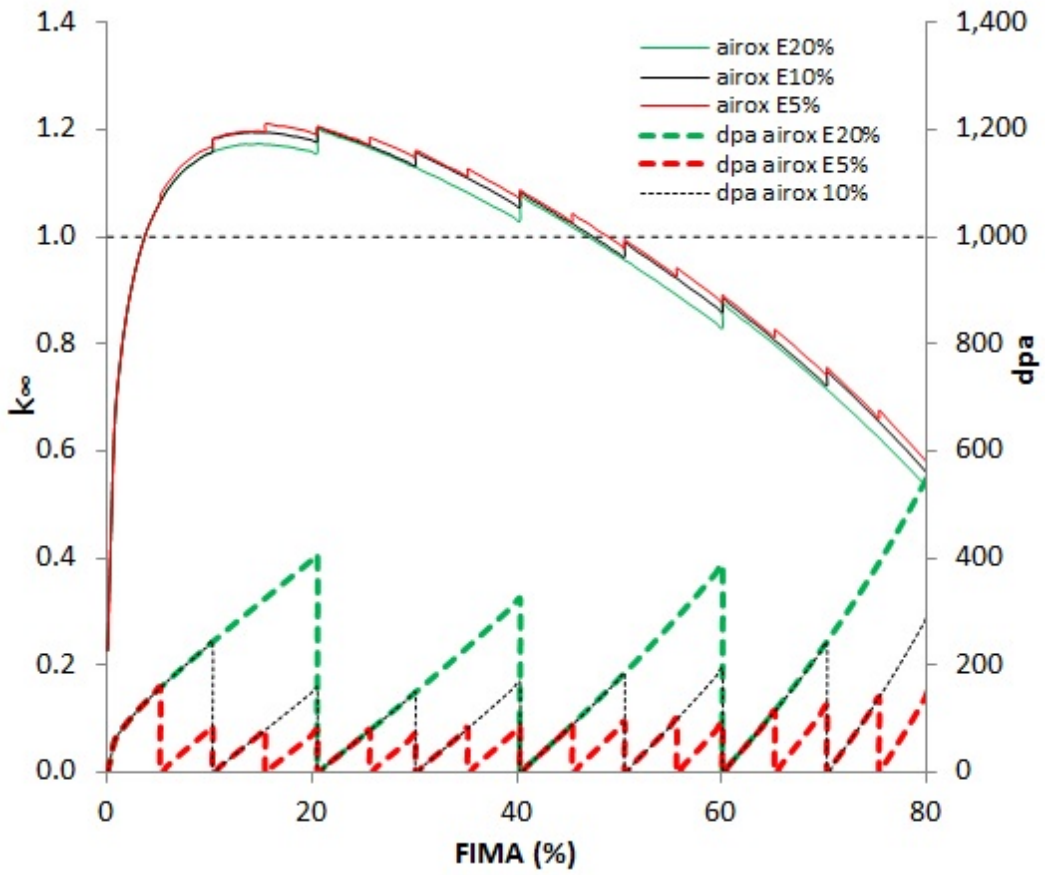

Figure 2.15: k_∞ evolution for U-10%Zr alloy fuel with AIROX every 5%, 10% or 20% FIMA; dpa accumulation in HT-9 is also plotted.

Figure 2.8 shows the neutron balance for the three AIROX cases. Discontinuities, though present, are not evident, for the 5% FIMA, as the change in slope is more subtle. Table 2.8 summarizes the results for AIROX cycles,

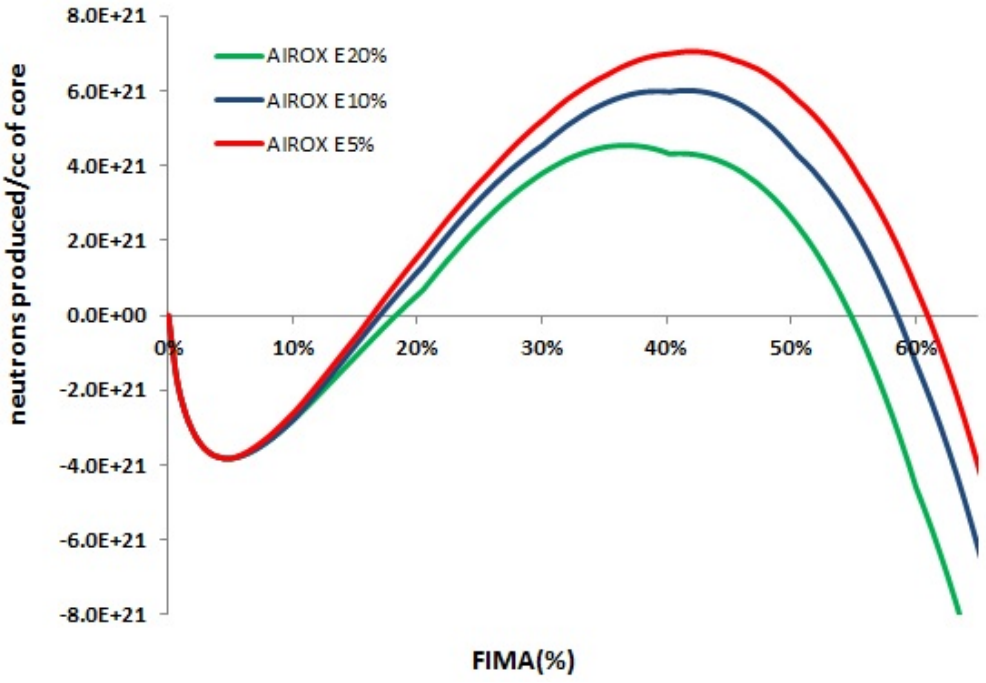

Figure 2.16: Neutron balance for U-10%Zr with P_{NL}=96% and P_{RC}=98% with AIROX reprocessing every 5%, 10%, 20% FIMA.

together with the dpa accumulated in the second step. It is observed that using AIROX every 5% average burnup, peak radiation damage does not exceed 117 dpa. With the limit of 200 dpa, an interpolation between the 5% and 10% AIROX cases, brings that recycling every 8% should cause a radiation damage to the cladding that does not exceed 200 dpa with a maximum burnup of $\sim$ 59%. This result is of great importance, as it tells that a B&B reactor could be designed without exceeding current material damage limitations, and therefore could be realized with current technologies, without need of new experiments to test material resistance beyond 200 dpa. However, a commercially viable AIROX like process will have to be developed and recycling of AIROX processed fuel demonstrated.

Table 2.8: Maximum burnup in % FIMA for AIROX fuel cycles.

AIROX every FIMA %	maximum burnup	dpa	peak dpa (dpa×1.5)
5%	60%	78	117
10%	58%	158	237
20%	54%	405	607

Lastly, we examine the effect of melt-refining actinide losses on the maximum burnup on B&B reactors. When melt refining is performed and heavy metal losses are present the FIMA at time t cannot be calculated as in Eq. (2.4). In fact, the term M_t does not include the HM that are lost in waste, since it represents the composition at time t, after recycling. When calculating the percent of initial HM that are burned, the HM in waste needs to be included back, since this are not properly burned, but lost into waste. Therefore, we can write:

$$FIMA(\%)_t = \frac{M_0 - M_t + M_{waste}}{M_0} \times 100 \tag{2.14}$$

where M_{waste} are the moles of actinides accumulated in the waste, from the beginning of burnup. Since these moles that are lost to waste constitute a part of material which will not be burned, the fuel cannot be burned to a full 100% FIMA.

Figure 2.17 shows the k_∞ evolution for U-10%Zr for reference melt refining and 1% and 10% actinide losses. It is observed that in the case of 10% losses

the melt refining k_∞ is lower than the k_∞ with no reprocessing at burnups higher than 43%.

Figure 2.18 shows the neutron balance for melt refining with losses and Table 2.9 summarizes the results. It is observed that, 1% losses decrease the maximum attainable burnup 1.3%, while 10% losses decrease the final burnup considerably down to 47.3% from 58%. However this burnup is still higher than the theoretical case of no reprocessing 45%. In the following chapter, B&B reactors utilizing limited separation recycling are analyzed. The results of this chapter are used to restrict the design space to reactors in the vicinity the attainable burnup calculated from the unit cell model.

Table 2.9: Maximum burnup for melt-refining fuel cycles with melt-refining every 20% FIMA

actinide losses %	maximum burnup
reference	58%
1%	56.7%
10%	47.3%

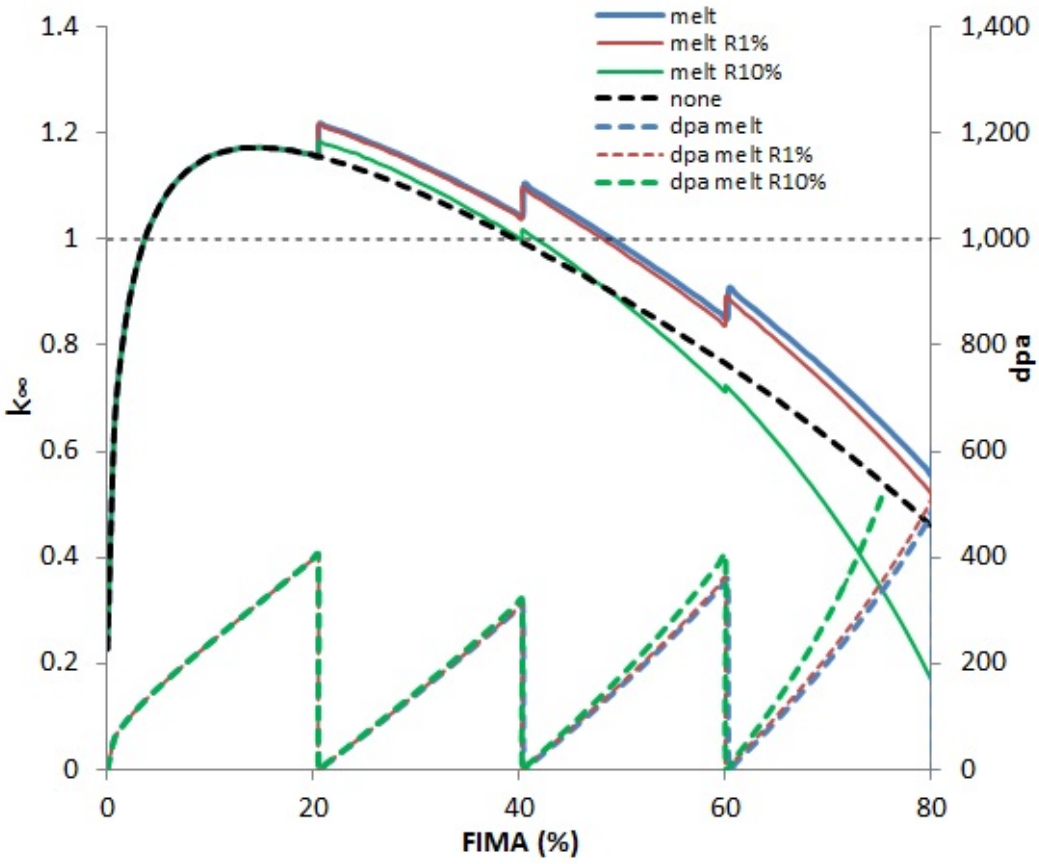

Figure 2.17: k_∞ evolution for U-10%Zr alloy fuel with melt-refining every 20% FIMA, assuming actinides losses equal to the reference case, to 1% and to 10%; dpa accumulation in HT-9 is also plotted

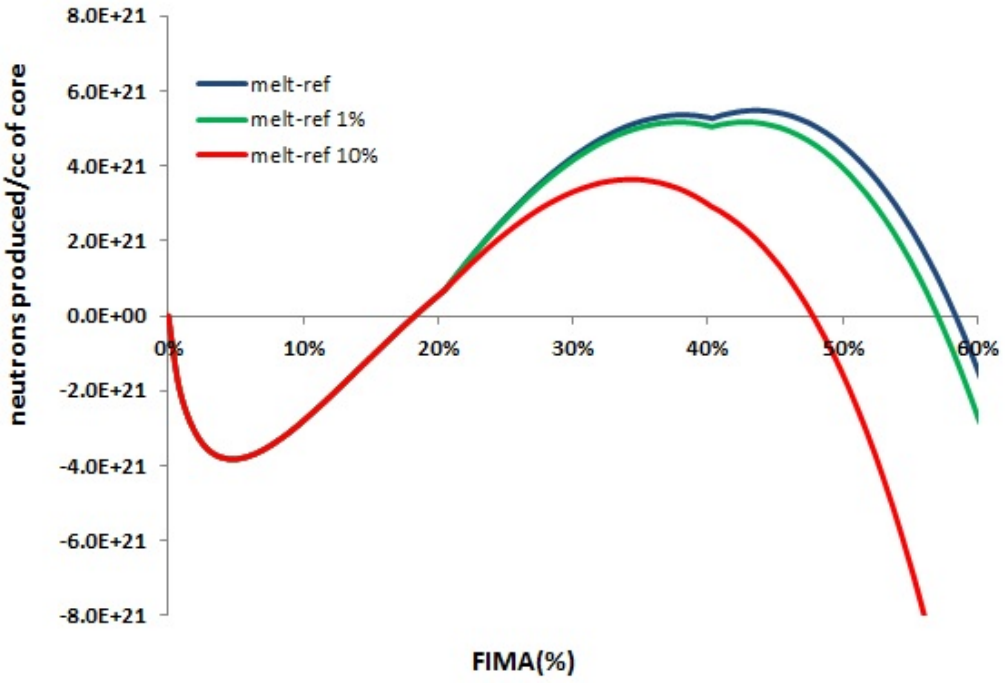

Figure 2.18: Neutron balance for U-10%Zr with P_{NL}=96% and P_{RC}=98% with melt-reprocessing every 20% FIMA with reference, 1% and 10% actinide losses

2.6 Computational Tools

In this Section, the computational tools used for simulation are presented. These tools have been used for all simulations described in this chapter, and they are used in the next chapters to simulate 3-D reactors.

2.6.1 MCNP5

MCNP5 is a Monte Carlo particle code, developed by Los Alamos National Laboratory (LANL). This code can simulate neutron transport using Monte Carlo techniques. Geometries can be freely defined by the user, and materials can be used from the material database and mixed to reproduce reactor core composition. The detailed capabilities of MCNP5 can be found in the MCNP5 manual [33]. Using Monte Carlo codes is computationally expensive when compared to deterministic codes. However, the use of this code allows to simulate modern advanced reactors without approximations on the physics or on geometric configurations. The main advantage is the use of point-wise energy cross-section data without the need for generation of problem-dependent multi-group cross sections, and therefore no need to know the neutron spectrum *a priori*.

2.6.2 ORIGEN 2.2

ORIGEN 2.2 is a depletion code released in 2002 by Oak Ridge National Laboratory [34]. It solves the Bateman-depletion equation using a matrix exponential method. This code is used to estimate the reactor fuel composition as a function of time, using the effective one-group cross-sections and total flux values generated by MCNP5. For reactions for which cross-sections are not provided by MCNP5, cross-sections from the default ORIGEN 2.2 library for liquid metal cooled cores with oxide fuel, LMFBR recycle Pu/U, are used. However, it is important to stress that these cross-sections do not represent a valid approximation of B&B reactors. Therefore MCNP5 is used to calculate cross-sections at each burn-up step, based on the real physics of the reactor. Unfortunately, no default library representing a fast reactor operating with metallic fuel is available in ORIGEN2.2. Due to the spectral difference between oxide and metallic fueled cores, it is important that the data generated by MCNP5 for isotopes represent at least 99% of the total fission and absorption cross-sections. For all the simulations performed with

MCNP5, the (n,f), (n,γ), (n,2n), (n,3n) and (n,α) one group cross-sections are generated for thirty-four actinide isotopes and ninety-nine fission product isotopes, given in Table 2 8. All the cross-section data used by MCNP5 for the present study are based on the ENDF/B-VII libraries.

2.6.3 MOCUP

MOCUP is the MCNP-ORIGEN Coupled Utility Program developed by Idaho National Laboratory (INL) in 1995 [35] and upgraded at UC Berkeley [17]. Its role is to interface ORIGEN 2.2 with MCNP5. In particular, it provides ORIGEN 2.2 with the initial fuel compositions, effective one-group cross-sections and total flux estimated by MCNP5 for each depletion zone, it creates the ORIGEN 2.2 input file, executes ORIGEN 2.2 and generates the new input file for MCNP5 using the updated fuel composition. The isotopes that are tracked in MOCUP are reported in Table 2.10 and Table 2.11 . The main function of MOCUP is to calculate the one group cross sections from MCNP5 results for these isotopes in each cell and transfer them to ORIGEN 2.2., as illustrated in Fig. 2.19. MOCUP results have been accurately bench-marked [39].

Table 2.10: List of Actinide Isotopes Tracked in MCNP5

Element	Isotope number
Thorium	232, 233
Protactinium	233
Uranium	234, 235, 236, 237, 238, 239
Neptunium	236,237, 238, 239
Plutonium	236,237, 238, 239, 240, 241, 242, 243, 244
Americium	241, 241m, 242, 243, 244
Curium	242, 243, 244, 245, 246, 247, 248
Berkelium	249
Molybdenum	95, 96, 97, 98, 100
Californium	249

Table 2.11: List of Fission Product Isotopes Tracked in MCNP5

Element	Isotope number
Bromine	81
Krypton	83, 84
Rubidium	85, 87
Strontium	90
Yttrium	89
Zirconium	90, 91, 92, 93, 94, 96
Technetium	99
Ruthenium	100, 101, 102, 103, 104, 105
Rhodium	103
Palladium	104, 105, 106, 107, 108, 110
Silver	109
Cadmium	110, 111, 112, 113, 114
Indium	115
Tin	117, 118
Antimony	121, 123, 125
Tellurium	125, 128, 130
Iodine	127, 129
Xenon	130, 131, 132, 134, 135
Caesium	133, 134, 135, 137
Barium	134, 137, 138
Lanthanum	139
Cerium	140, 142
Praseodymium	141
Neodymium	143, 144, 145, 146, 148, 150
Promethium	147
Samarium	147, 148, 149, 150, 151, 152, 154
Europium	151, 152, 153, 154, 155
Gadolinium	154, 155, 156, 157, 158
Terbium	159

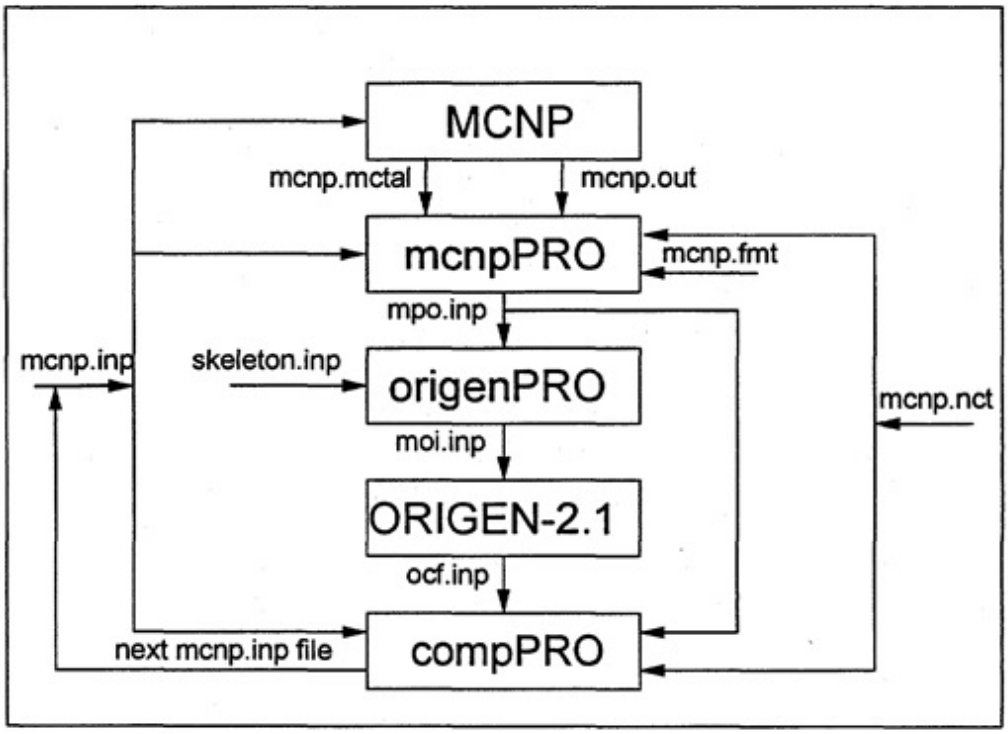

Figure 2.19: Flow path of MOCUP 2.1

2.6.4 Additional tools

The MOCUP code is able to transfer data from MCNP to ORIGEN and the other way around. However, scripts for fuel shuffling and reactor equilibrium need to be added to find a core equilibrium composition. The aforementioned operations have been implemented in MOCUP through the use of external scripts, written in bash shell in UNIX. These scripts have been developed as part of this study, though code previously developed at UC Berkeley [17] has been used as a basis.

-*fuel shuffling script*: this script exchanges material compositions so that it can simulate shuffling of different batches in different geometrical areas of the reactor

-*equilibrium composition script*: this script searches for an equilibrium composition. After a transport calculation is executed for a reactor cycle. This script uses cross section data thus obtained to run depletion-only calculations until material composition converge. Then a neutron transport calculations is run again, and the procedure is repeated until equilibrium is found . The reactor equilibrium cycle is defined as convergence on two subsequent cycles having each value of k at each step of the cycle during within two times the MCNP calculated statistical uncertainty, σ. The statistical uncertainty for simulation is 70 pcm thorough this entire work, except when noted.

2.7 Conclusions

In this chapter, the synergies of B&B reactors with limited separation fuel cycles were analyzed, thorough the neutron balance method. It was found that for typical values of leakage and reactivity control losses the maximum burnup is in the range of 54% to 58% depending on the recycling process used, if AIROX or melt refining.

Chapter 3

Fuel Cycle of B&B Reactors with limited separation reprocessing

In this chapter we will describe the current status of B&B reactor designs at UC Berkeley and we will analyze the current fuel cycle issues, through a waste analysis of B&B reactors. Alternatives to the fuel cycles presented in this chapter will be the subject of the following chapters.

3.1 Issues with B&B fuel cycle

The current objective of B&B reactor research is to realize a B&B cycle that is inherently proliferation resistant. This objective could be achieved with a B&B reactor working at the minimum burn-up ($\sim$ 18-20%) with no reprocessing. If materials that can withstand a radiation damage of about 500 dpa became available, this objective could be realized. TerraPower is working on this objective with new experiments, simulations and material testing [15]. In the rest of this study, it will be assumed that such an objective will be achieved and cladding materials able to withstand 20% FIMA in a B&B reactor will be available. In this chapter, the issues of B&B reactors working with minimum burn-up are analyzed and benefits of using limited separation fuel cycles are assessed.

Table 3.1 reports the uranium utilization of B&B reactor using 20% discharge burn-up, compared to uranium utilization in current Light Water

Reactors.

Table 3.1: Uranium utilization of Breed and Burn Reactor Discharge Burnup

reactor	discharge burnup (% FIMA)	depleted/natural uranium utilization (%)	depleted/natural uranium utilization compared to PWR
PWR	4.36	0.53	N/A
B&B	20	20	38

Figure 3.1 shows the evolution of plutonium concentration in B&B fuel along with the burnup in FIMA for U-10%Zr. It is observed that the concentration peak of ^{239}Pu happens at $\sim$ 16% FIMA which is very close the minimum burnup (18-20% FIMA). This means that the reactor at minimum burnup discharges significant quantity of ^{239}Pu to waste. Moreover, it needs to be considered that the fuel form of B&B reactors is metallic and therefore it is not a stable form as uranium dioxide. The disposal of such a high content of ^{239}Pu in metallic fuel poses both waste disposal and proliferation concerns.

As is observed in Figure 3.2, the fissile content in B&B discharged fuel is more than twice the one in LWRs per unit of electricity generated. This is of great concern, since the use the disposal of such a fuel could pose environmental concerns and high proliferation risks, which are exactly what B&B fuel cycle should prevent.

Moreover this high fissile content can be utilized for energy production. Chapter 4 and Chapter 5 explore methods for using the discharge fuel through an additional burn-up step in a different type of reactor, while this chapter analyzes the results increasing fuel utilization in B&B reactor with limited separation in terms of radiotoxicity and ^{239}Pu fuel content.

3.2 UC Berkeley B&B designs

At UC Berkeley, Heidet & Greenspan have designed various versions of B&B reactors [14, 17, 27, 29, 40], all based on a cylindrical arrangement of hexagonal assemblies. The two main designs studied are:

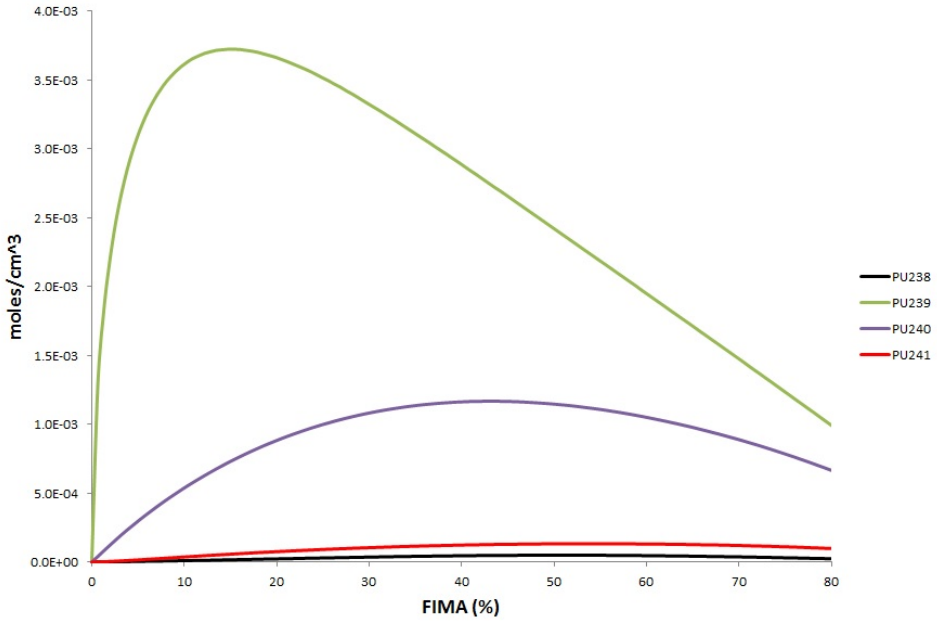

Figure 3.1: Pu content evolution with burnup in a B&B reactor unit cell with fuel U-10%Zr.

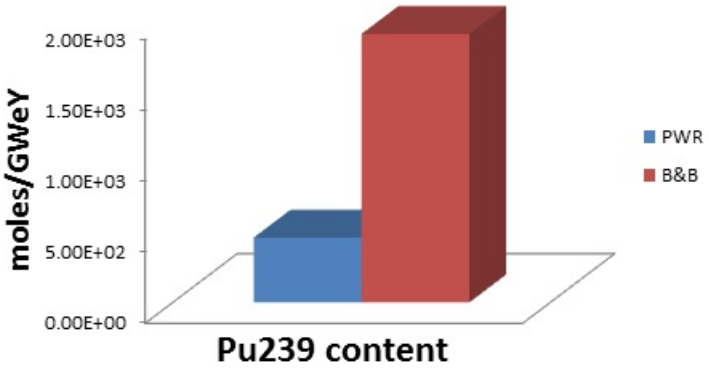

Figure 3.2: Pu content in B&B and LWR discharged fuel

- a large B&B reactor of 3000 MW_{th} [13];
- a medium size B&B reactor [27] of 1200 MW_{th} that has dimensions similar to S-PRISM fast reactor, developed by General Electric [31]. The studies were summarized in Heidets thesis at UC Berkeley [17].

Two versions of this reactor have been developed:

- 55% burnup B&B reactor. A large B&B reactor consisting of 8 radial batches, with a cycle length of 8.8 years and 55% discharge burnup.
- 20% burnup B&B reactor. A B&B reactor with 12 radial batches, with cycle length of 2.06 years and discharge burnup of about 20%.

Both reactor cores have same dimensions with an active fuel length of 209 cm and a diameter of 400 cm. For burn-up simulations each axial batch is divided in 3 zones, within each the core composition is homogenized.

The 20% B&B reactor uses a metallic alloy of U-10%Zr as fuel. The fuel goes once through the reactor and it is then discharged at 20% burn-up. The 55% reactor uses a fuel reprocessing, happening every 20% FIMA, since the cladding radiation damage limit is assumed to be 20%. The fuel will be recycled two times to reach a 55% burn-up. In this chapter, the previous analysis will be expanded to study the effect of plutonium concentration in waste of the two different recycling process analyzed in Chapter 2: AIROX and melt refining.

The large B&B reactor designed by Heidet & Greenspan is schematically represented in Figure 3.3, while Table 3.2 reports reactor dimensions and compositions of the reactor components.

Figure 3.4 shows the fuel management scheme of the 20% B&B reactor. This shuffling scheme is optimized for the reactor to operate at 20% FIMA. The 20% average burn-up is the minimum discharge burn-up for B&B mode of operation at this fuel composition. It is assumed that material improvements will enable to produce cladding that can withstand 20% burn-up and therefore there is no need of reprocessing and the 20% burned batch is discharged and sent to repository.

Figure 3.5 shows the fuel management scheme of the 55% reactor. This reactor uses 8 fuel batches with an out-to-in shuffling scheme. In this design, it is assumed that cladding, through material improvements, will be able to withstand about 20% burnup, therefore the fuel needs to be reprocessed

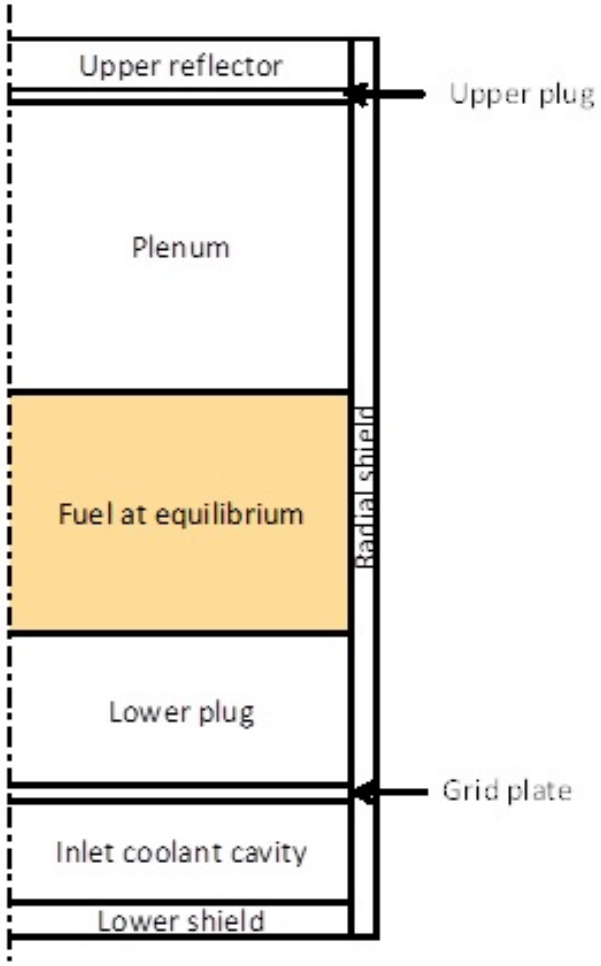

Figure 3.3: Design scheme of the large B&B reactor [13].

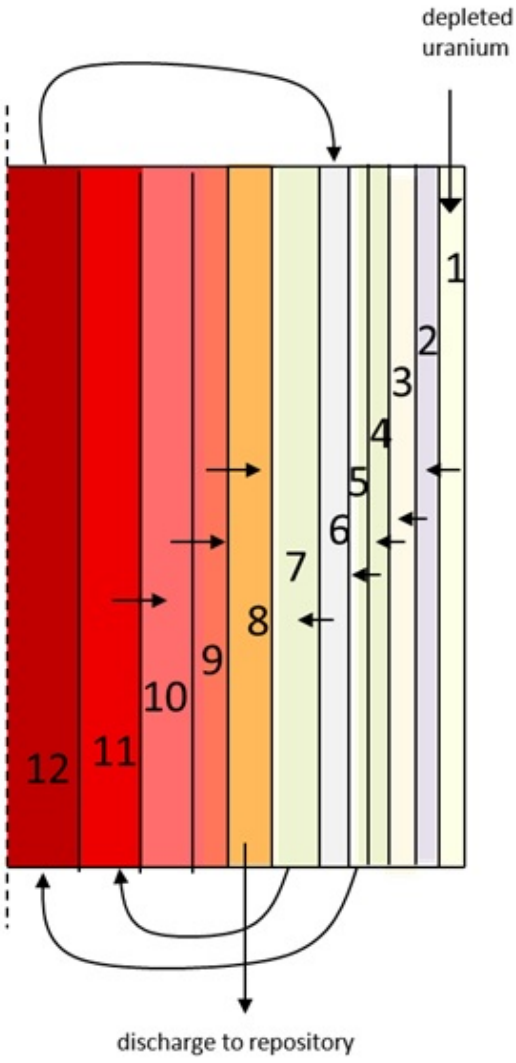

Figure 3.4: Shuffling scheme of the 20% B&B reactor; depleted uranium is charged in batch 1 and shuffled according to the arrows.

Table 3.2: Dimensions and compositions of the regions of B&B reactors [13].

Region	Height (cm)	Thickness (cm)	Material (Volume %)	T [K]
Upper reflector	34.93	242.2	50% HT9- 50% Na	783
Upper end plug	2.54	201.36	22% HT9 - 78% Na	783
Plenum	209.36	201.36	22% HT9 - 28% Na	783
Enriched fuel	209.36	142.38	37.5% Fuel - 22% HT9 - 28% Na	800
Blanket	209.36	58.98	37.5% Fuel - 22% HT9 - 28% Na	800
Lower end plug	90.42	201.36	22% HT9 - 78% Na	628
Grid plate	5.18	242.2	50% HT9 - 50% Na	628
Coolant inlet	60	242.2	22% HT9 - 78% Na	628
Lower shield	20	242.2	43.1% B4C - 29.7% HT9 - 27.2% Na	628
Radial reflector	511.58	40.84	50% HT9 - 50% Na	628
Radial shield	631.79	20.5	43.1% B4C - 29.7% HT9 - 27.2% Na	628

at least two times before final discharge from the reactor. The reprocessed batches are batch #4 and in batch #6, where the fuel reaches at the end of cycle, 20% and 41.4% FIMA, respectively. The recycling process chosen can be the melt-refining or AIROX process.

3.3 B&B waste characteristics

The purpose of this section is to compare waste characteristics of B&B reactors which discharge their fuel at the bounding burnup levels, 20% and 55%. The following fuel reconditioning scenarios are examined for the 55% reactor:

- Melt refining whenever 20% BU is reached.
- Melt refining whenever 20% BU is reached; the recovery efficiency of all actinides is 99%; 1% lost in the crucible.
- Melt refining whenever 20% BU is reached; the recovery efficiency of all actinides is 90%; 10% lost in the crucible.
- AIROX reprocessing whenever 20% BU is reached, using the reference AIROX recovery efficiency The 20% reactor is assumed to discharge its fuel without reconditioning. The melt refining (MR) and AIROX

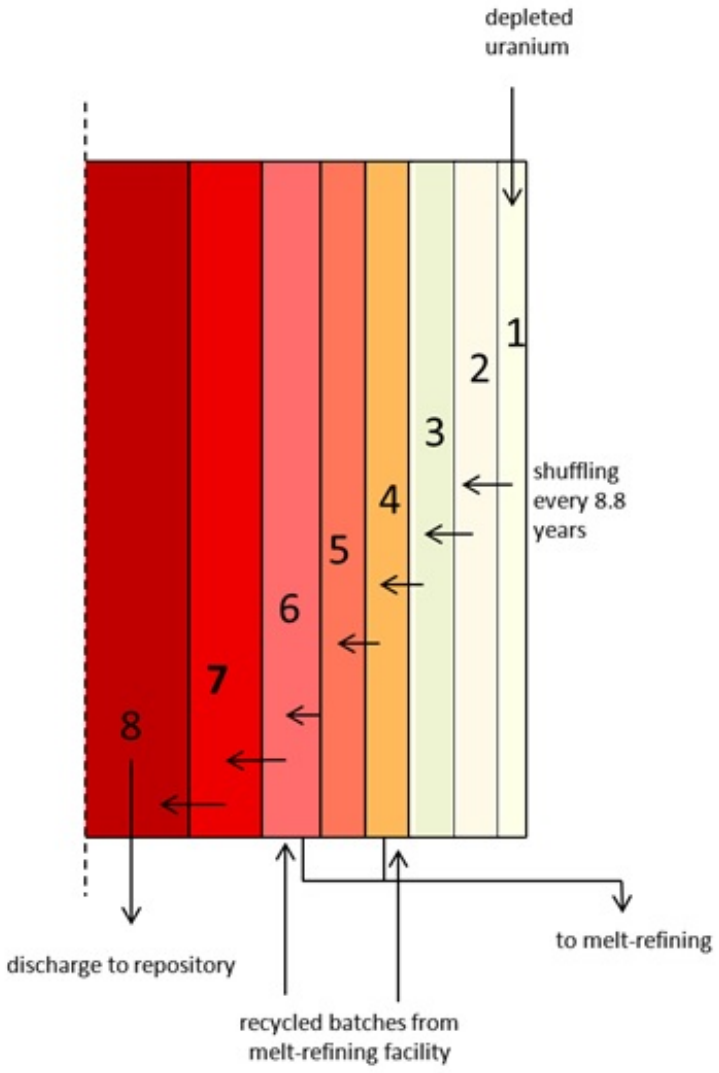

Figure 3.5: Shuffling scheme of the 55% B&B reactor; depleted uranium is charged in batch 1 and shuffled inward to the inner batch, where it is discharged after reaching 55% FIMA. Batch #4 and #6 are sent to the melt-refining facility and substituted with recycled batches.

recovery fractions were discussed in Chapter 2 and are reported in Table 2.6.

The characteristics of the B&B waste are compared to those of other three reference systems:

- a PWR operating on the once-through cycle;
- a sodium-cooled Advanced Burner Reactor (ABR) having a conversion ratio of CR=0.5 [41] and,
- an Advanced Recycling Reactor (ARR) having a conversion ratio CR=1 [41].

The reference PWR uses 4.5% enriched fuel up to 50,000 MWd_{th}/MT_{HM}, while the ABR and ARR wastes are derived from ANL data for reactor at equilibrium assuming 99% recovery of actinides in the recycling process (possibly a pyro-metallurgical fuel reprocessing). Fuel from ABR and ARR is discharged with a burnup of, respectively, 73,000 MWd_{th}/MT_{HM} and 131,900 MWd_{th}/MT_{HM} [41]. Table 3.3 summarizes the burn-up characteristics of the reactor systems inter-compared. For B&B reactors, it is also assumed that 75% of the gaseous FPs generated in the B&B reactor fuel migrate out from the fuel and accumulates in the fission-gas plenum. The gaseous fission products that are removed this way are: H, He, N, O, F, Ne, Cl, Ar, Kr, Xe and Rn.

Table 3.3: Burnup and thermal conversion efficiency of studied reactors.

	PWR	55% B&B	20% B&B	ARR	ABR
final burnup (MWd_{th}/MT)	50,000	540,930	189,455	73,000	131,900
Fuel cycle	Once-thru	Once-thru via reconditioning	Once-thru	Recycled	Recycled
thermal conversion efficiency	33%	40%	40%	40%	40%

As depleted uranium is charged into the reactor and recycling takes place at the pre-determined steps, the reactor reaches an equilibrium composition.

It is assumed that the MCNP calculated one group cross-sections at equilibrium, using reference melt-refining, do not vary when using other recycling processes, so that it is possible to use one-group cross-sections previously calculated in all the scenarios. In fact, the one-group cross sections for each single nuclide vary weakly with the reactor composition, while composition varies only of about 10% between a scenario and another. We will therefore assume cross-sections independent of the actinide fraction lost and of the specific recycling process, being melt refining or AIROX. This approximation can be justified based on the results of chapter 2 for AIROX, melt refining operating at reference recovery fractions and with 1% actinides losses, as the resulting burnup are all very close, from 54% to 58%. For the 10% losses this assumption is only a preliminary assessment to compare with the 1% scenario. It is to be added that 10% losses is a large upper bound estimate, and a recycling process with 10% losses would be highly inefficient, and it would necessitate make-up fuel as well.

For each fuel cycle, a mass flow of materials is established at equilibrium. Tables 3.4 , 3.5, 3.6, 3.7, 3.8 summarize the fuel specific mass flow, in Kg/GW_eY, for each of the reactor systems examined. Included in the tables are the important actinides as well as ^{90}Sr and Cs which are responsible for most of the short-term radio-toxicity and decay heat of the waste, as seen in the following sections. The data shown in these tables is for the equilibrium composition cores; it does not include the initial fissile fuel feed that is required for start-up of a new B&B reactor. The mass flow is attained normalizing the feed and the materials discharged from the reactor at the beginning and end of each cycle to the energy produced during the cycle.

Figure 3.6 shows the flow streams for the 55% B&B reactor. Every 8.8 years batch # 8 is discharged at 55% FIMA and melt-refining or AIROX waste streams are generated from the reprocessing of batch #4 and #6. The latter include the waste stream of gaseous FPs; their mass is 6% of the initial fuel mass. The total produced waste is normalized to the electrical energy production during the cycle (in this case 540,930 $MW_{th}d/MT$ or 216,372 MW_ed/MT). For the ARR and ABR the waste stream consists of only the FPs and unrecovered actinides (1% loss) each time the fuel is recycled. The waste stream for the PWR and 20% B&B reactor is just the discharged fuel.

Table 3.9 compares selected fuel cycle characteristics of the reactor systems excluding that of the ABR the primary mission of which – LWR TRU transmutation, is different. It is observed that the B&B cores feature the lowest specific HM loading i.e., the heavy metal that needs to be loaded into

Table 3.4: Mass flow in kg/GW_eY of PWR, 20% B&B. The streams of B&B reactor are: discharge, i.e. the discharged fuel, MR waste, i.e. waste from melt-refining process, and gas FP, i.e. the gaseous fission products accumulated in the plenum.

	PWR		B&B-20%		
	charge	discharge	charge	discharge	gas FP
mass	2.21E+04	2.21E+04	4.82E+03	4.72E+03	9.78E+01
U	2.21E+04	2.07E+04	4.82E+03	3.41E+03	-
Pu		2.25E+02	-	4.76E+02	-
Np		1.86E+01	-	3.49E+00	-
Am		5.38E+00	-	1.43E+00	-
Cm		2.03E+00	-	1.30E-01	-
U-235	9.95E+02	1.56E+02	9.64E+00	7.17E-01	-
Pu-238		6.97E+00	-	1.70E+00	-
Pu-239		1.10E+02	-	3.80E+02	-
Pu-240		5.89E+01	-	8.55E+01	-
Pu-241		3.31E+01	-	8.05E+00	-
Pu-242		1.59E+01	-	1.31E+00	-
Am-241		1.49E+00	-	1.24E+00	-
Np-237		1.73E+01	-	2.94E+00	-
Cm-245		6.03E-02	-	5.25E-03	-
Sr-90		1.75E+01		7.05E+00	-
Cs		9.44E+01		9.62E+01	-
U-235/U	4.50%	0.75%	0.20%	0.02%	-
HM		2.21E+04	-	3.89E+03	-
TRU		1.39E+03	-	4.81E+02	-
TRU/HM		6.29%	-	12.37%	-
Fiss. Pu		1.43E+02	-	3.88E+02	-
Fiss. Pu/HM		0.65%		9.97%	-
Fiss. Pu/Pu		63.69%		81.43%	-

Table 3.5: Mass flow in kg/GW_eY of 55% B&B reactor (reference recovery). The streams of B&B reactor are: discharge, i.e. the discharged fuel, MR waste, i.e. waste from melt-refining process, and gas FP, i.e. the gaseous fission products accumulated in the plenum.

	B&B-55%			
	charge	discharge	MR waste	gas FP
mass	1.69E+03	1.23E+03	3.56E+02	9.64E+01
U	1.69E+03	6.24E+02	-	-
Pu	-	1.30E+02	-	-
Np	-	7.23E-01	-	-
Am	-	2.24E+00	2.29E+00	-
Cm	-	3.95E-01	-	-
U-235	3.37E+00	4.92E-02	-	-
Pu-238	-	1.27E+00	-	-
Pu-239	-	8.18E+01	-	-
Pu-240	-	3.98E+01	-	-
Pu-241	-	4.59E+00	-	-
Pu-242	-	2.35E+00	-	-
Am-241	-	1.79E+00	1.90E+00	-
Np-237	-	6.61E-01	-	-
Cm-245	-	4.40E-02	-	-
Sr-90	-	1.59E+00	4.62E+00	-
Cs	-	2.31E+01	7.01E+01	-
U-235/U	0.20%	0.01%	-	-
HM	-	7.57E+02	2.29E+00	-
TRU	-	1.33E+02	-	-
TRU/HM	-	17.58%	-	-
Fiss. Pu	-	8.64E+01	-	-
Fiss. Pu/HM	-	11.41%	-	-
Fiss. Pu/Pu	-	66.55%	-	-

Table 3.6: Mass flow, in kg/GWeYr, of three variants of 55% B&B reactor: 1) MR with 1% actinides lost in the process; 2) MR with 10% loss; and 3) using AIROX reprocessing. 2) and 3) are reported in Table 3.7.

		B&B-55% - 1% rec.		
	charge	discharge	MR waste	gas FP
mass	1.69E+03	1.21E+03	3.79E+02	9.64E+01
U	1.69E+03	6.04E+02	2.00E+01	-
Pu	-	1.26E+02	3.16E+00	-
Np	-	7.02E-01	2.20E-02	-
Am	-	2.17E+00	2.27E+00	-
Cm	-	3.99E-01	3.12E-03	-
U-235	3.37E+00	4.73E-02	2.81E-03	-
Pu-238	-	1.24E+00	1.85E-02	-
Pu-239	-	7.93E+01	2.34E+00	-
Pu-240	-	3.88E+01	7.10E-01	-
Pu-241	-	4.51E+00	7.37E-02	-
Pu-242	-	2.33E+00	2.13E-02	-
Am-241	-	1.73E+00	1.88E+00	-
Np-237	-	6.39E-01	1.92E-02	-
Cm-245	-	4.47E-02	2.40E-04	-
Sr-90	-	1.59E+00	4.62E+00	-
Cs	-	2.30E+01	7.01E+01	-
U-235/U	0.20%	0.01%	0.01%	-
HM	-	7.34E+02	2.54E+01	-
TRU	-	1.30E+02	5.46E+00	-
TRU/HM	-	17.66%	21.47%	-
Fiss. Pu	-	8.38E+01	2.41E+00	-
Fiss. Pu/HM	-	11.42%	9.49%	-
Fiss. Pu/Pu	-	66.40%	76.29%	-

Table 3.7: Mass flow, in kg/GWeYr, of two variants of 55% B&B reactor: 1) MR with 10% loss; and 2) using AIROX reprocessing. Charge is same as in Table 3.7.

	B&B-55% - 10%			B&B-55% AIROX		
	discharge	MR waste	gas FP	discharge	waste	gas FP
mass	1.02E+03	6.72E+02	9.65E+01	1.36E+03	2.28E+02	9.61E+01
U	4.40E+02	1.89E+02	-	6.25E+02	-	-
Pu	9.52E+01	3.00E+01	-	1.31E+02	-	-
Np	5.20E-01	2.09E-01	-	7.33E-01	-	-
Am	1.61E+00	2.09E+00	-	2.49E+00	-	-
Cm	4.40E-01	3.25E-02	-	5.02E-01	-	-
U-235	3.12E-02	2.71E-02	-	5.36E-02	-	-
Pu-238	9.49E-01	1.73E-01	-	1.50E+00	-	-
Pu-239	5.81E+01	2.21E+01	-	8.20E+01	-	-
Pu-240	3.03E+01	6.73E+00	-	4.01E+01	-	-
Pu-241	3.79E+00	7.09E-01	-	4.62E+00	-	-
Pu-242	2.09E+00	2.09E-01	-	2.47E+00	-	-
Am-241	1.21E+00	1.72E+00	-	1.97E+00	-	-
Np-237	4.58E-01	1.81E-01	-	6.70E-01	-	-
Cm-245	5.24E-02	2.63E-03	-	6.07E-02	-	-
Sr-90	1.59E+00	4.62E+00		3.33E+00		
Cs	2.27E+01	6.99E+01		2.30E+01	6.55E+01	
U-235/U	0.01%	0.01%	-	0.01%	-	-
HM	5.38E+02	2.22E+02	-	7.59E+02	-	-
TRU	9.78E+01	3.24E+01	-	1.34E+02	-	-
TRU/HM	18.18%	14.60%	-	17.71%	-	-
Fiss. Pu	6.19E+01	2.28E+01	-	8.66E+01	-	-
Fiss. Pu/HM	11.51%	10.31%	-	11.41%	-	-
Fiss. Pu/Pu	65.01%	76.25%	-	66.30%	-	-

Table 3.8: Mass flow, in kg/GWeYr, of the ABR and ARR

	ARR		ABR	
	Charge	Discharge	Charge	Discharge
U	1.04E+04	9.46E+03	4.47E+03	3.94E+03
Pu	1.62E+03	1.65E+03	1.98E+03	1.60E+03
Np	1.10E+01	1.20E+01	4.80E+01	2.70E+01
Am	3.50E+01	3.30E+01	1.42E+02	1.16E+02
Cm	9.00E+00	1.00E+01	6.50E+01	6.80E+01
U-235	4.00E+00	2.00E+00	3.00E+00	2.00E+00
Pu-238	1.80E+01	1.80E+01	7.40E+01	6.40E+01
Pu-239	1.07E+03	1.09E+03	8.61E+02	6.54E+02
Pu-240	4.43E+02	4.50E+02	6.86E+02	5.94E+02
Pu-241	5.40E+01	5.70E+01	1.44E+02	1.03E+02
Pu-242	3.70E+01	3.70E+01	2.09E+02	1.82E+02
Am-241	2.30E+01	2.10E+01	7.00E+01	5.10E+01
U-235/U	0.04%	0.03%	0.08%	0.06%
HM	1.21E+04	1.12E+04	6.70E+03	5.75E+03
TRU	1.68E+03	1.70E+03	2.23E+03	1.81E+03
TRU/HM	13.86%	15.25%	33.26%	31.43%
Fiss. Pu	1.13E+03	1.14E+03	1.01E+03	7.57E+02
Fiss. Pu/HM	9.30%	10.24%	15.00%	13.16%
Fiss. Pu/Pu	69.33%	69.35%	50.92%	47.39%

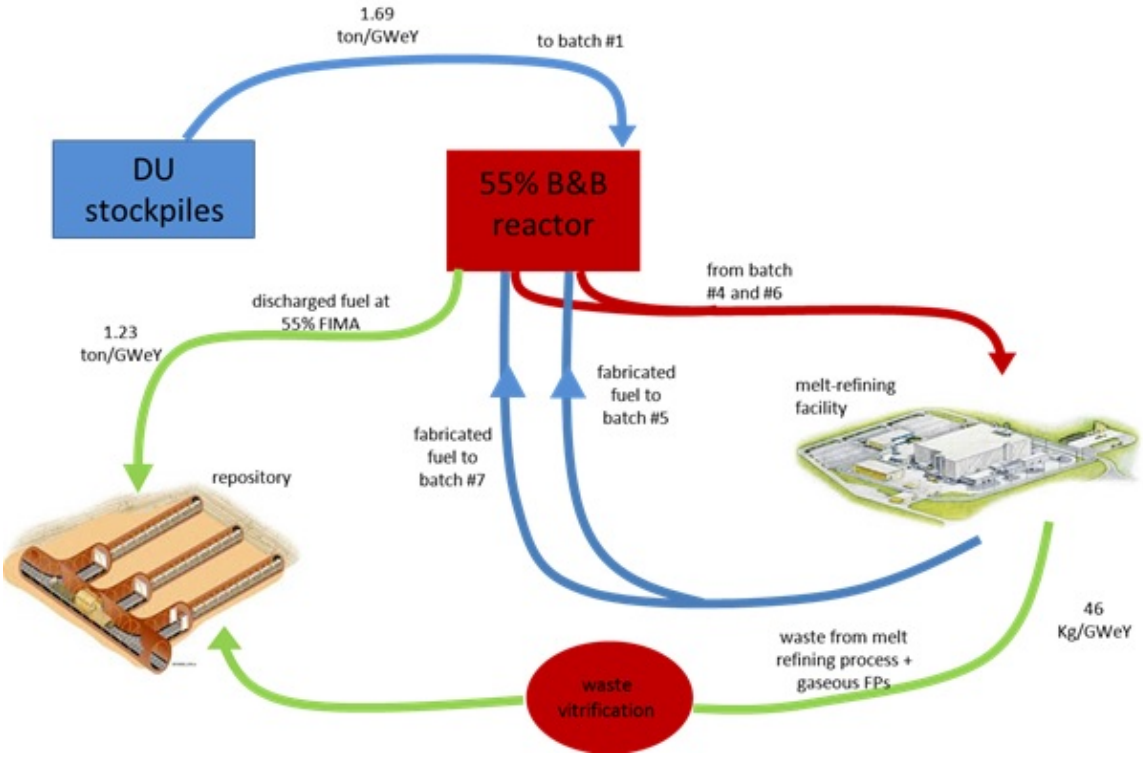

Figure 3.6: Fuel cycle of the 55% B&B reactor.

the core per unit of electricity the core generates.

The natural (depleted, in case of the fast reactors) uranium utilization of the B&B reactors far exceeds that of the PWR but do not match that attainable in fast breeder reactors that recycle their fuel, after reprocessing, unlimited number of times.

On the other hand, the specific inventory of fissile plutonium discharged from the B&B cores is significantly smaller than that discharged from the ARR. The fissile Pu specific inventory of the 55% B&B is even smaller than that of the PWR. The fissile Pu isotopes (239+241) fraction in the plutonium in the fuel discharged from the 55% B&B core is only slightly higher than that from PWR, but slightly lower than that of the ARR. However, the 20% B&B discharged fuel has a significantly higher fissile Pu fraction.

Relative to a PWR, the net amount of plutonium accumulated per GWe-Year of electricity generated in close to one-half for the 55% B&B reactor, but approximately double in case of the 20% B&B reactor. There is practically no Pu accumulation in the ARR, while there is a net plutonium destruction in the ABR.

Table 3.9: Comparison of selected fuel cycle characteristics of the 20% B&B, 55% B&B, ARR and PWR

Characteristic	PWR	ARR	20% B&B	55% B&B
HM loading (Kg/GWeY)	2.21E+4	1.25E+4	4.72E+3	1.69E+3
fuel type	Enriched U	Recy U+TRU	Depleted U	Depl+Recon U
uranium utilization (%)	0.6	>99	20	55
fis. Pu discharge (Kg/GWeY)	143	1140	388	86
fis. Pu/ tot. Pu (%)	63.7	69.3	81.4	66.6
Pu generated (Kg/GWeY)	224	∼0	477	129

The following sections compare additional waste characteristics of the reactor systems examined.

3.4 Ingestion radiotoxicity

The ingestion radiotoxicity is the main measure to assess the hazard of the waste from a nuclear fuel cycle. It is a measure of how much the waste needs to be diluted in water so that it is not dangerous for the population.

This section compares the specific ingestion radiotoxicity of the 5 reactor systems; it is measured in m^3 of water by which the waste generated per GW_eYr of generated electricity needs to be diluted. Figure 3.7 compares the total radiotoxicity of the fuel and waste streams discharged from the different reactor systems examined. Time zero is taken to be the moment of fuel discharged from the core and, in case of the 55% B&B reactor, the associated waste streams from fuel reconditioning. No cooling time and no reprocessing time are assumed. In this way it is possible to fairly assess the different reactor systems and fuel cycles, independently from the particular reprocessing technology used. In fact, different cooling times might be needed for the different technologies inter-compared. Since the discharged fuel and waste streams need to be managed from the moment they are created, an analysis without a cooling time will show up the intrinsic differences between the characteristics of the waste from the different reactor systems.

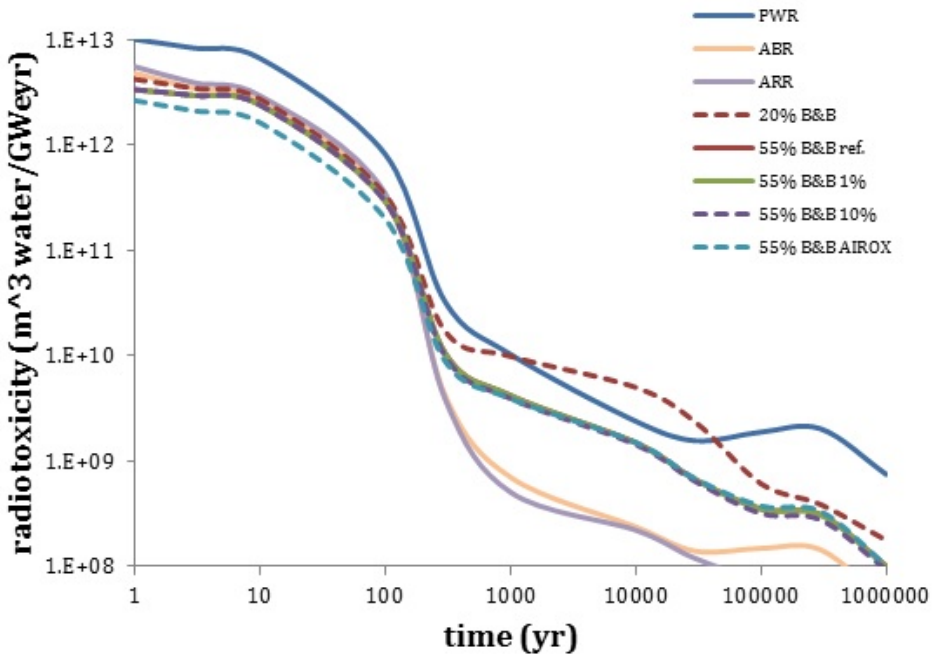

Figure 3.7: Total specific radiotoxicity for the studied reactor fuel cycles

Figure 3.8 shows that the total specific radiotoxicity of all the fast reactor

systems examined is smaller than that of PWR with one exception - the radiotoxicity of the 20% B&B reactor around the 10,000 year time range. This is due, in particular, to the contribution of ^{239}Pu – the specific ^{239}Pu content in the 20% B&B reactor discharged fuel is ∼3.5 times that in PWR. The 55% B&B reactor has a lower long-term specific radiotoxicity because their specific ^{239}Pu and other TRU inventories are smaller. Notice that the specific radiotoxicity of all four 55% B&B scenarios is very similar. This is due to the fact that the sum of the actinides in the discharged fuel and in the reconditioning process waste stream is practically the same, regardless of the fraction that remains in the reconditioning waste streams. The specific radiotoxicity of both the ARR and ABR fast reactors is significantly lower, after several hundred years, than the specific radiotoxicity of all the other systems. This low long-term radiotoxicity level is due to the fact that these reactors keep recycling all their actinides, with the exception of 1% that gets to the reprocessing waste stream. Up to several hundred years from discharge, the specific radiotoxicity of all the B&B reactors is very similar to that of the ARR and ABR with the exception of the 55% B&B scenario that recondition its fuel using an AIROX-like process; the latter is smaller. The lower short-term specific radiotoxicity of the 55% B&B reactor that reconditions its fuel using an AIROX process is due to the fact that the AIROX process does not separate ^{90}Sr from the fuel while the melt-refining process does. As shown in Figure 3.9, ^{90}Sr is the dominant contributor to the short term radiotoxicity of both the PWR and the reference 55% B&B reactor (which uses the melt-refining process). In the 55% AIROX scenario the Sr is recycled with the fuel back to the core. As long as ^{90}Sr resides in the core, it does not contribute to the radiotoxicity of the waste streams and discharged fuel. While in the core the ^{90}Sr keeps decaying and, as illustrated in Figure 3.9, its concentration levels off towards an equilibrium value. The sum of the three ^{90}Sr peaks in MR fuel cycle shown in Figure 3.9, makes the ^{90}Sr inventory in MR waste. This sum is significantly larger than the amount of ^{90}Sr inventory discharged with the fuel that is reconditioned with the AIROX process. The inventory differences are also reported in Table 3.6 - the specific ^{90}Sr discharge with the MR process is nearly twice that in the AIROX process.

Strontium-90 is also responsible for the higher short-term radiotoxicity of the PWR discharged fuel. As shown in Figure 3.9, the ^{90}Sr build-up rate in PWR fuel is higher than in fast reactors. Contributing to this difference are the relative short fuel residence time (relative small fraction of the ^{90}Sr decays before fuel discharge, different fission yield, as well as smaller thermal

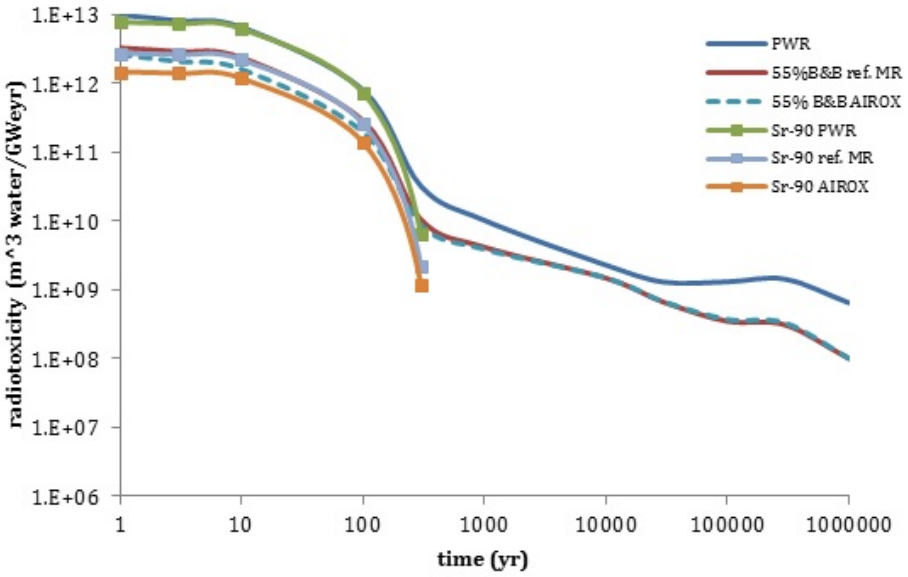

Figure 3.8: Total radiotoxicity and ^{90}Sr-only radiotoxicity for PWR once-through, 55% B&B AIROX, and 55% B&B using reference MR. It is shown that, for PWR and MR, ^{90}Sr radiotoxicity is the major component of total short-term radiotoxicity.

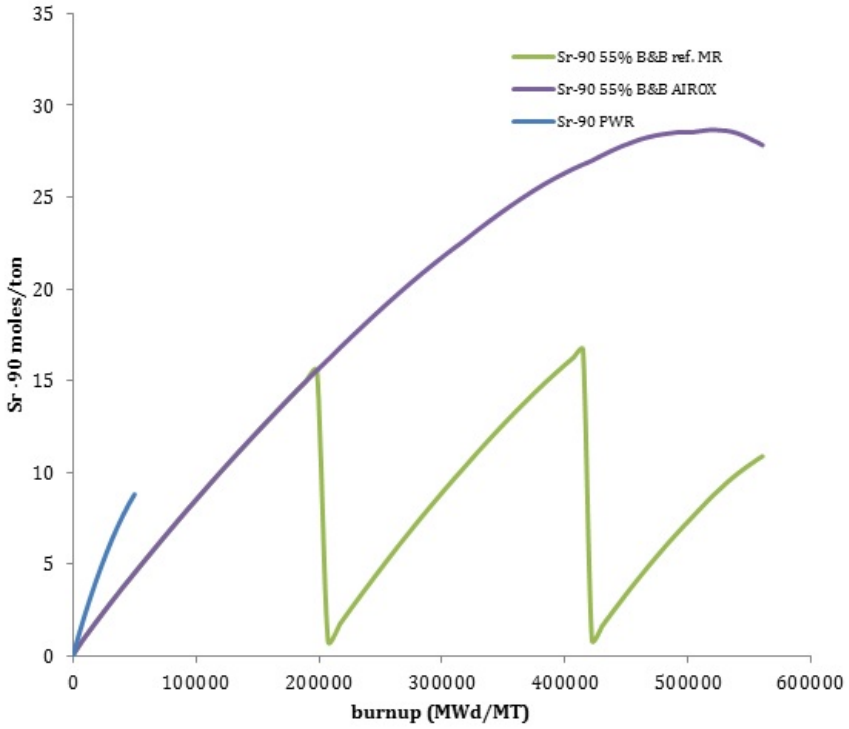

Figure 3.9: ^{90}Sr concentration evolution with burn-up in PWR, 55%B&B ref. MR and AIROX cycle.

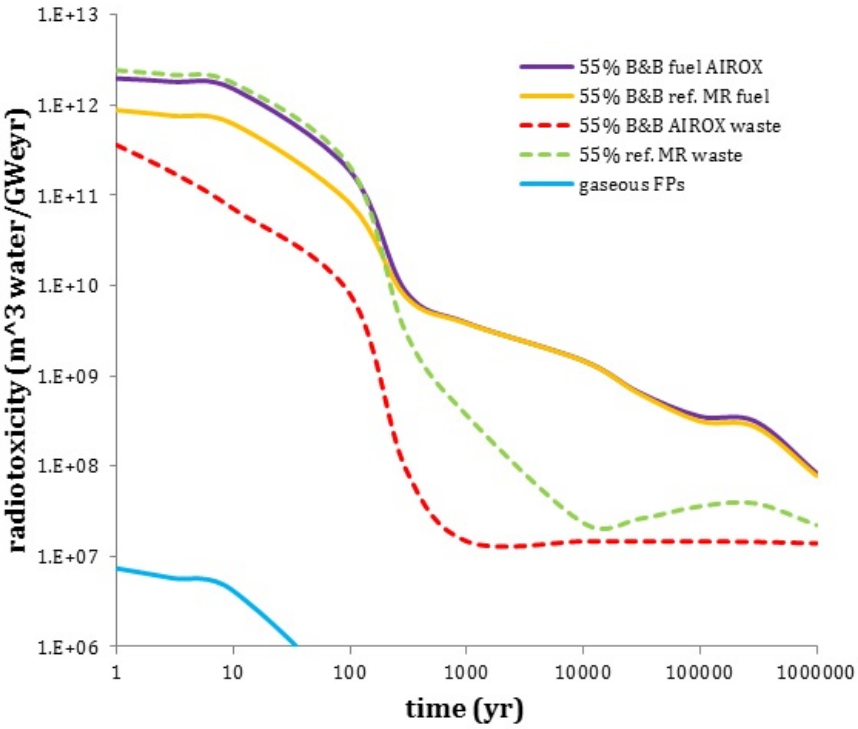

Figure 3.10: Radiotoxicity components of the 55% B&B reactor system using either MR or AIROX reconditioning.

conversion efficiency). Figure 3.12 shows the contribution of the discharged fuel and of the waste streams for the two 55% B&B reactor systems one using the reference melt-refining and the other using AIROX for fuel reconditioning. In the long term, the discharged fuel for AIROX and MR has essentially the same radiotoxicity. However, in the short term, most of the radiotoxicity of the reference MR system comes from the MR waste stream (dashed green line) rather than discharged fuel (yellow line); this is due mostly to the ^{90}Sr that ends up in this stream. With AIROX reconditioning, the trend is the opposite - the discharged fuel (purple solid line) has a higher radiotoxicity than the waste stream (dashed red). The radiotoxicity contribution of the gaseous FPs, also shown in Fig. 3.10, is negligible compared to the other contributions; it will be neglected in all the subsequent analysis.

The effect of different recovery efficiencies in the melt refining on the radiotoxicity contribution of the Melt-refining waste (MRW) and of the discharged fuel is shown is Figure 3.11. It is observed that the discharge fuel radiotoxicity is the same for all the 3 cases in the short term but somewhat differ in the long-term it is lower for the 10% loss fraction. This is expected since nearly 30% of the actinides end up in the waste stream. As a summary of this section, Figure 3.12 plots the ratio of the total radiotoxicity of each of the fast reactor systems examined to the of the PWR radiotoxicity. The 55% reference MR B&B reactor represents the other 55% B&B reactors, since the total radiotoxicity of all these systems is very close. It is concluded that with fuel reconditioning, the specific radiotoxicity of B&B reactors can be lower than that of a once-through PWR while the uranium utilization the B&B reactors offer is higher by up to 2 orders of magnitude. Without fuel reconditioning the radiotoxicity of the B&B reactors is comparable to that of the PWR – it is approximately half the PWR radiotoxicity up to $\sim$ 200 years and up to twice as much 10,000 years from discharge. The 20% B&B reactor offers, though, nearly 40 times the PWR uranium utilization and requires a very small fraction of the PWR uranium enrichment capacity.

3.5 Decay heat

The total decay heat from the discharged fuel and waste streams from the analyzed reactor systems is compared in Figure 3.13. The overall trend is similar to that of the radiotoxicity; there is no significant difference for the total decay heat of the 55% reactors, using MR with different recovery

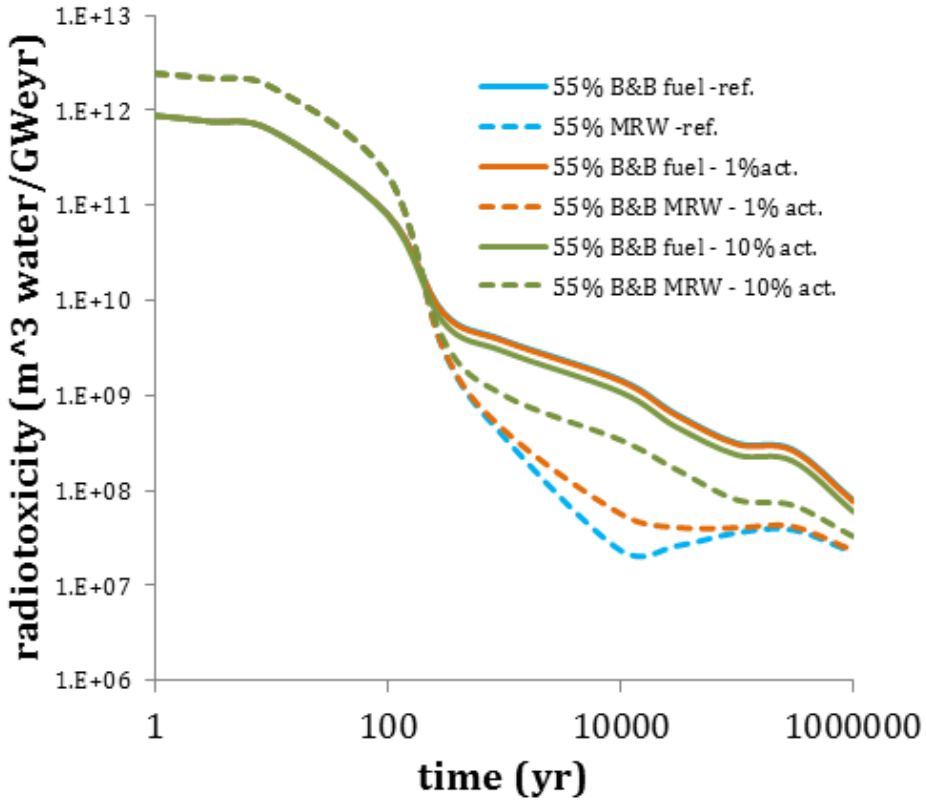

Figure 3.11: Radiotoxicity MR 55% B&B cycles, using different recovery efficiency. Melt-refining waste (MRW) is plot together with discharged fuel for reference recoveries and 1% and 10% actinides lost in waste.

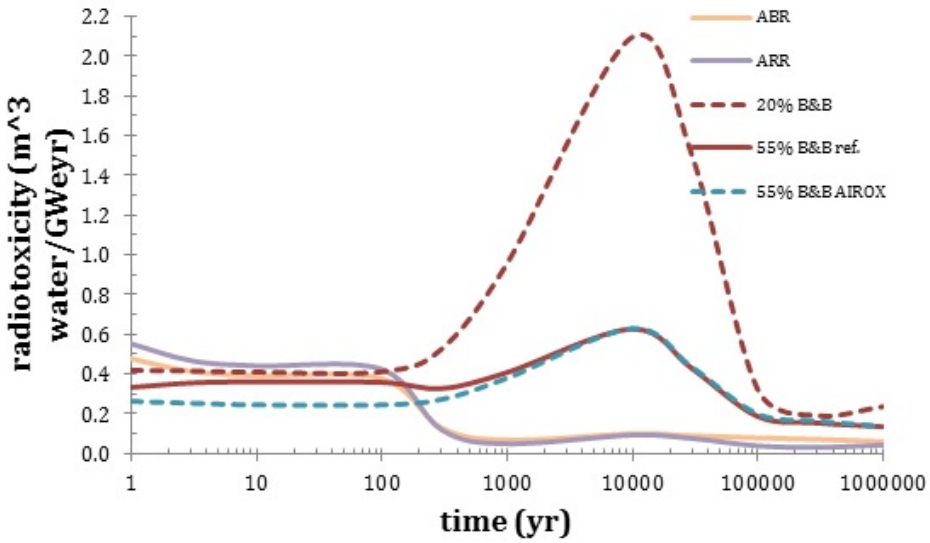

Figure 3.12: Radiotoxicity of the various fuel cycles as a ratio to PWR once-through radiotoxicity

efficiencies. The specific decay heat of all fast reactor systems is smaller than that of the PWR with the exception of the 20% B&B reactor system that has a higher decay heat around the 10,000 years. In the short term, the B&B reactors specific decay heat is even somewhat smaller than that of the ARR and ABR but after $\sim$ 100 years the ARR and ABR specific decay heat becomes significantly smaller. This is again attributed to the low amount of actinides that get into the ARR and ABR waste stream combined with lack of discharged fuel for disposal.

Figure 3.14 shows the difference in the decay heat of the 55% B&B reactor systems when using the MR versus the AIROX process for fuel reconditioning. The discharged fuel decay heat is essentially the same but there is a significant difference in the decay heat emitted by the waste streams – the AIROX waste stream specific decay heat is higher in the short-term but gets significantly lower after $\sim$ 100 years. This difference is due to the actinide contribution that is only present in melt-refining waste. Figure 3.15 shows the effect of the MR recovery fraction on the 55% B&B system decay heat. Very small difference is observed in the short term decay heat from the waste

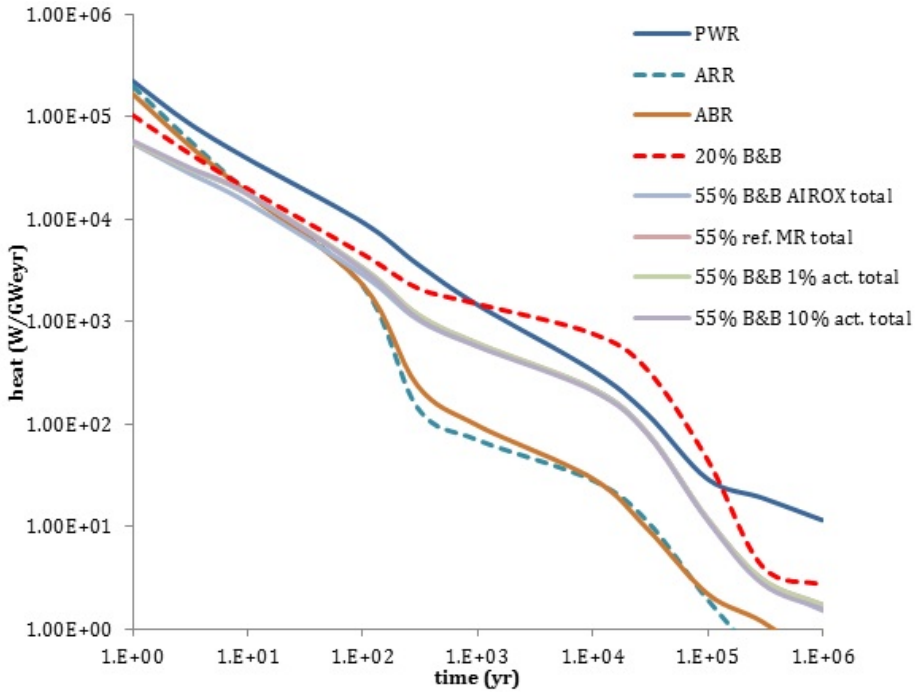

Figure 3.13: Total specific decay heat of analyzed fuel cycles

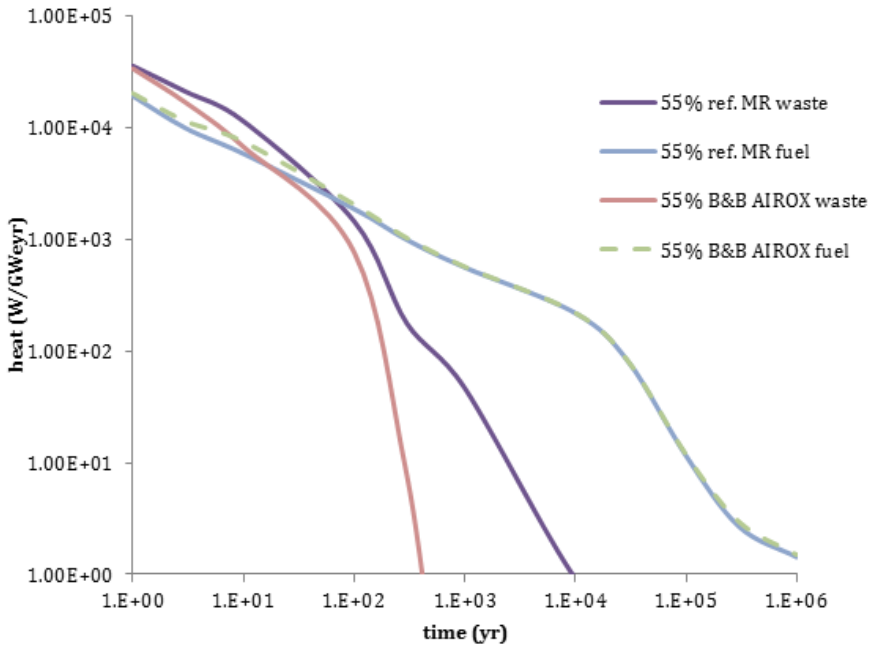

Figure 3.14: Specific decay heat of the reference 55% B&B reactor system using the melt-refining and AIROX reconditioning

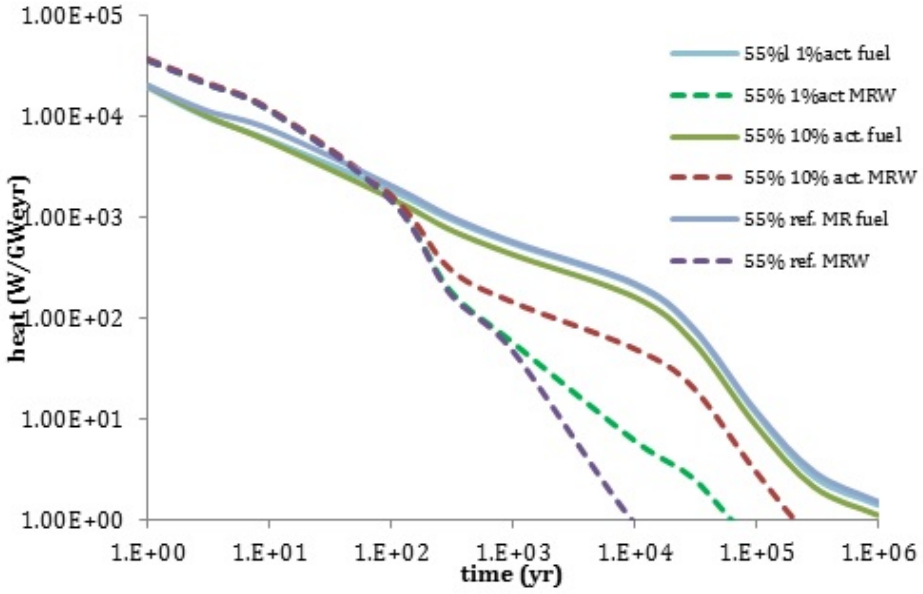

Figure 3.15: Effect of recovery efficiency on the decay heat of the discharged fuel and waste streams from the 55% B&B reactor systems

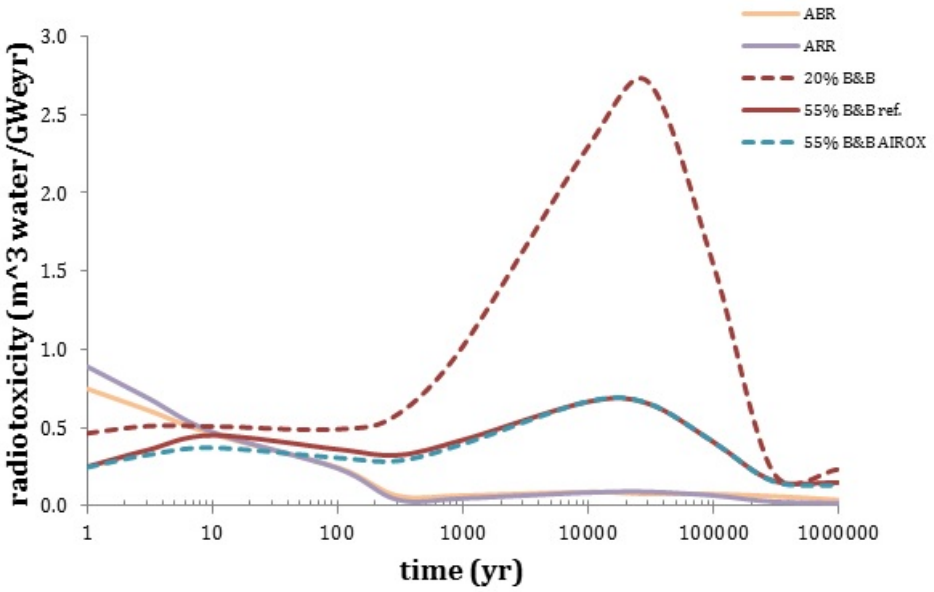

Figure 3.16: Decay heat of the various fuel cycles as a ratio to PWR once-through radiotoxicity.

streams but the difference becomes significant in the long time range when the majority of the heat comes from actinides decay. Figure 3.16 shows the decay heat as a ratio of decay heat of PWR. It is observed that the 55% B&B reactors have significant less decay heat than PWR. On the other side, the 20% B&B reactor has a significant higher decay heat than PWR, still due to the high content of ^{239}Pu.

3.6 Proliferation resistance

The proliferation resistance of the fuel and of the waste discharged from the B&B reactor systems examined is compared against that of the fuel and waste discharged from the reference PWR, ARR and ABR systems using a recently proposed Figure of Merit, [42–44].

$$FOM = 1 - log_{10}\left(\frac{M}{800} + \frac{Mh}{4500} + \frac{M}{50}\left[\frac{D}{500}\right]^{\frac{1}{log_{10}2}}\right) \tag{3.1}$$

where M is the bare critical mass in kg, h is the heat content in W/kg, and D is the dose rate of 0.2×M evaluated at 1 m from the surface in rad/h. The more negative the FOM is, the higher is the proliferation resistance of the fuel.

A fuel is considered to be proliferation resistant if its FOM value is negative; the more negative the more proliferation resistant the fuel is; and vice versa – the larger positive, of more proliferation concern the material is. The values of critical mass are calculated as a weighted average of the mass reported in Table 3.10.

Tables 3.11 and 3.12 give the relative composition of the actinides in the discharged fuel and in the waste streams of each of the reactors systems examined. Table 3.11 also compares the FOM of the TRU present in each of these systems. It is found that none of the B&B reactor systems have negative FOM, although the 55% B&B discharged fuel comes very close to it. The FOM strongly depends on the mass percent of fissile Pu. As this is highest in the 20%B&B reactor, this reactor fuel features the highest FOM. The reference 55% B&B MR waste stream has the smallest FOM of -3.17. This is due to the fact that this waste stream has only a very little amount of TRU, consisting only of the 95% Th and Am that remains stuck to the crucible.

Table 3.10: Nuclide data for FOM calculations

Isotope	M(kg)	Mh(W)	Dose(rad/h @ 1 m for 0.2M)	FOM
227Ac	>5E11			
228Th	>6E11			
229Th	2780.3	1.69E4	6.18E0	0.1
230Th	>6E11			
232Th	>6E11			
231Pa	>1E12			
232Pa	105.3	2.96E8	3.64E8	-18.8
233Pa	>6E10			
232U	6.7	4.76E3	2.82E-1	1.0
233U	15.3	4.30E0	1.46E-4	2.7
234U	126.1	2.26E1	3.59E-4	1.8
235U	46.5	2.79E-3	1.04E-5	2.2
236U	>1E12			
238U	>1E11			
236Np	7.0	1.88E-1	1.10E-2	3.1
237Np	62.8	1.26E0	4.69E-4	2.1
236Pu	7.2	1.31E5	6.98E0	-0.5
238Pu	9.7	5.51E3	2.11E-1	0.9
239Pu	10.0	1.92E1	3.95E-4	2.8
240Pu	37.3	2.64E2	7.17E-3	2.0
241Pu	13.0	4.27E1	1.45E-3	2.6
242Pu	89.1	1.04E1	5.45E-3	1.9
244Pu	256.2	1.29E-1	1.50E-2	1.5
241Am	57.3	6.55E3	1.22E0	0.8
242Am	10.9	1.01E7	1.29E5	-6.4
242mAm	11.7	4.94E1	2.74E-1	2.6
243Am	144.8	9.30E2	2.82E-1	1.4
242Cm	368.2	4.45E7	8.55E2	-3.0
243Cm	11.9	2.25E4	1.37E2	0.3
244Cm	27.1	7.66E4	1.40E1	-0.2
245Cm	9.5	5.43E1	1.47E-1	2.6
246Cm	49.4	4.93E2	1.67E1	1.8
247Cm	8.4	2.42E-2	1.62E-3	3.0
248Cm	42.5	5.06E0	7.25E1	2.2
250Cm	24.8	3.66E3	5.04E3	-2.0
249Bk	193.7	6.20E4	7.49E-1	-0.1
249Cf	7.2	1.10E3	5.36E1	1.6
250Cf	6.6	2.64E4	2.95E3	-0.7
251Cf	5.6	3.16E2	1.59E0	2.1
252Cf	5.8	1.12E5	5.77E5	-8.2

Table 3.11: Fraction of TRU nuclides to the total TRU in each waste stream and Figure of Merit for each waste stream; *fuel* indicates the discharged assembly; MRW indicates the Melt Refining Waste stream; *ref.* indicates melt refining with reference removal fractions for melt refining and *act.* indicates melt refining with the specified percent of actinide losses.

Nuclide	PWR	AIROX	1% act. fuel	1% act. MRW	10% act. fuel	10% act. MRW
NP236	1.45E-09	6.92E-10	3.36E-10	3.58E-10	4.29E-10	6.19E-10
NP237	6.93E-02	6.28E-03	4.93E-03	3.41E-03	4.69E-03	5.57E-03
PU236	2.08E-07	1.76E-07	1.20E-07	9.15E-08	1.33E-07	1.53E-07
PU238	2.79E-02	6.22E-03	9.55E-03	3.29E-03	9.71E-03	5.35E-03
PU239	4.41E-01	7.18E-01	6.12E-01	4.17E-01	5.94E-01	6.83E-01
PU240	2.36E-01	2.29E-01	3.00E-01	1.27E-01	3.09E-01	2.08E-01
PU241	1.33E-01	2.40E-02	3.48E-02	1.31E-02	3.87E-02	2.19E-02
PU242	6.35E-02	6.46E-03	1.79E-02	3.79E-03	2.14E-02	6.45E-03
PU244	4.08E-06	1.76E-07	9.75E-07	1.22E-07	1.47E-06	2.27E-07
AM241	5.95E-03	6.46E-03	1.34E-02	3.36E-01	1.24E-02	5.29E-02
AM242m	1.36E-04	5.76E-04	1.07E-03	2.86E-02	1.09E-03	4.59E-04
AM242	1.36E-04	5.76E-04	1.07E-03	2.86E-02	1.09E-03	4.59E-03
AM243	1.55E-02	6.93E-04	2.33E-03	3.97E-02	2.94E-03	6.86E-03
CM242	2.05E-03	2.94E-04	4.42E-04	1.57E-04	5.43E-04	2.67E-04
CM243	7.40E-05	2.68E-05	4.74E-05	1.43E-05	6.21E-05	2.48E-05
CM244	5.73E-03	5.15E-04	2.16E-03	3.35E-04	3.22E-03	6.16E-04
CM245	2.41E-04	6.08E-05	3.45E-04	4.27E-05	5.36E-04	8.12E-05
CM246	4.07E-05	6.88E-06	7.89E-05	5.99E-06	1.33E-04	1.21E-05
CM247	4.89E-07	3.37E-07	6.17E-06	3.46E-07	1.09E-05	7.16E-07
CM248	3.32E-08	2.55E-08	9.61E-07	3.59E-08	1.92E-06	7.81E-08
CM250	1.48E-16	2.29E-17	1.59E-15	5.08E-17	4.83E-15	1.34E-16
BK249	3.38E-10	3.06E-10	1.01E-08	4.80E-10	2.66E-08	1.17E-09
CF249	7.86E-11	5.08E-10	3.55E-08	9.26E-10	7.26E-08	2.01E-09
CF250	8.08E-11	1.04E-10	8.01E-09	2.24E-10	2.03E-08	5.40E-10
CF251	3.42E-11	6.88E-12	7.74E-10	1.84E-11	2.08E-09	4.55E-11
CF252	2.55E-11	2.73E-13	3.25E-11	8.85E-13	1.09E-10	2.40E-12
FOM	-0.32	0.37	0.16	-1.78	0.10	-0.14

Table 3.12: Fraction of TRU nuclides to the total TRU in each waste stream and Figure of Merit for each waste stream; *fuel* indicates the discharged assembly; MRW indicates the Melt Refining Waste stream; *ref.* indicates melt refining with reference removal fractions for melt refining and *act.* indicates melt refining with the specified percent of actinide losses.

Nuclide	ref. fuel	ref. MRW	20% B&B	ABR	ARR
NP236	3.28E-10	0.00E+00	7.44E-10	0.00E+00	0.00E+00
NP237	4.96E-03	0.00E+00	6.12E-03	1.41E-02	6.03E-03
PU236	1.19E-07	0.00E+00	1.74E-07	3.20E-07	9.89E-08
PU238	9.52E-03	0.00E+00	3.55E-03	3.54E-02	1.05E-02
PU239	6.14E-01	0.00E+00	7.90E-01	3.61E-01	6.38E-01
PU240	2.99E-01	0.00E+00	1.78E-01	3.28E-01	2.64E-01
PU241	3.44E-02	0.00E+00	1.67E-02	5.70E-02	3.33E-02
PU242	1.76E-02	0.00E+00	2.72E-03	1.01E-01	2.21E-02
PU244	9.36E-07	0.00E+00	3.87E-08	6.78E-07	1.03E-07
AM241	1.34E-02	7.77E-01	2.57E-03	2.81E-02	1.25E-02
AM242m	1.06E-03	6.61E-02	1.71E-04	2.03E-03	8.18E-04
AM242	1.06E-03	6.61E-02	1.71E-04	2.03E-03	8.18E-04
AM243	2.28E-03	9.10E-02	2.19E-04	3.38E-02	5.99E-03
CM242	4.32E-04	0.00E+00	1.28E-04	1.78E-03	6.47E-04
CM243	4.61E-05	0.00E+00	1.00E-05	1.67E-04	4.47E-05
CM244	2.07E-03	0.00E+00	1.20E-04	2.51E-02	3.64E-03
CM245	3.30E-04	0.00E+00	1.09E-05	6.55E-03	8.89E-04
CM246	7.50E-05	0.00E+00	7.94E-07	3.58E-03	4.72E-04
CM247	5.84E-06	0.00E+00	2.89E-08	3.05E-04	3.57E-05
CM248	8.97E-07	0.00E+00	1.41E-09	1.44E-04	1.69E-05
CM250	1.43E-15	0.00E+00	1.12E-18	6.70E-11	5.62E-12
BK249	9.19E-09	0.00E+00	1.78E-11	3.23E-06	3.17E-07
CF249	3.31E-08	0.00E+00	1.61E-11	9.89E-06	1.12E-06
CF250	7.30E-09	0.00E+00	3.44E-12	2.27E-06	1.95E-07
CF251	7.02E-10	0.00E+00	1.70E-13	2.92E-07	2.30E-08
CF252	2.89E-11	0.00E+00	5.73E-15	2.00E-08	1.38E-09
FOM	0.17	-3.17	0.77	-0.36	0.08

In chapter 5 we found that it is possible to greatly reduce the fissile plutonium content in the fuel discharged from B&B reactors at an average burnup of 20% FIMA by irradiating this fuel in a soft neutron spectrum for few % FIMA. After such a soft-spectrum irradiation the FOM of the fuel discharged from the 20% B&B core will be negative.

Chapter 4

Double cladding for Breed and Burn reactors

4.1 A new reconditioning process: double cladded fuel

When the fuel reaches high burnups, such as the ones necessary for the B&B mode of operation, the fuel swells and the mechanical properties of the cladding deteriorates due to neutron-induced radiation damage, thermal creep and irradiation creep. The most proliferation resistant process to recycle this fuel is to use the discharged fuel *as is* and insert the entire fuel rod, including the irradiated cladding after venting the gaseous fission products, into a new larger diameter clad; we will refer to this process as *double cladding reconditioning*. A purely mechanical process, based on double cladding, is briefly mentioned as one of the possible options for DUPIC process [45], but it was not pursued in favor of an OREX process. However, the DUPIC studies do not give any detail on the actual double cladding process and how this was envisioned to be executed. The double-cladding fuel reconditioning envisioned in this study is described in this section. This process is to be used in B&B reactors, with the goal of increasing the fuel utilization beyond the material damage limits with minimum possible fuel reconditioning. The goals of this process are:

- avoid any type of chemical reprocessing,
- maintain a strong proliferation resistance in synergy with the B&B

mode of operation,

- reduce number and complexity of processes involved in fuel reconditioning.

The double-cladding reconditioning process considered in this study consists of the following operations:

- Removing the fuel rods from the discharged fuel assemblies;
- Relieving the pressure accumulated in the fuel rod by, primarily, the gaseous fission products (while capturing these FP);
- Inserting the fuel rod into a new clad (made of, say, HT-9);
- Reconstituting a new fuel assembly out of the double-cladding fuel rods;
- Loading these fuel assemblies into the B&B reactor. Sodium bonding may be used to fill the gap between the old and new cladding so as to minimize the gap resistance to heat transfer.

Figure 4.1 shows a graphical illustration of fuel unit cell before and after the double-clad reconditioning process.

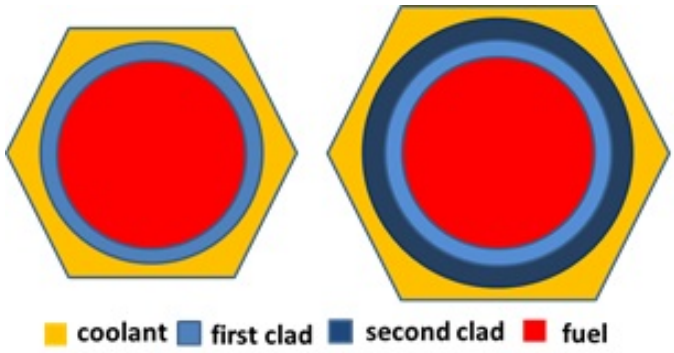

Figure 4.1: Unit cell of B&B reactor fuel (left) and unit cell of the double-clad fuel (right).

Table 4.1 reports the dimensions of the unit cell for single clad case, with a pitch-to-diameter ratio of 1.122, as used by Heidet for single clad [13]. It

is assumed that the cooling requirements of double cladded fuel will substantially be the same as the single clad fuel (this will be later confirmed by a thermal-hydraulics verification), therefore the reconstituted fuel assembly examined has the same coolant cross-section area of the original unit cell. In this way, the total coolant volume in the reactor is the same. The resulting volume fractions of the unit cell elements are given in Table 4.2, based on the geometrical parameters of Table 4.1.

Table 4.1: Unit cells geometrical parameters for single and double clad

Dimension	single clad (cm)	double clad (cm)
Rod outer diameter	1	1.166
Clad thickness	0.083	0.166
P/D	1.122	1.079

Table 4.2: Unit cells volume fractions for single and double clad

Volume fraction	single clad (cm)	double clad (cm)
coolant	28%	22%
fuel+gap	50%	40%
clad	22%	38%

4.2 Neutron balance for double cladded fuel

An insight into the neutron balance of the B&B reactors using double-cladded fuel can be obtained from the k_∞ evolution with burnup of a single unit cell. The unit cell consists of a homogenized composition of fuel, coolant and cladding, as is commonly the practice for fast spectrum neutronic analysis. The analysis is performed using MCNP5 1.51 and the ORIGEN 2.2 codes that are coupled with the MOCUP 2.0 driver, as described in Section 2.6. The initial heavy metal fuel composition is depleted uranium (^{238}U/0.2%^{235}U) and the clad is assumed to be HT-9 - 12% Cr ferritic-martensitic steel. The reactor coolant is sodium. The power density assumed is 300 W/cm^3, which is

well within the heat removal capability of liquid metal cooled cores. Figure 4.2 shows the calculated k_∞ as a function of burn-up for a unit cell that undergoes reconditioning at 20% FIMA. It is found that at 20% FIMA the single-clad fuel unit cell has a k_∞ of about 1.18 and is therefore still a net neutron producer. By double cladding the fuel at 20% FIMA k_∞ drops to approximately 1.05. This fuel is therefore still reactive. This suggests that after recladding the fuel can still be used in a B&B reactor for further burning. Using the neutron balance method described in Section 2.3, Figure 4.3 can be derived for various values of leakage probability (L) and neutron loss in Reactivity Control systems (RC). As seen in Figure 4.3, the neutron balance for a reactor working with double-cladded fuel and 4% leakage probability and 2% loss in control rods can sustain B&B mode of operation up to about 30% burn-up. Based on these results, it is possible to envision applications of double cladded fuel with the goal of increasing fuel utilization. The main idea of this study is to add to the B&B fuel cycle, based on the 20% reactor, a second tier reactor that would further burn this fuel. The first tier brings the reactor from 0% to 20% FIMA, while the second tier takes the fuel from 20 to the highest possible burn-up (however not beyond 40% as the new cladding will also have a material limit). The two following designs are envisioned:

1. The double-cladded fuel is used in a sodium-cooled fast reactor for a second-tier fuel cycle. This new reactor which we call Second-Tier B&B or (2TB&B) uses double cladded fuel as feed and burn it up to what burn-up can be sustained, the identification of which is the point of this design study. This design is described in Section 4.3

2. The double cladded fuel is used in a subcritical core in which the final burn-up can be higher percentages than 30% FIMA derived by neutron balance for a critical core subjected to 2% RC and 4% L. The subcritical core, also referred to as a blanket, is driven by an external neutron source, provided by a lead spallation target that is bombarded by accelerator high energy protons. This design is called Accelerator Driven Reactor (ADR) and it is described in Section 4.5.

Both these designs are able to achieve higher burn-up and reduce the fissile content of ^{239}Pu in the reactor.

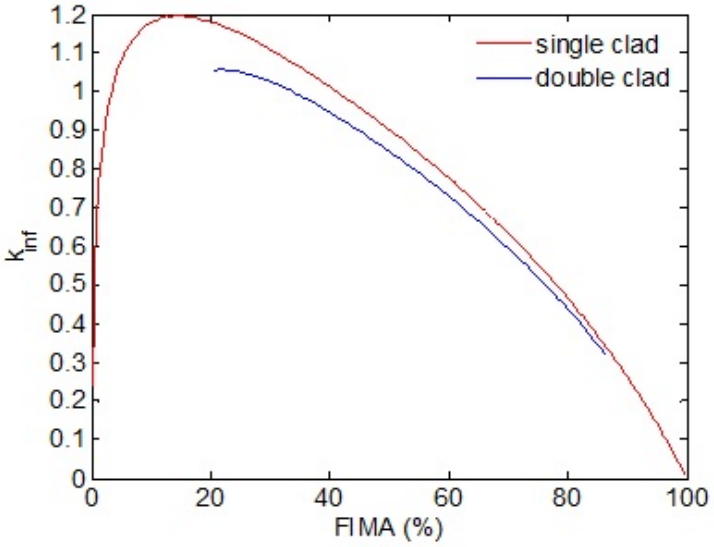

Figure 4.2: Single clad and double-clad unit cell k_∞ as a function of burn-up.

4.3 Second-tier double cladded sodium cooled fast reactor (ADR)

The Second-Tier Breed and Burn reactor (2TB&B) uses the fuel discharged at 20% FIMA from the B&B reactor described in Chapter 3. The core geometrical parameters are the same, as reported in Table 3.2, but the fuel is replaced with double cladded fuel at 20% FIMA, and it is shuffled with an in-to-out shuffling scheme. The in-to-out fuel scheme is used since the most reactive fuel will be the 20% FIMA fuel and it will be shuffled outside increasing the burn-up and decreasing outside leakage. For all simulations the ENDF-VII/B cross-sections are used with temperature of 900 K. The analysis is aimed to identify the conditions of the cycle at equilibrium, thus the performances will be reported analyzing the equilibrium cycle, without analyzing start-up phase. The batch composition is not uniform in the axial direction due to the different axial burning of the fuel rods. In these simulations, three axial zones were considered sufficient for a realistic assessment of fuel composition. The composition of the fuel elements at 20% FIMA was given in Table 3.4 which reports the discharge mass per GW_eYr for the

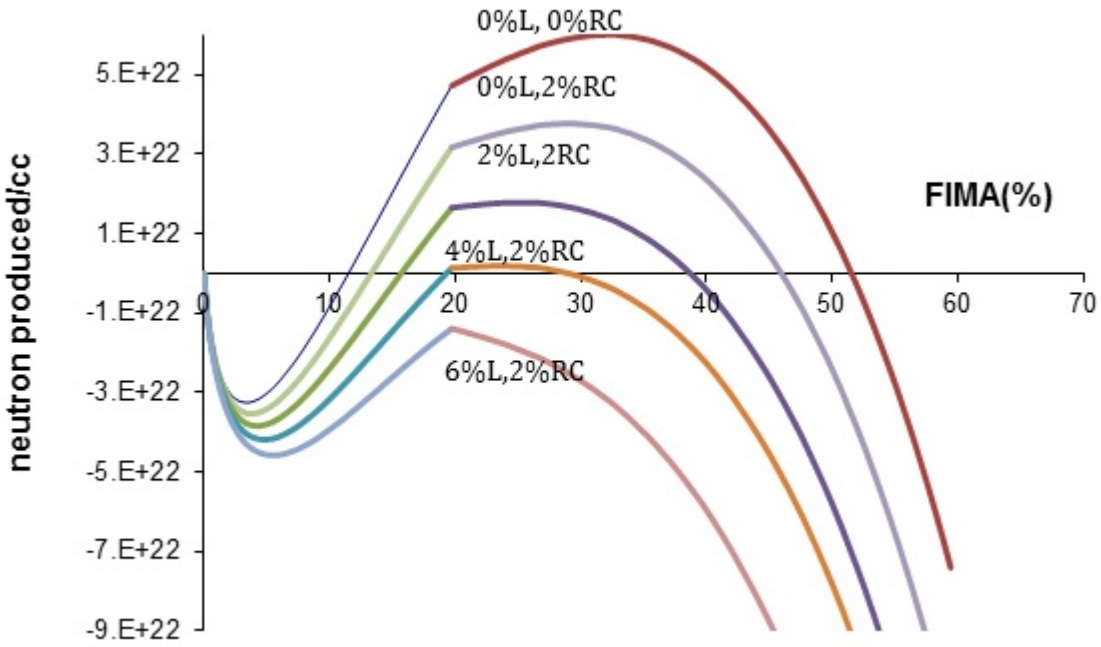

Figure 4.3: Neutron balance for double cladded fuel; Double cladding happens at 20% FIMA. Different curves are for different values of leakage probability (L), and loss in Reactivity Control systems (RC).

nuclides of most interest. It is assumed that 75% of the gaseous FPs are removed at each end of step. The fission products that are removed are: H, He, N, O, F, Ne, Cl, Ar, Kr, Xe and Rn. Figure 4.4 shows a cross view of the actual geometry used to simulate the 2TB&B. The fuel plenum is represented by the zone above the fuel, while the core zones represent the various burn-up zones used in the simulations. The fuel is divided in 8 radial batches and each batch is divided into 3 axial zones for burn-up simulation for a total of 24 zones. The representative real core uses a geometry with hexagonal fuel assemblies arranged in a cylindrical pattern. However, for Monte Carlo simulations in fast reactor, given the fact that the mean free path of the neutrons is much large than the fuel pin characteristic diameter, the zones can be homogenized. Moreover, the geometry to be used can be represented by a series of concentric cylinders, so that the simulated geometry is actually cylindrical. This approximation has been proven to yield accurate results [17].

Figure 4.5 shows the k_{eff} equilibrium evolution over a cycle for the 2TB&B with a 500 days cycle. "This is the maximum cycle length that enables maintaining criticality at the end of the cycle. The burnup accumulated as the fuel is shuffled from the innermost to the outermost batch is nearly 10% FIMA – making the combined Tier 1 and Tier 2 depleted uranium utilization of 30%. Figure 4.6 shows the batch burn-up distribution at Beginning of Cycle (BOC) and End of Cycle (EOC). Figure 4.7 shows the power distribution across the core in W/cm^3.

4.4 Thermal-Hydraulics validation

The main objectives of the T-H validation are to: validate reactor core's ability to handle peak power density without violating the design constraints and optimize the coolant system parameters for the final core design. In order to meet these objectives an adaptable sub-channel analysis model was developed in MATLAB that can quickly be applied to evaluate the effect of any design change.

The T-H design constraints are reported in Table 4.3:

Other channel parameters that are used in the sub-channel analysis are

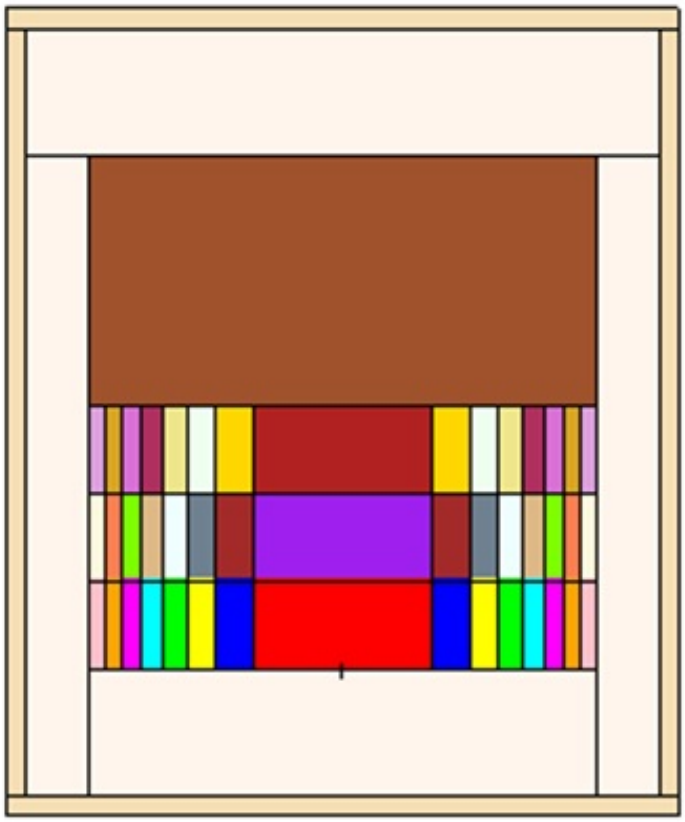

Figure 4.4: Second Tier Breed and Burn Reactor Schematic Cross Sections. The zone of different color represents the various burn-up regions used in the simulations. The radial separation represents the fuel batches. The Reactor has 8 radial fuel batches and 3 axial zones. Beyond the core there is 50 cm thick 50% Na/50% HT9 reflector and a shielding 50% Na/50% B_4C.

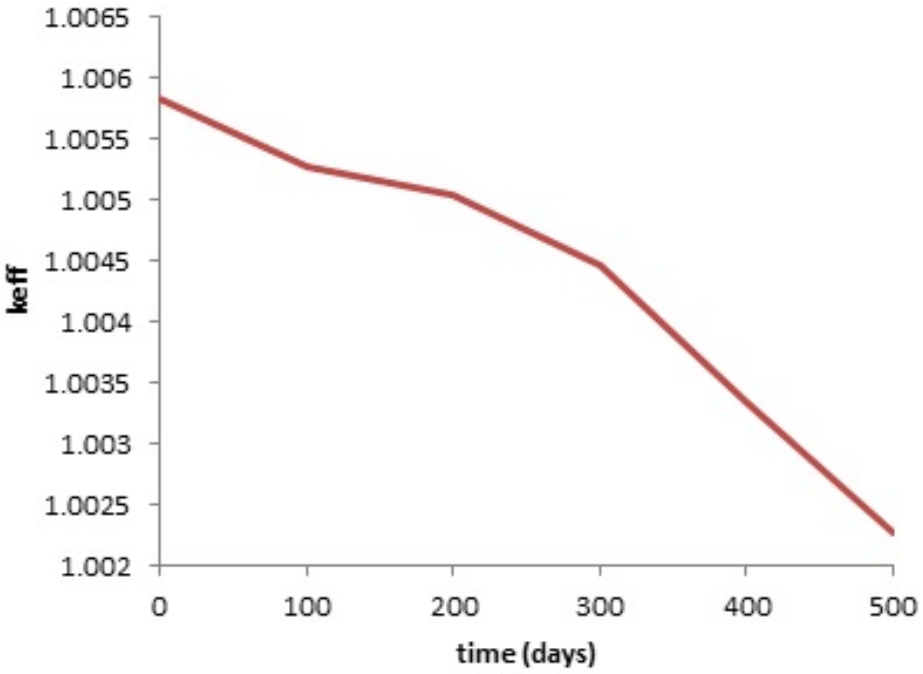

Figure 4.5: keff at equilibrium for 2TB&B

Table 4.3: TH Constraints

Peak fuel temperature	<melting
Maximum Inner Clad Temperature	$< 650\,^{\circ}C$
Coolant Pressure Drop Across Core	<1 MPa
Coolant ΔT Across Core	$< 200\,^{\circ}C$
Coolant Flow Velocity	< 12 m/s

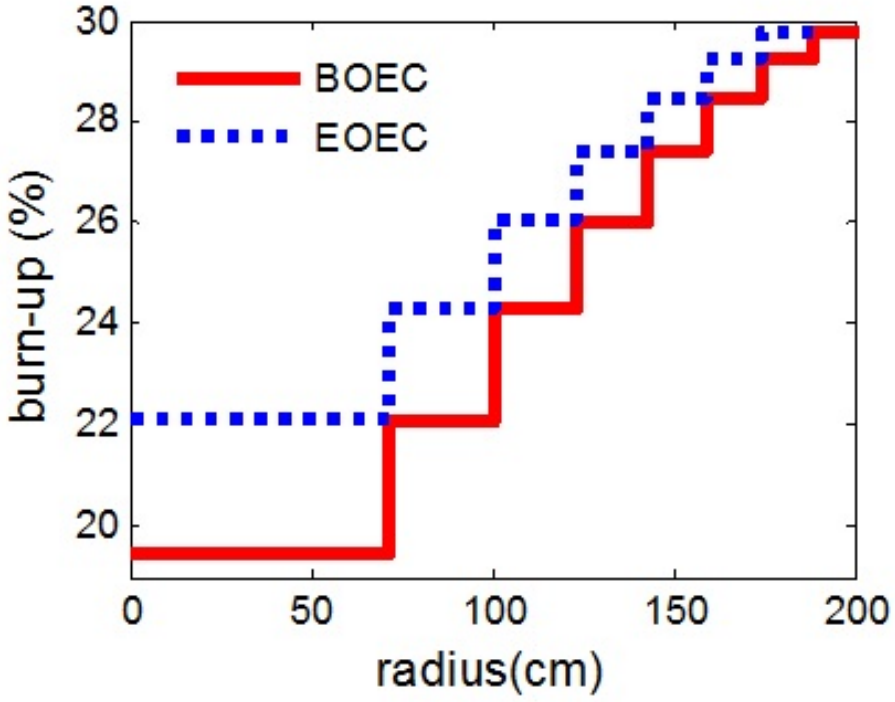

Figure 4.6: Burn-up distribution for 2TB&B

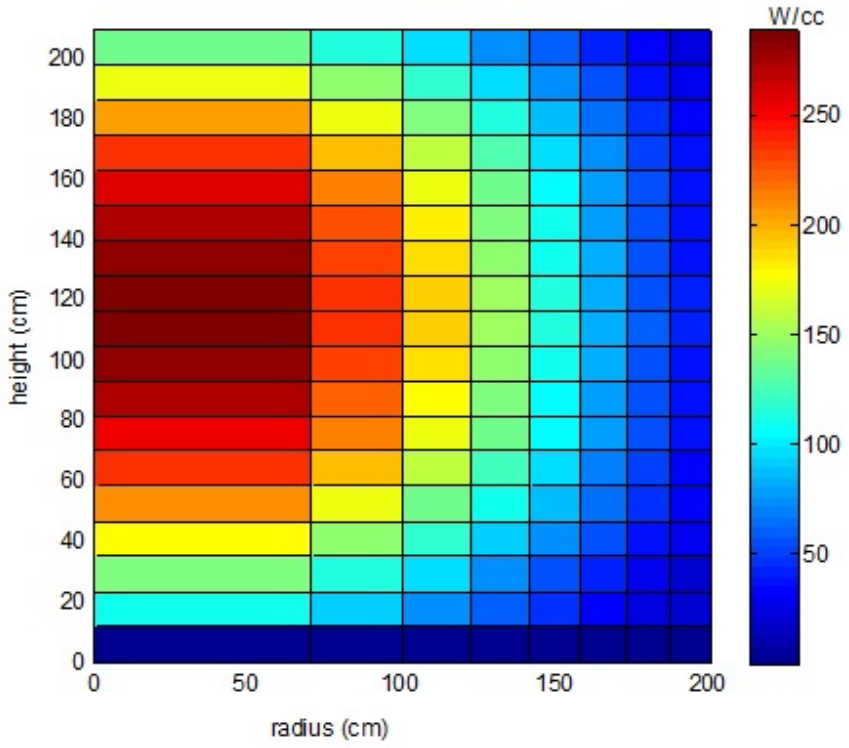

Figure 4.7: Power density distribution in 2TB&B in W/cm^3

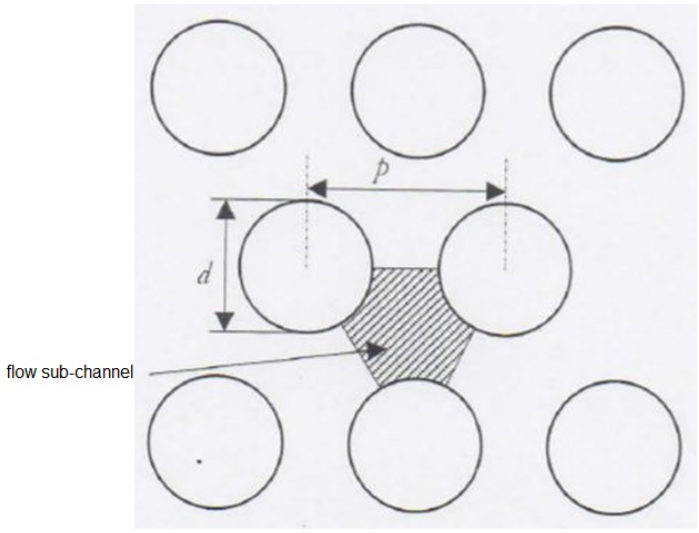

Figure 4.8: Triangular Lattice

defined below:

$$area\,of\,lattice\,unit\,cell,\ A_{lat} = \frac{\sqrt{3}}{4}P^2 \quad [cm^2] \tag{4.1}$$

$$flow\,area,\ A_{flow} = \frac{\sqrt{3}}{4}P^2 - \frac{\pi d^2}{8} \quad [cm^2] \tag{4.2}$$

$$wetted\,perimeter,\ P_W = \frac{1}{2}\pi d \quad [cm] \tag{4.3}$$

$$hydraulic\,perimeter,\ D_h = d\left[\frac{2\sqrt{3}}{\pi}\left(\frac{P^2}{d}\right)^2 - 1\right] \quad [cm] \tag{4.4}$$

The properties of the liquid sodium coolant were taken from a technical report by Fink [46]. These properties are a function of temperature and are listed below.

$$\rho_{Na} = \rho_{crit} + 275.32\left(1 - \frac{T}{T_{crit}}\right) + 511.58\left(1 - \frac{T}{T_{crit}}\right)^{0.5} \quad \left[\frac{kg}{m^3}\right] \tag{4.5}$$

$$\mu_{dyn,Na} = \frac{e^{-6.4406-0.3958ln(T)+\frac{556.835}{T}}}{100} \quad \left[\frac{kg}{cm \times s}\right] \tag{4.6}$$

$$C_{p,Na} = (1.6582 - 8.479 \times 10^{-4}T + 4.4541 \times 10^{-7}T^2 \\ -2992.6 \times T^{-2}) \times 1000 \quad \left[\frac{J}{kg \times K}\right] \tag{4.7}$$

$$k_{Na} = \frac{124.67 - 0.11381T + 5.5226 \times 10^{-5}T^2 - 1.1842 \times 10^{-8}T^3}{100} \quad \left[\frac{W}{cm \times K}\right] \tag{4.8}$$

where ρ_{Na} is the density of liquid sodium [kg/m^3]; ρ_{crit} is the critical density of sodium = 219 kg/m^3; T_{crit} is the critical temperature of sodium = 2503.7 K; μ_{dyn} is the dynamic viscosity of sodium [kg/m^3]; C_p is the heat capacity of liquid sodium [$\frac{J}{kg \times K}$]; k_{Na} is the thermal conductivity of liquid sodium [$\frac{W}{cm \times K}$].

A fluid is also characterized by dimensionless numbers. The following correlation for Reynold's number, Re, Nusselt's number, Nu, and Prandtl's number, Pr were used.

$$Re = \frac{\rho_{Na} \nu D_h}{\mu_{dyn}} \tag{4.9}$$

$$Pr = \frac{C_p \mu_{dyn}}{k_{Na}} \tag{4.10}$$

$$Nu = 0.023 Re^{0.8} Pr^{0.4} \tag{4.11}$$

$$f = 0.184 Re^{-0.2} \tag{4.12}$$

The Nusselt Number uses the Dittus-Boelter correlation. The friction factor, f, uses the McAdams relation, which is best for Reynold's number between 30,000 and 1,000,000. The lowest Reynold's number expected at slowest velocity – assumed 6 m/s, and coldest temperature, 350 °C, is calculated to be 56,499. The highest Reynold's number – expected to be at the fastest velocity 12 m/s, and hottest coolant temperature, approximately 550 °C – is calculated to be approximately 148,410. Both are within the range for the McAdams relation.

The sodium coolant is in contact with the fuel rod cladding, made of HT9. The heat transfer coefficient between the two materials must be defined, as well as the thermal conductivity of the cladding and the fuel. The heat transfer coefficient is defined in relation to the Nusselt number. The thermal conductivities used are given by Leibowitz for HT9 [47] and Bauer for the fuel [48].

$$h_{HT9-Na} = \frac{k_{Na} Nu}{D_h} \quad \left[\frac{W}{cm^2 \times K}\right] \tag{4.13}$$

$$k_{HT9} = \frac{17.622 + 2.428 \times 10^{-2} T - 1.696 \times 10^{-5} T^2}{100} \quad \left[\frac{W}{cm \times K}\right] \tag{4.14}$$

$$k_{fuel} = 0.25 \quad \left[\frac{W}{cm \times K}\right] \tag{4.15}$$

where h_{HT9-Na} is the heat transfer coefficient $\left[\frac{W}{cm^2 \times K}\right]$; k_{HT9} is the thermal conductivity of HT9 $\left[\frac{W}{cm \times K}\right]$; T is the temperature in K; k_{fuel} is the thermal conductivity of metallic fuel $\left[\frac{W}{cm \times K}\right]$.

Heat transfer through sodium between the first cladding and the fuel was not accounted for due to the assumption that after 20% FIMA, the fuel and first cladding are essentially bonded together. Moreover, k_{HT9} calculated for the expected fuel temperature range is approximately equal to k_{fuel}.

When using the power distribution of Figure 4.7, it is found that the most limiting constraint is the pressure drop, and the parameters are all within the limits with a coolant velocity v = 10.48 m/s and a temperature difference across the core of ΔT = 187 K.

4.5 Second-tier double cladded Accelerator Driven Reactor

To increase fuel utilization beyond what is feasible with a critical reactor, a new type of second tier reactor is studied. As the absorptions in nuclear fuel become strong and since it is not deemed feasible to perform another double cladding operation after the first one, the idea of using an external neutron source to increase the fuel utilization is appealing. In this section, the possibility of using an accelerator neutron source to drive a subcritical blanket of double-cladded fuel is examined.

The Accelerator Driven Reactor (ADR) consists of a central spallation neutron source surrounded by a subcritical radial blanket. The spallation neutron source is provided by a 20 MWe cyclotron that accelerate protons to an energy of approximately 1 GeV. These high energy protons impinge on a central cylindrical lead target, as shown in Figure 4.9. The beam tube is cooled from the outside by liquid-lead which flows from bottom to top in the central channel and functions as both coolant and spallation target. For neuton transport simulations, the central lead target is a source of 20 cm diameter and 20 cm in height. A 3 mm HT9 wall separates the central channel from the sodium cooled subcritical blanket and it is surrounded by a 50% HT-9 / 50% coolant 1 m thick reflector. A schematic of ADR is provided in Figure 4.9. The accelerator beam tube is inserted from the top into a central cavity in the subcritical blanket. The subcritical fission blanket is divided in 15 radial batches for fuel shuffling. The blanket geometry is simplified, as for the 2TB&B, modeling the fuel batches as concentrically cylinders. For depletion analysis, each batch is split into 3 axial zones. The external radius of the blanket is 225 cm. With this radius, ADR contains the same HM mass as the first-tier B&B reactor. The fuel elements are 209 cm long and a 2 m plenum is designed to accommodate gaseous fission products. The fission blanket coolant is sodium, but a lead-cooled variation is also studied. However, it is shown that sodium guarantees significantly better T-H performance.

4.5.1 Neutron Source Description

In this study, the accelerator physics is not simulated, but a neutron source is defined in the transport code, without modeling the proton beam. The neutron source energy distribution is based on a typical energy spectrum of spallation neutrons from lead targets that are bombarded by 1 GeV protons [49, 50]. The spectral energy distribution used in the simulations is showed in Figure 4.10. The maximum neutron source intensity is calculated to be $1.25\times10^{1}8$ neutron/second. This estimation of the source is based on the assumption that a 20 MWe accelerator is used with a 50% efficiency to produce energetic protons with 1 GeV energy. It is further assumed that 1 GeV proton produces 20 neutrons when impinging on the lead target.

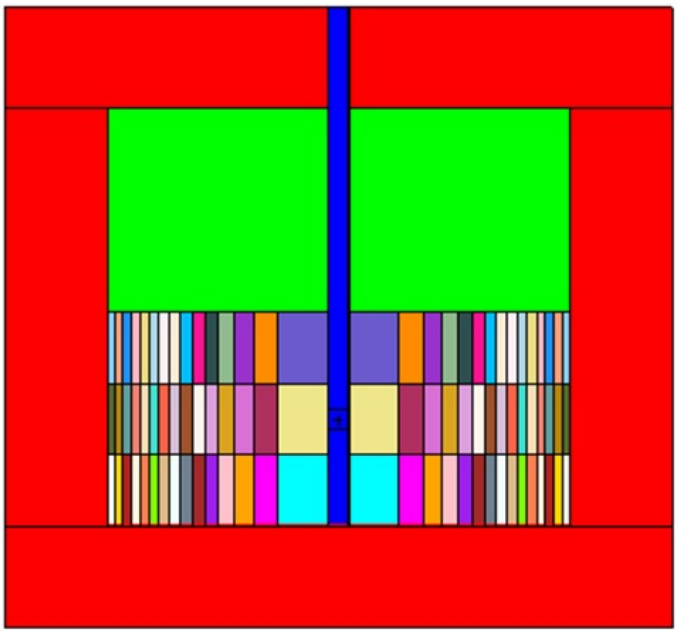

Figure 4.9: ADR geometry as simulated with MCNP 1.51; the blue center represents the penetration for the spallation source; the red part represents the sodium/FT9 reflector, while in green is the plenum, and multi-color is the fuel. Vacuum tube is not simulated.

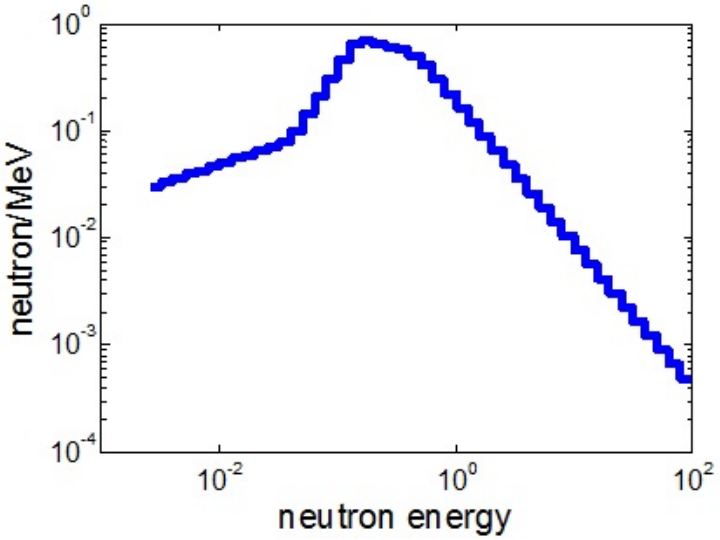

Figure 4.10: Energy spectral distribution of the spallation neutron source simulated in MCNP

4.5.2 Preliminary assessment of energy gain for subcritical system

To estimate the blanket power that can be established by ADR, a simple formula can be used for the energy multiplication:

$$energy\ gain = 0.2\frac{k}{(1-k)\nu}\frac{N}{E} \tag{4.16}$$

where k is the subcritical multiplication factor, E is the energy of impinging particles (1 GeV in this case), ν is the number of neutrons per fission, N is the number of neutrons generated per impinging proton (20 in this case) and 0.2 represents the energy released per fission which is 0.2 GeV. Figure 4.11 shows a plot of the energy gain as a function of k. Expression 4.16 can be used to properly calculate the thermal energy gain. From the thermal gain, the electrical gain can be derived assuming 50% efficiency for the accelerator and 40% conversion efficiency for ADR; therefore the electrical gain is 20% of the corresponding thermal gain, derived by Eq. 4.16. For Figure 4.11, ν is assumed to be 2.91.

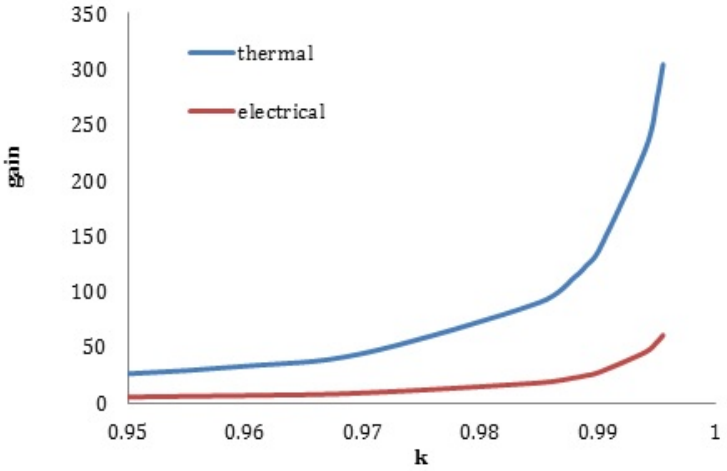

Figure 4.11: Thermal and electrical gain for Accelerator Driven Systems

The subcritical multiplication factor k in Eq. 4.16 is defined as:

$$k = \frac{F}{F+1} \tag{4.17}$$

where F is the number of fission neutrons in the subcritical system. Accounting for (*n,xn*) reactions it is also possible to write the source multiplication factor as:

$$k_{src} = \frac{F+N}{F+N+1} \tag{4.18}$$

where N indicates the number of neutrons produced by (*n,xn*) reactions. The source multiplication factor k_{src} will be used in the following analysis. However, for ADR the amount of neutrons from (*n,xn*) reactions is about two order of magnitudes lower than the amount of fission neutrons. If the ADR is to produce the same thermal energy as the first-tier B&B reactor (3000 MWth), a thermal energy multiplication of 300 is needed for a 10 MW proton beam. Figure 4.11 implies that such a high multiplication corresponds to k of 0.9955. Since the multiplication factor will decrease during ADR cycle, to obtain a reasonable energy gain ADR should operate with a k between 0.9955 and 0.985, with a thermal output that varies between 3000 MWth and 1000 MWth. Figure 3.12 it is also inferred that a change in k of 1000 pcm, e.g. from 0.994 to 0.995, implies a change in thermal output of up to 200

MW for k > 0.99, since the energy gain behaves exponentially as the fission neutron population. Consequently small modification on the design, such as neutron leakage reduction with better reflector, can significantly change the thermal output of ADR.

4.5.3 Sodium cooled ADR

In the assumed cycle the fuel batches are shuffled from in-to-out every 1000 days and a 20% (properly 19.5%) burned batch is introduced in the central zone at Beginning of Equilibrium Cycle (BOEC). Figure 4.12 shows reactor k_{src} during a cycle and the corresponding reactor electrical power, assuming 40% conversion efficiency. The proton beam is assumed to operate at 10 MW during the entire cycle.

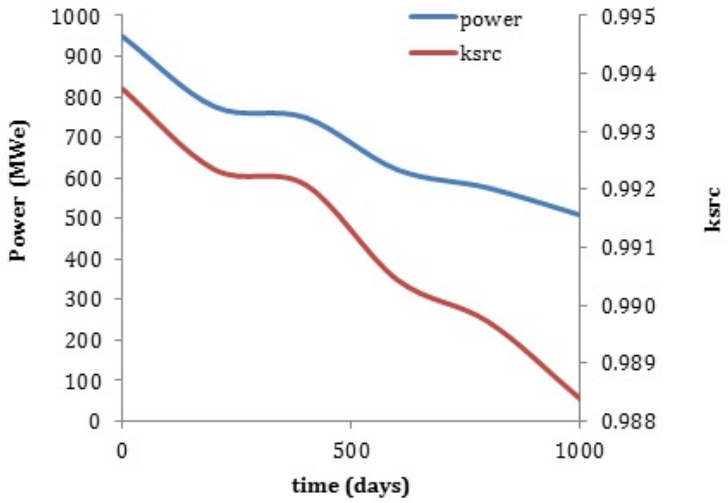

Figure 4.12: k_{src} and electrical power for sodium cooled ADR during equilibrium cycle.

The source multiplication factor k_{src} varies from 0.9937 at BOEC to 0.9883 EOEC, with a statistical uncertainty σ =50 pcm. The resulting power varies from 945 MWe at BOEC to 508 MWe at EOEC. The electrical gain varies therefore from 48 to 25. The power in Figure 4.12 is the result of transport calculation and accounts for all reactions in ADR and for proper

Q-value for all actinides; it is therefore a more precise estimate than the energy gain estimation of Figure 4.11 which is derived with approximated Eq. 4.16. Figure 4.13 shows the burn-up that is reached in each batch in a cycle. It is observed that the inner 6 batches undergo a significant burning in a cycle, while the outermost batches do not burn significantly. The final burn-up reached is about 38%, close to the design goal of 40 %. In this design, the radial leakage is only 2.19% (expressed as a fraction of fission neutrons) at BEOEC; bottom and top leakages are both 2.10%. Small reduction in radial leakage could significantly increase the output power. To verify if the sodium blanket can be effectively cooled with the given pitch and the accelerator uneven power distribution, a basic T-H analysis was performed. Figure 4.14 reports the power density at BOEC in ADR in W/cm^3, where each batch has been split into 18 axial zones for power assessment. The represented profile is a crosscut view of ADR where left side represents the HT9 separator between lead target and the blanket. The maximum power density is reached in proximity of the lead target and it is about 310 W/cm^3. The 8 outermost batches have very low power densities ranging from 50 to 10 W/cm^3.

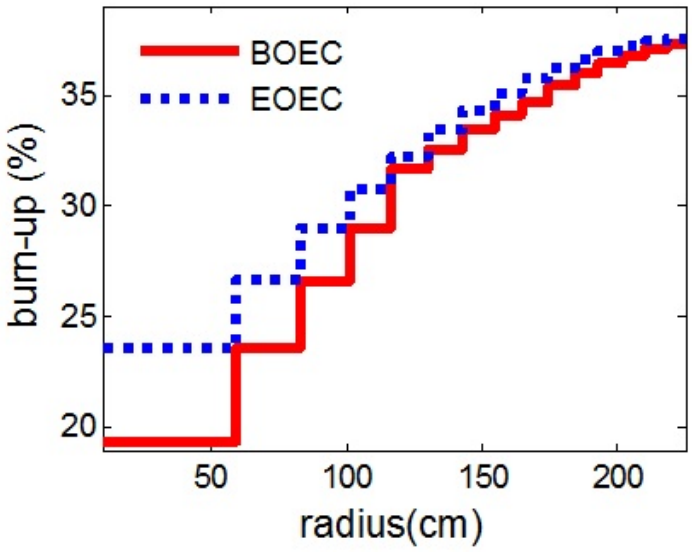

Figure 4.13: Average Batch burn-up at BOEC and EOEC.

A T-H verification is performed based on the procedure outlined in Sec-

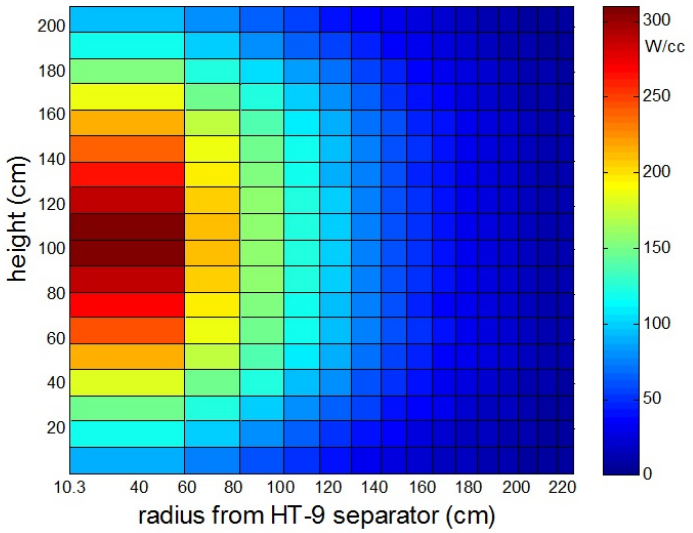

Figure 4.14: Thermal power density (W/cm^3) in ADR at BEOC. Left side represents HT9 separator between lead target and the blanket.

tion 4.4. The T-H balance is performed on the innermost batch which is the one with the highest power density. With the constraints on $\Delta T < 200$ K and $\Delta P < 1$ MPa, it is found that the peak power density that can be removed is 350 W/cm^3 , with a coolant velocity of 10.4 m/s. Consequently, the ΔT can be lowered to 180 K, still guarantying a feasible design.

4.5.4 Lead-cooled ADR

The use of lead as a coolant for ADR has the advantage of simplifying the design using the same coolant for blanket and accelerator target. Moreover, thanks to the better neutronics properties of lead as neutron reflector, the design could give a higher k_{src}. However, a T-H analysis based on lead properties proves that the cooling is not as effective when using the above outlined constraints ($\Delta T < 200$ K and $\Delta P <1$ MPa) and the peak power density that can be removed is about 130 W/cm^3 when the previously derived power shape is used. Consequently, it is necessary to reduce the beam power to 4 MW (8 MWe) to obtain an acceptable power density. Figure 4.12 shows the k_{src} and output power variation during a cycle where the beam power is

assumed constant at 4 MW. The cycle length is proportionally increased to 2500 days to obtain the same discharge burn-up. It is observed that the ADR has a higher k_{src} at BOEC, thanks to lead reflective properties. The source multiplication factor k_{src} varies from 0.9948 at BOEC to 0.9869 at EOEC. However, the output power varies from 446 MWe to 170 MWe during the cycle. The electrical gain is still significant varying from 58 to 21.

Figure 4.13 shows the batch burn-up, where the discharged fuel has reached a burn-up of 39.2%. Figure 4.14 shows the power density at BOEC

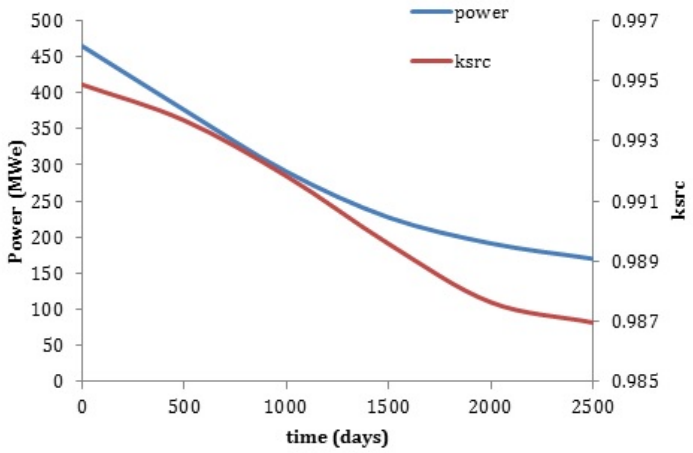

Figure 4.15: k_{src} and electrical power for lead cooled ADR during equilibrium cycle.

in lead cooled ADR for a 4 MW proton beam, where the peak power density is 127 W/cm^3. Using the outlined T-H analysis with this power distribution and lead properties, the maximum power density is calculated to be the 128 W/cm^3 with the usual constraints of ΔT and ΔP, and resulting flow velocity of 2.73 m/s. The reduced maximum allowable power density is a consequence of lower specific heat of lead, 144 J/(Kg K) against 1260 J/(Kg K) of sodium, and the lower coolant velocity, dictated by the pressure drop. For same pressure drop the flow velocity is lower for lead due to its higher density (10.4 g/cc against 0.83 g/cc for sodium).

The lead cooled ADR is therefore running at the maximum allowable power with a 4 MW proton beam and 446 MWe output power at BOEC.

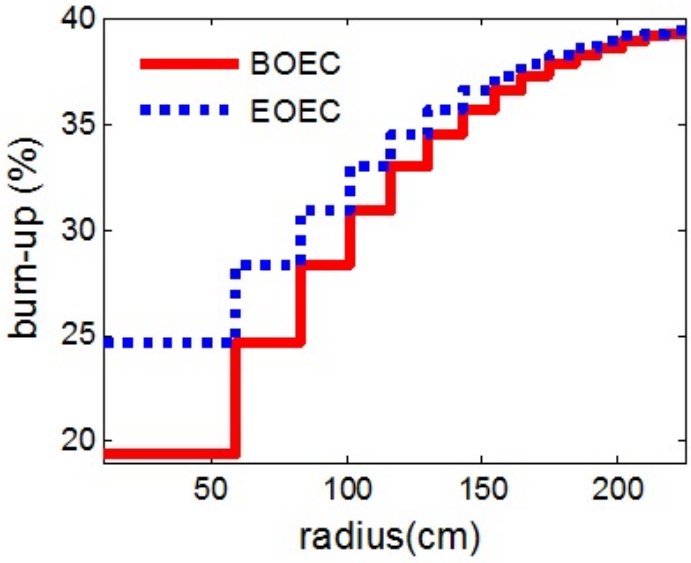

Figure 4.16: Batch burn-up in lead-cooled ADR.

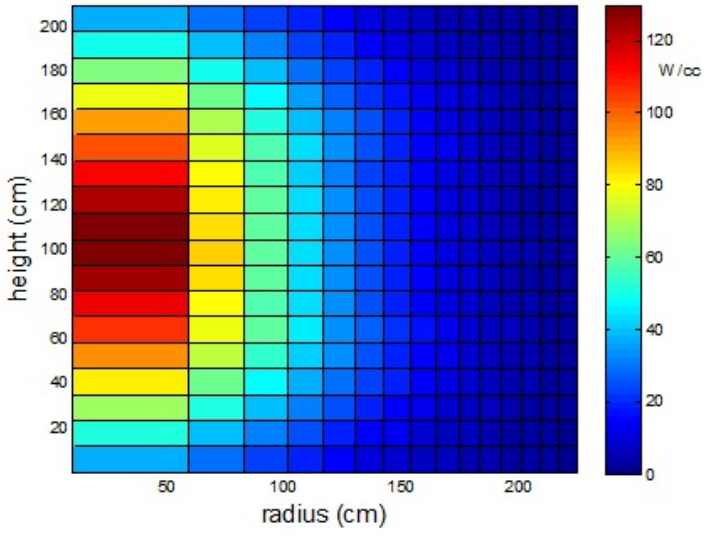

Figure 4.17: Thermal power density (W/cm^3) in lead cooled ADR at BOEC.

However, since the beam does not run at full power as in the sodium cooled case, it is possible to increase the beam power as k_{src} decreases and run ADR at a constant 500 MWe output power. Another approach to increase output power is to reduce the peaking power in the center, as to allow the use of a more powerful beam. To reduce power peaking a possibility is to use a longer target, where the neutron generation is dispersed in a 1-m long cylinder, instead of a 20 cm tall cylinder. Using the same composition as the calculated lead cooled BOEC, MCNP simulation with a lead target 1 m long were performed resulting in a reduction of the power peak by about 13% with a maximum peak of 110 W/cm^3. The reduction is not particularly significant, since most of the peaking is given by fission power cosine-type shape rather than by the accelerator peaking. However, spreading the source implies a small decrease in k_{src}, since the leakage is increased compared to the compact target design. Consequently, though it is possible to increase the beam power of approximately 13%, the output power is basically unchanged (465 MWe) due to a corresponding decrease in k_{src} (down to 0.9944).

In conclusion, the sodium cooled ADR is proven to be able to burn the fuel up to about 38%, with an average electricity gain of about 37 over a cycle and an output power up to 95 MWe. The lead cooled ADR is proven to be less effective, mainly because of T-H constraints due to thermodynamical properties of lead coolant.

4.6 Summary

In this chapter, an innovative reconditioning process has been clearly defined to increase fuel utilization. A sodium cooled fast reactor was designed to used 20% burned fuel and bring it up to the maximum possible in a critical reactor. It was foudn this maximum to be 30% FIMA. An Accelerator Driven Reactor using an external neutron source was also designed to increase fuel utilization up to 40%. It was found to be feasible, and the preferred cooling option was found to be sodium.

Chapter 5

Feasibility of recycling B&B discharged fuel in PWRs

5.1 Motivations

So far, we have explored the possibility of re-utilizing the B&B fuel in the same B&B type reactor as in Chapter 3 or in a different B&B reactor as in Chapter 4. However, the fuel discharged by B&B reactors working at 20% FIMA contains a considerable amount of fissile plutonium, so that its use in a Light Water Reactor (LWR) could be attractive on two counts – increasing the depleted uranium fuel utilization and reducing the fissile contents in, and proliferation resistance of the discharged fuel. This possibility is explored in this chapter.

This study has been developed in collaboration with Terrapower, LLC. The composition used in this study to simulate the discharge fuel has been provided by Terrapower [51]. The composition represents discharge fuel from a B&B reactor using U-5%Zr alloy fuel and discharged at 18% FIMA. In this chapter, we will refer to the B&B reactor with the name given by Terrapower to their specific design, the Traveling Wave Reactor, or TWR. The composition is reported in Table 5.1.

It is assumed that the discharged TWR fuel undergoes a 100% effective decladding process, before undergoing a recycling-reconditioning process. Two recycling scenarios are analyzed: 1) the fuel is converted to oxide and undergoes an AIROX-like process; and 2) the fuel undergoes a melt

Table 5.1: Composition of fuel provided by Terrapower. Fuel is U-5%Zr alloy discharged at 18% FIMA. The composition is at 1000 days after discharge.

Nuclide	Mass fraction
U-238	8.74E-01
Np-236	1.26E-20
Np-237	7.85E-04
Pu-238	4.40E-04
Pu-239	9.95E-02
Pu-240	2.16E-02
Pu-241	9.55E-04
Pu-242	2.93E-04
Am-241	1.41E-03
Am-242m	1.29E-20
Am-242	1.29E-20
Am-243	2.44E-05
Cm-243	4.34E-07
Cm-244	2.66E-06
Cm-245	4.62E-07
Cm-246	2.16E-08
Cm-247	4.43E-10
Cm-248	1.32E-20
Pu/HM	12.28%
Fis. Pu/Tot.	Pu 81.81%

refining process and it is then converted to oxide fuel. The oxide fuel is then fabricated into Zircaloy clad PWR fuel rods and fuel assemblies. The recycling process is assumed to happen at 1000 days after discharge. The discharged TWR fuel undergoes an ideal melt-refining process after which it is converted to oxide fuel and fabricated into Zircaloy clad PWR fuel rods and fuel assemblies.

5.2 Density of oxide fuel

It is assumed that the 18% FIMA TWR discharged fuel is converted, after reconditioning, into oxide form. The fuel to be loaded into the PWR includes most of the actinides, the 5% Zr (used in the metallic alloy), and whatever fission products left over after either an AIROX-like process or a melt-refining process. The Zr and fission products reduce the HM density in the oxide fuel beyond the dilution caused by the oxidation.

The reprocessed oxide fuel density is estimated as follows:

$$\rho_{mixture} = \frac{1}{(\frac{w_1}{\rho_1} + \frac{w_2}{\rho_2} + ... + \frac{w_i}{\rho_i})} \tag{5.1}$$

where the i terms at the denominator are the densities of the oxides of the constituents of the fuel mixture while w_i is their weight %. Table 5.2 and Table 5.3 give the density of the oxides of the elements we could find information for. The oxide in the table is assumed to be the only chemical form this element is present in the fuel. Some elements do not form oxides, or their oxide densities are unknown. For elements with unknown oxides, the pure element density is used. Table 5.4 reports the removal fractions of elements from the TWR discharged fuel that underwent either the AIROX or the melt-refining process. This is the same as Table 2.6 and it is reported here for convenience.

The resulting density of TWR fuel that underwent reconditioning 1000 days after discharge is calculated to be 9.95 g/cm^3 for the melt refining process and 9.7 g/cm^3 for the AIROX process. Both resulting densities are smaller than the density of pure UO_2that is 10.97 g/cm^3. The inferior value of AIROX fuel density is due to the higher content of fission products left over in the fuel. Table 5.5 compares the density of actinides in the various fuels.

Table 5.2: Fission Product oxide densities.

oxide	g/cc	oxide	g/cc
GeO_2	4.228	TeO_2	5.67
As_2O_3	3.74	I_2O_5	4.98
SeO_2	3.954	XeO_3	4.55
Br	-	Cs_2O	4.65
Kr	-	BaO_2	5.68
Rb_2O	4	La_2O	6.51
SrO	4.7	Ce_2O	6.2
Y_2O_3	5.01	Pr_2O	6.9
ZrO_2	5.68	Nd_2O	7.24
NbO	7.3	Pm_2O	6.85
MoO_2	6.47	Sm_2O	8.347
TcO_2	6.9	Eu_2O	7.4
RuO_2	6.97	Gd_2O	7.407
Rh_2O_3	8.2	Tb_4O	7.3
PdO	8.3	Dy_2O	7.8
Ag_2O	7.14	Ho_2O	8.41
CdO	6.95	Er_2O	8.64
In_2O_3	7.179	Tm_2O	8.6
SnO	6.45	Yb_2O	9.17
Sb_2O_3	5.67		

Table 5.3: Actinide and daughters oxide densities.

oxide	g/cc
Ac2O3	-
AmO2	11.68
At	-
Bi2O3	8.9
Cm	-
Fr	-
He	-
NpO2	11.1
Pa	
PbO	9.53
PoO2	8.9
PuO2	11.5
Ra	-
Rn	-
ThO2	10
Tl2O	10.45
UO2	10.97

Table 5.4: Summary of removal fractions in AIROX and melt-refining.

	AIROX	melt-refining
Actinides	0%	95 % Th, Am 0% others
Fission Products	100% H,C,Kr,Xe,I 90% Cs,Ru 75% Te,Cd	100% Br,Kr,Rb,Cd,I,Cs 95% Sr,Y,Te,Ba, La-Lu
Gaseous Fission Products	100% H,He,N,O,F,Ne,Cl,Ar,Kr,Xe,Rn	

Table 5.5: Density of oxide fuels.

type of fuel	HM mass fraction	fuel density (g/cm^3)	HM density (g/cm^3)
UO_2	88.1%	10.97	9.65
TWR-melt refining	75.8%	9.95	7.54
TWR-AIROX	72.6%	9.70	7.04

5.3 PWR core presentation

The PWR core is represented, in this very preliminary feasibility study, by a single fuel pin unit cell shown in Figure 5.1. Table 5.6 gives the dimensions assumed for the reference PWR unit cell [52]. The MCNP5 model is 10 cm tall. Reflective boundary conditions are applied to all the outside boundaries of the unit cell.

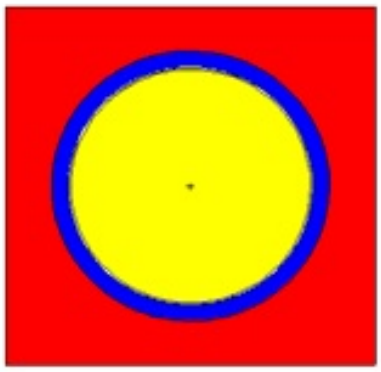

Figure 5.1: MCNP5 model of the unit cell of PWR used in this study: fuel (yellow); clad (blue); coolant (red).

From this simple unit cell model, it is possible to infer the reactor behavior. To infer reactor behavior, the core average reactivity can be estimated

Table 5.6: PWR unit cell dimensions [52].

outer rod diameter, D (mm)	9.5
clad thickness (mm)	0.57146
gap thickness (mm)	0.08243
lattice pitch, P (square) (mm)	12.6
P/D	1.326
Moderator/Fuel volume ratio (M/F)	1.6

as a power weighted average of the batch reactivities [53]. The reactivity of batch i is defined as:

$$\rho_{\infty,i} = \frac{k_{\infty,i} - 1}{k_{\infty,i}} \tag{5.2}$$

The value of $k_{\infty,i}$ can be calculated from the unit cell k_∞ evolution with burnup, knowing the burnup. For a core with n batches, the core reactivity can be estimated as:

$$\rho_{\infty,core} = \frac{f_1\rho_{\infty,1} + f_1\rho_{\infty,1} + ... + f_n\rho_{\infty,n}}{n} \tag{5.3}$$

The value of f_i can be determined from a 3-D analysis of a representative core; for this preliminary analysis it is assumed to be $1/n$. This is a good approximation for PWRs [53]. For a realistic approach, leakage needs to be included. Leakage depends on the fuel management scheme decided by the fuel manager. However, at a first approximation, a typical value for PWRs can be used. The values used in this study is 0.025. Therefore 5.3 can be re-written as:

$$\rho_{core} = \frac{f_1\rho_{\infty,1} + f_1\rho_{\infty,1} + ... + f_n\rho_{\infty,n}}{n} - 0.025 \tag{5.4}$$

Batch burnup and batch k_∞ depend on the residence time of the fuel in the reactor. In this study, we assuming a PWR working with 5 batches For

a fixed Fuel-Cycle-Length (FCL), it is possible to write the Beginning-Of-Cycle (BOC) reactivity and End-Of-Cycle (EOC) reactivity for a five batch reactor as:

$$\rho_{core,BOC} = \frac{\rho_0 + \rho_{FCL} + \rho_{2\times FCL} + \rho_{3\times FCL} + \rho_{4\times FCL}}{n} - 0.025 \qquad (5.5)$$

$$\rho_{core,BOC} = \frac{\rho_{FCL} + \rho_{2\times FCL} + \rho_{3\times FCL} + \rho_{4\times FCL} + \rho_{5\times FCL}}{n} - 0.025 \qquad (5.6)$$

where ρ_0 is the reactivity at time zero (fresh fuel), ρ_{FCL} is the reactivity after the fuel has resided in the core one cycle, $\rho_{2\times FCL}$ is the reactivity of the fuel that resided in the core two cycles and so on. The cores of interest are the ones for which both ρ_{BOC} and ρ_{EOC} are > 1 for the highest possible discharge burn-up.

In this study we limit the analysis to four and five batch cores, so as to get an upper practical estimation of the attainable burnup. It will be shown that using 5 batches, it is possible to obtain a discharge burn-up closer to the typical PWR discharge for melt-refining in the reference case. The goal is to increase burn-up which can be obtained by increasing the batches; however a high number of batches would imply a unrealistically short cycle length. A 5-batch core represents a good compromise between these two needs.

5.4 PWR reference core

Figure 5.2 shows the k_∞ evolution with burnup of the reference PWR that is fueled with reconditioned TWR fuel as well as with a standard 4.5% enriched uranium dioxide. The initial (maximum) value of k_∞ calculated for the AIROX treated TWR fuel is only 0.97, implying that this fuel cannot establish criticality, but using a melt-refining processed fuel it is possible to establish criticality in the reference PWR core. Although the beginning of life k_∞ of 1.08 is significantly smaller than in a standard enriched uranium fuelled PWR, its rate of decline is significantly smaller. This is due to a combination of a couple of reasons: a higher initial inventory of fissile fuel

and a significant initial inventory of fission products in the fuel originating from the TWR discharged fuel. Figure 5.3 shows the evolution with burnup of selected isotopes in the 4.5% enriched UO_2, while Figure 5.4 shows such evolution in the melt refined TWR fuel. It is observed that the fraction of initial TWR ^{239}Pu decline per burnup unit is not as sharp as in the case of ^{235}U in UO_2. This is due to the more than double initial inventory of fissile plutonium in the melt-refined fuel. As the melt-refined fuel also contains high concentration of fission products, its beginning-of-life k_∞ is significantly lower than that of the enriched uranium fuel. The fission products also function as burnable poisons thus further flattening the k_∞ drop with burnup. The very fortunate combination of features makes the burnup reactivity swing of the melt-refined fueled core much smaller than that of the conventional enriched uranium fueled core. Most likely there will be no need to add burnable poison, such as gadolinium or boron, to the TWR discharged fuel.

To identify the behavior of fission products during burn-up in the PWR, the evolution of the 879 Fission Products (FP) tracked by ORIGEN 2.2, is analyzed. Figure 5.5 shows a plot of fractional absorptions of all the Fission Products that at any point of the burn-up have a fractional absorption above 1% of all FP absorptions. Figure 5.6 shows a plot of the absorption rate (neutrons/sec) of these selected FPs, which are 24. It is observed that FPs can be roughly divided in three categories: 1) FPs that have an absorption rate almost constant with burn-up such ^{103}Rh, ^{109}Ag; 2) FPs that are initially present, but are burned with time such as ^{149}Sm,^{157}Gd; 3) FPs that are not initially present, but are produced during the burning in PWR such as ^{131}Xe,^{153}Eu. It is observed that ^{149}Sm is the only Fission Product of the second category that has a significant fractional absorption. It is roughly responsible for 10% of the absorption at BOL and it is rapidly burned until it reaches equilibrium at roughly 10,000 MWd/MT_{HM}. Gadolinium-57 has a similar behavior, but it is responsible for only 1.5% of the absorption at BOL and much less after that. The burning of ^{149}Sm helps to compensate the effect of newly produced FPs, so that no sharp decrease in k is present at the beginning of life such as in uranium dioxide fuel. Among the most absorbing FPs are ^{103}Rh, ^{109}Ag. Both of them are present at BOL and their absorption rate is almost constant along the burn-up. However, their mass decreases along the burn-up, as it is shown in Figure 5.7. As their mass decreases, their capture cross section increases slightly due to a softening of the spectrum and their absorption rate is almost constant. At BOL, they contribute for about 25% and 15% of all FP absorption. Their contribution

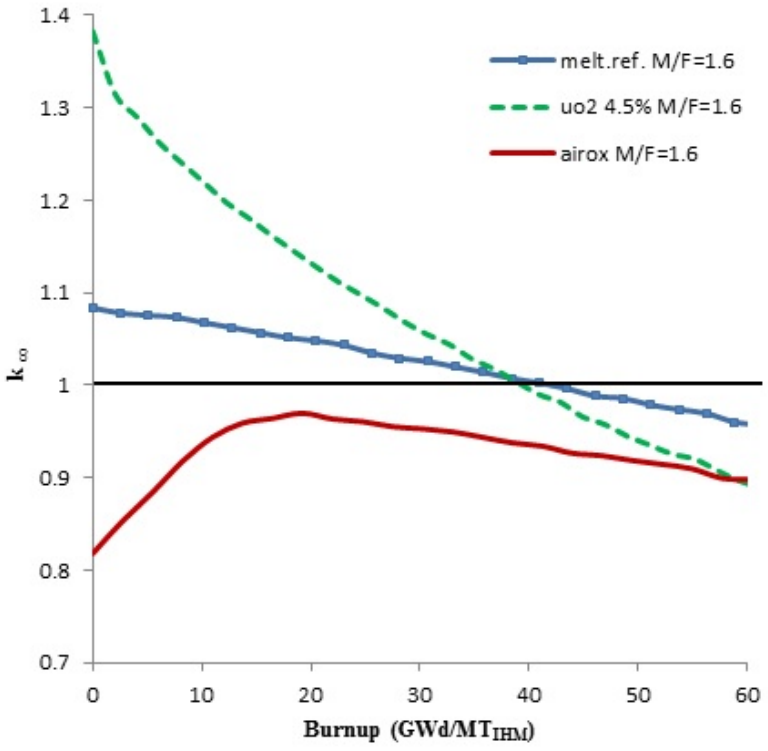

Figure 5.2: k_∞ evolution in the reference PWR unit cell using 18% FIMA TWR fuel reconditioned using an AIROX-like or a melt-refining process, as well as using standard UO_2 fuel with 4.5% ^{235}U enrichment.

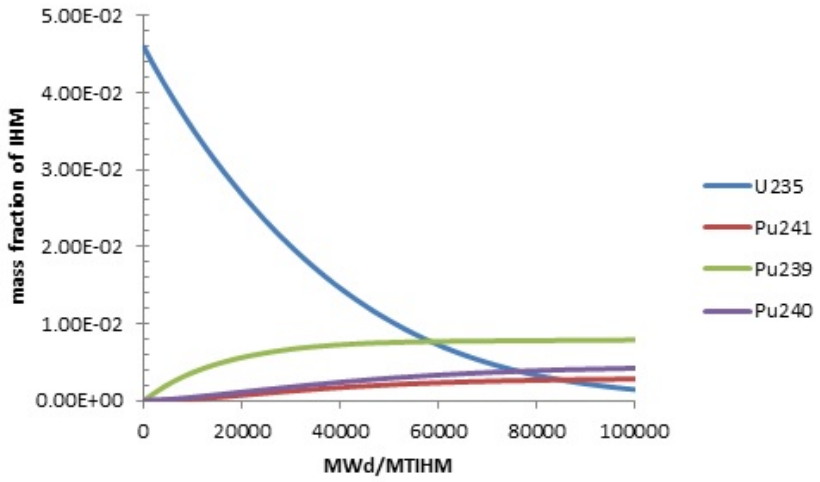

Figure 5.3: Evolution of selected isotope concentration in a 4.5% enriched UO_2 fueled PWR

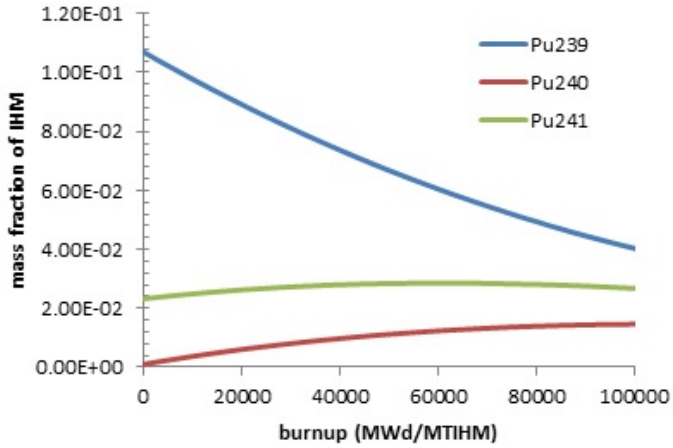

Figure 5.4: Evolution of selected isotope concentration in a TWR discharged and melt-refined fuel in PWR

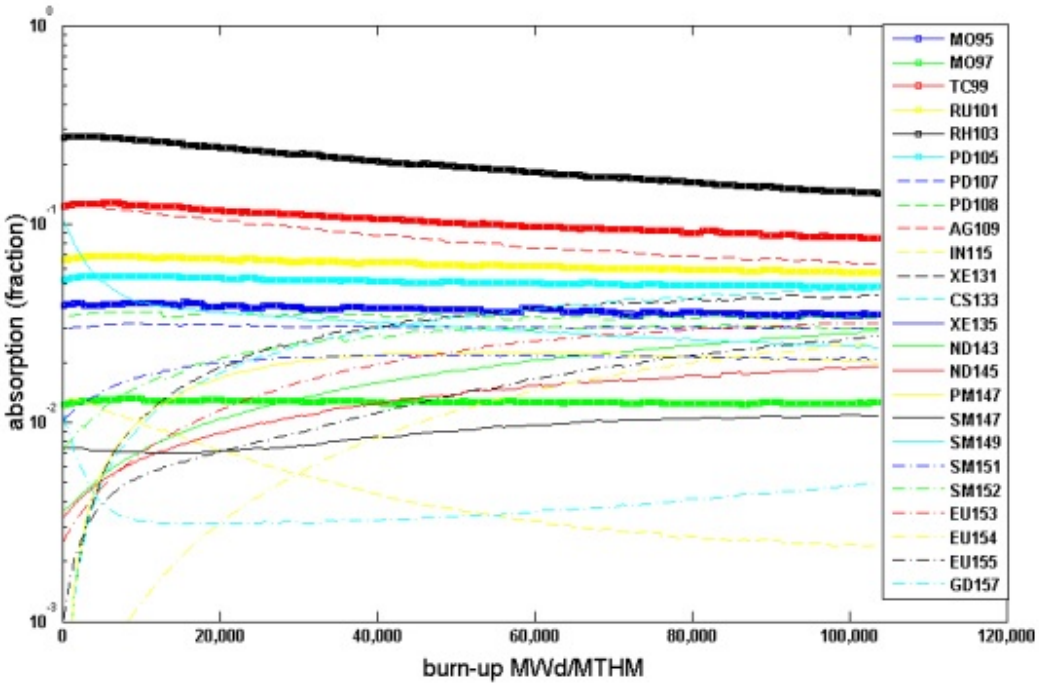

Figure 5.5: Fission Product fractional absorption as a function of burnup in TWR discharged fuel in a PWR. Only fission products that have a higher than 1% fractional absorption at any point of the burnup are plotted.

to Fission Products absorption decreases to about 20% and 9% at 100,000 MWd/MTHM.

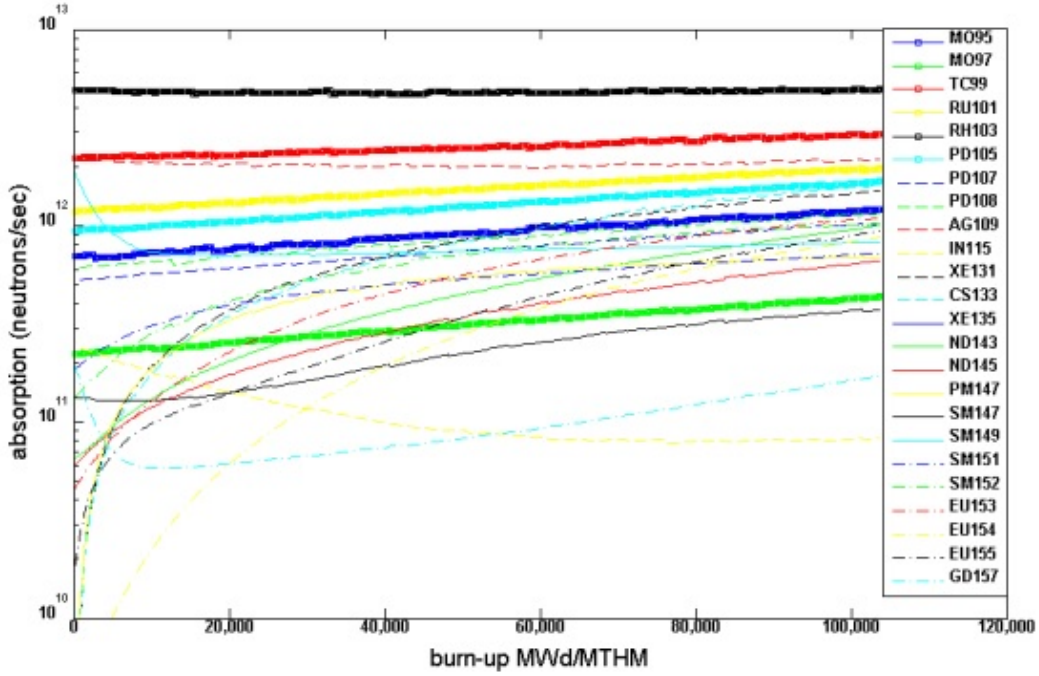

Figure 5.6: Absorption rates as a function of burn-up in TWR discharged fuel in a PWR. Only fission products that have a higher than 1% fractional absorption at any point of the burn-up are plotted.

A comparison of the neutron spectra at beginning of life is shown in Figure 5.8 for three different fuels. The spectrum is harder in the TWR melt-refined and AIROX treated fuel due to the higher fissile content than in the 4.5% UO_2 fuel and due to the fact that the absorption cross section of the plutonium isotopes is larger than that of ^{235}U. The fission products and zirconium in the TWR discharged and melt-refined fuel also contribute to the harder spectrum. The three pronounced depressions in the spectra are due to the strong absorbing resonances of ^{239}Pu and ^{241}Pu at ∼0.3 eV, of ^{240}Pu at ∼1 eV and of ^{238}U at ∼6.67eV.

The PWR fuel discharge burn-up is estimated using the linear reactivity theory assuming either a 4 or 5 batch fuel management scheme. An average power density of 322 W/cm^3 of fuel is assumed for estimating the cycle length

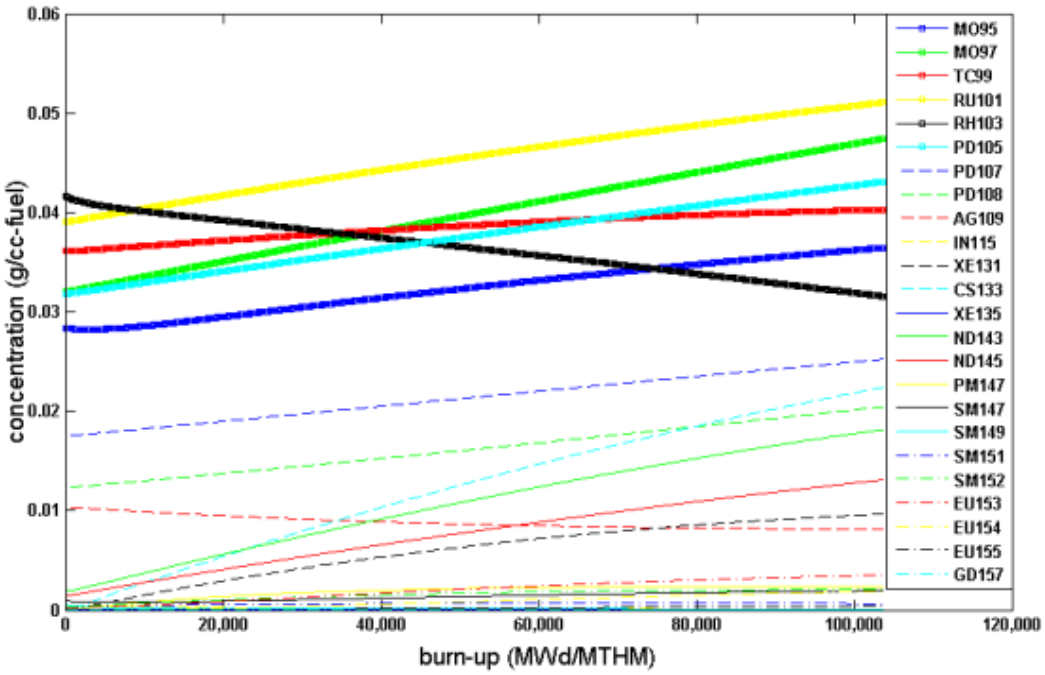

Figure 5.7: Fission Product concentration in fuel as a function of burn-up in TWR discharged fuel in a PWR. Only fission products that have a higher than 1% fractional absorption at any point of the burn-up are plot.

and the assumed neutron leakage probability from the core is 2.5%. Table 5.7 compares the discharge burn-up and cycle length for the TWR discharged and melt-refined fuel with those obtained using uranium dioxide of different enrichments. It is found that the discharge burnup of the melt-refined TWR fuel in the PWR is comparable to that of a 3.8% UO2 fueled PWR. However, for a comparable burnup, the cycle length with the melt-refined TWR fuel is shorter by approximately 20%. This is because the TWR melt-refined fuel has a lower HM density.

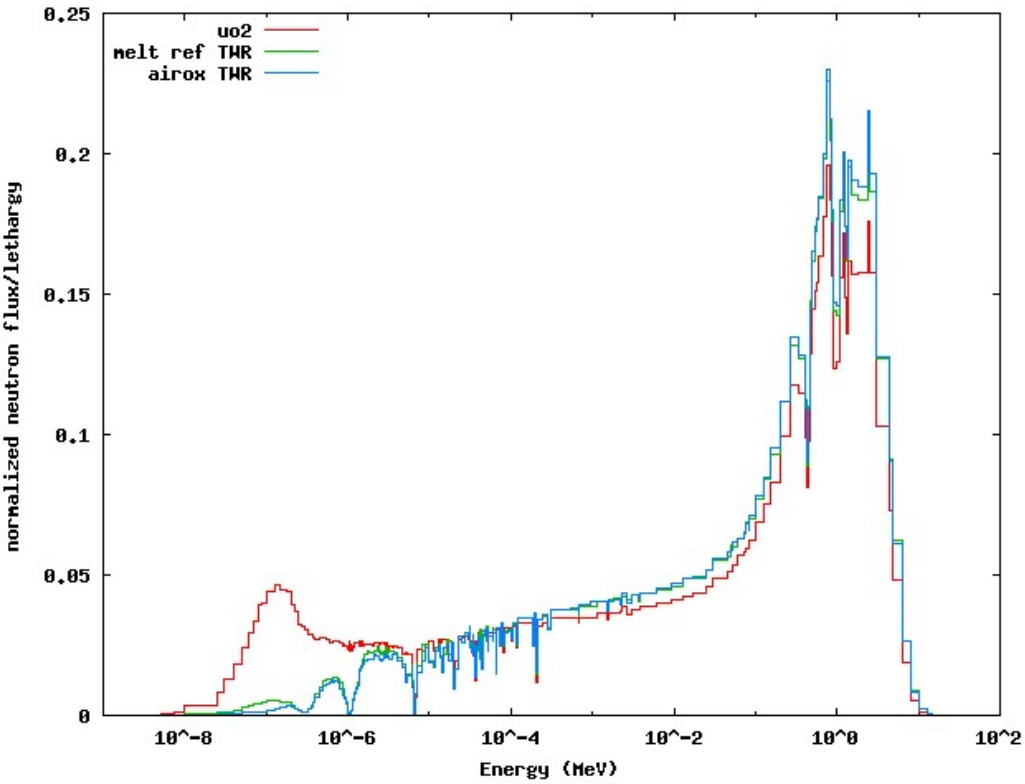

Figure 5.8: Normalized flux for TWR discharged melt-refined fueled, AIROX treated fuel and 4.5% UO_2 fueled PWR; M/F=1.6

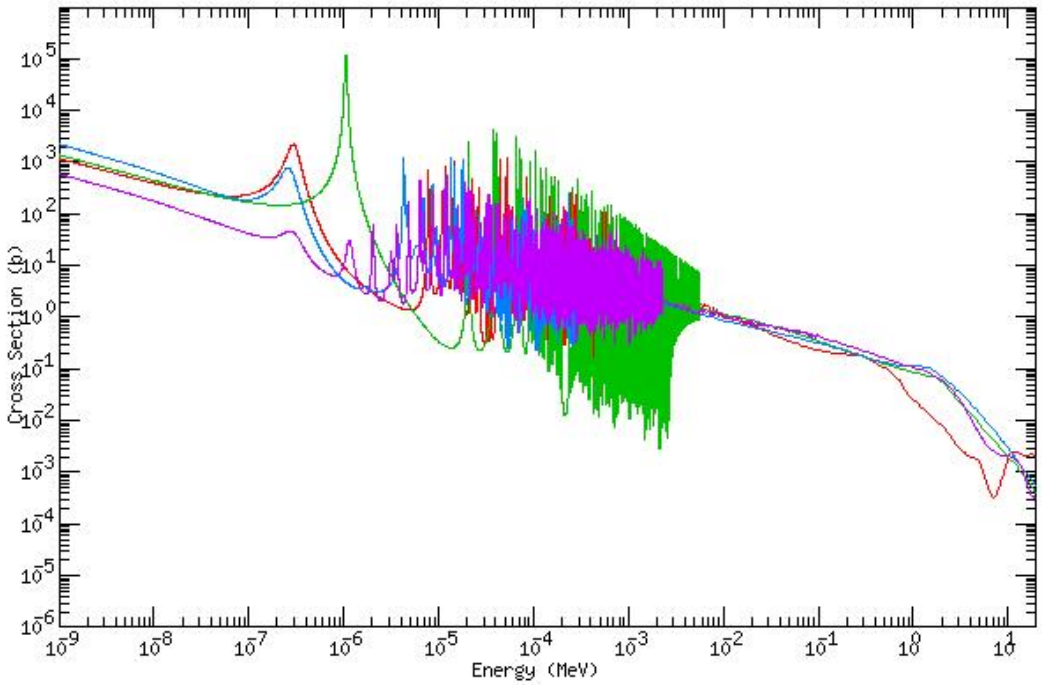

Figure 5.9: Capture cross sections for ^{239}Pu (green); ^{240}Pu (blue); ^{241}Pu (red), ^{235}U (purple).

Table 5.7: Discharge Burnup and Cycle Length of PWR Cores Fueled with TWR Melt-Refined fuel and with UO_2. 2.5% Leakage Probability. M/F=1.6.

n=5			
fuel type	discharge burnup MWd/MTIHM	cycle burnup MWd/MTIHM	cycle lenght (days)
melt-ref	50,933	10,186	238
4.5% UO_2	59,921	11,984	352
4% UO_2	53,381	10,676	313
3.5% UO_2	46,246	9,249	271
n=4			
fuel type	discharge burnup MWd/MTIHM	cycle burnup MWd/MTIHM	cycle lenght (days)
melt-ref	48,896	12,733	298
4.5% UO_2	57,524	14,381	422
4% UO_2	51,246	12,811	376
3.5% UO_2	44,396	11,099	326

5.5 Modified PWR core

5.5.1 Melt-refining

The water to heavy-metal ratio of a standard PWR fuel assembly design is optimized for enriched uranium dioxide fuel having 4% to 5% enrichment. The TWR discharged and melt-refined fuel features a significantly larger macroscopic absorption cross section than the reference enriched uranium fuel and is therefore expected to benefit from a larger moderator-to-fuel volume ratio. A parametric study was performed to estimate to what extent increasing the water volume fraction can increase the attainable discharge burnup in a PWR. The k dependence on the moderator-to-fuel volume ratios is shown in 5.13. It is found that increasing the moderator-to-fuel volume ratio (M/F) increases the initial k_∞ value but reduces the conversion ratio causing the k to decrease with burn-up more rapidly. $\rho = 0$ is arrived at approximately the same burnup for M/F in the range from 4 to 6. The reference case with P/D = 1.32 (M/F = 1.6) is the worst case.

Evolution of k for moderator-to-fuel volume ratio M/F = 1.6, 2.8, 4.1, 5, 6.2, 9.9 are shown in Figure 5.13. The initial increase in reactivity becomes more pronounced for higher M/F cores; it is due to the increase rate of neutron capture in strongly absorbing fission products loaded with the reconditioned B&B fuel. Using a polynomial fit to each of the curves of Figure 5.13, the 5-batch EOC core average, k_{core}, was calculated using Equation (5.6) as a function of the cycle length. Figure 5.13 reports the results obtained. Table 5.8 summarizes the maximum attainable discharge burn-up. It is observed that the burn-up attainable in the reference M/F ratio of 1.6 of 49 GWd/MTHM is close to that being achieved in today's PWR using enriched uranium – $\sim$ 55,000 MWd per Metric Ton of Initial Heavy Metal (MT_{IHM}). However, by increasing the moderator-to-fuel volume ratio the attainable burn-up can be doubled. The reduction in the attainable burnup for M/F > 4.1 indicates that these cores are over-moderated.

Figure 5.11 shows the various spectra in comparison to the spectrum of a PWR. It is noted that that only the case of M/F = 9.9 presents an over moderated neutron spectrum at BOL, all other M/F have a spectrum that is harder than the PWR. Figure 5.12 shows the spectra of selected M/F at the discharge burn-up of Table 5.8; there is a significant change in the spectrum for melt-refined fuel.

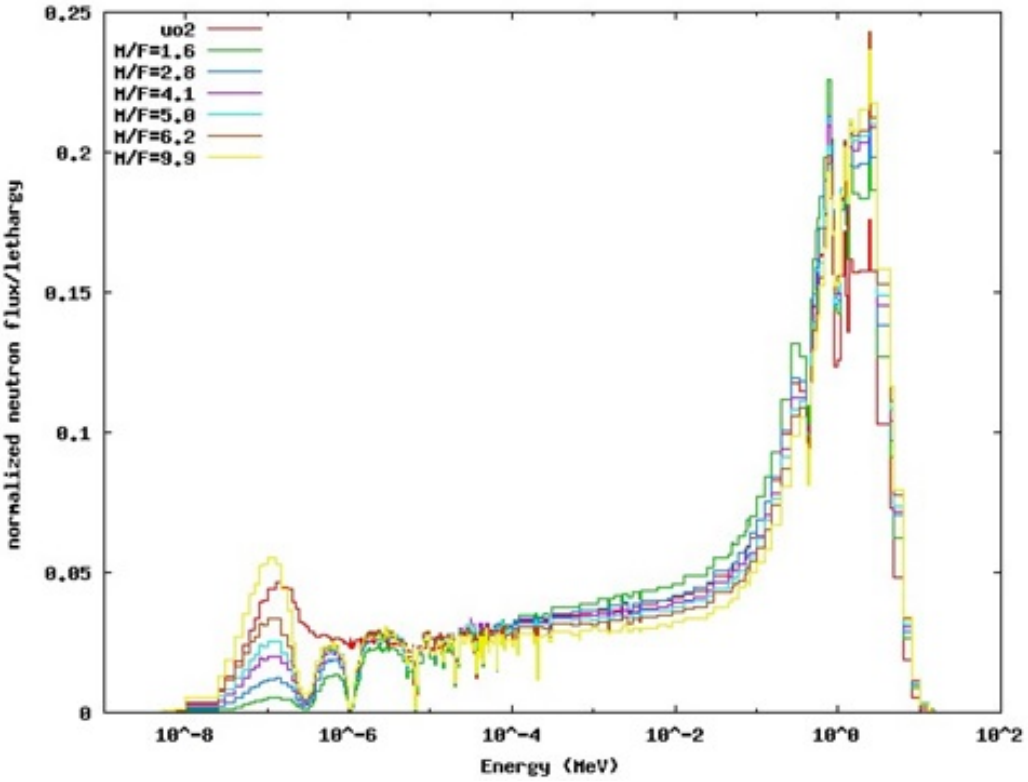

Figure 5.10: Normalized flux for TWR discharged melt-refined fueled and 4.5% UO2 fueled PWR at BOL

Table 5.8: Maximum Discharge Burn-up for Melt-refined Fuel for Various Moderator-to-Fuel Volume Ratios

M/F	P/D	discharge burnup MWd/MTIHM	Cycle length (days)
1.6	1.32	49,485	232
2.8	1.57	94,704	444
4.1	1.79	105,583	495
5.0	1.92	104,516	490
6.2	2.11	102,596	481
9.9	2.56	92,998	436

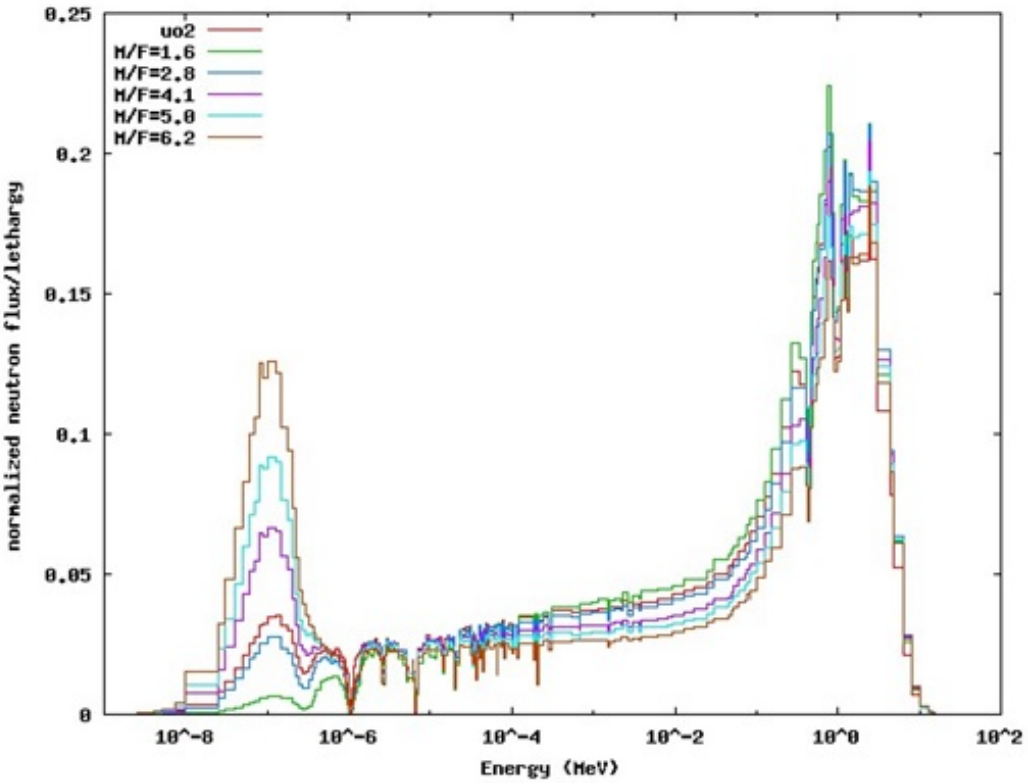

Figure 5.11: Normalized flux for TWR discharged melt-refined fueled and 4.5% UO2 fueled PWR at discharge burn-up.

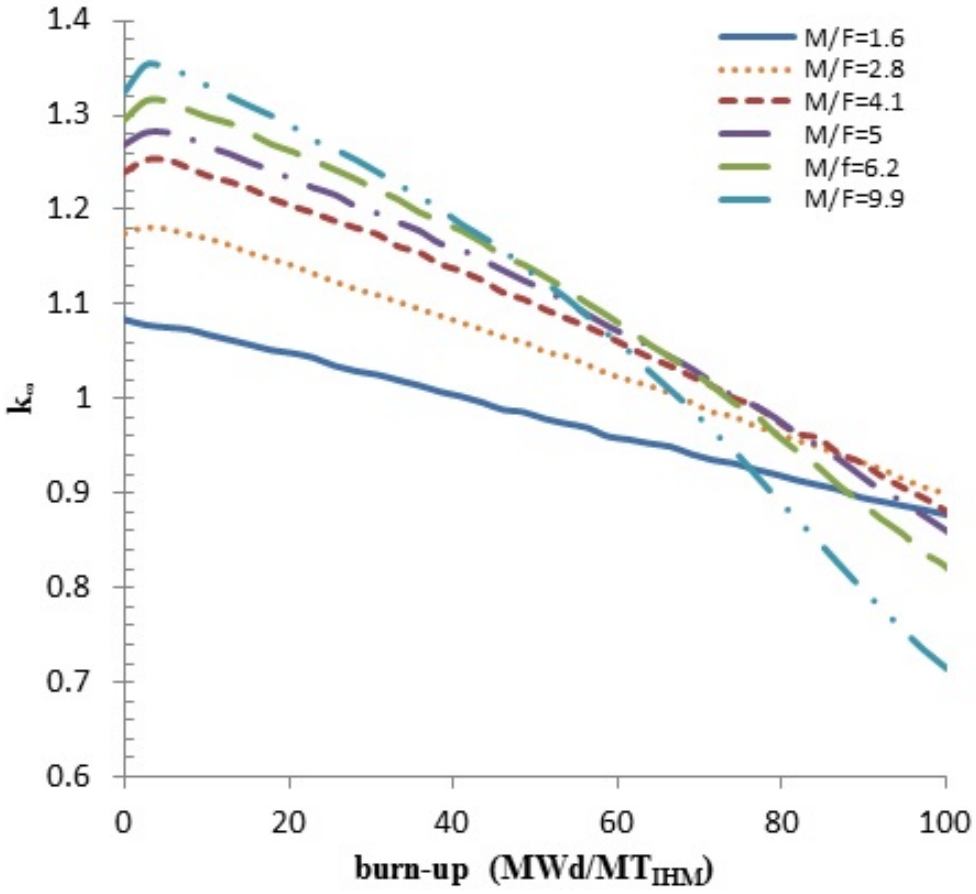

Figure 5.12: k_∞ evolution in the reference PWR unit cell using 18% FIMA TWR fuel reconditioned using a melt-refining process for various moderator-to-fuel volume ratios

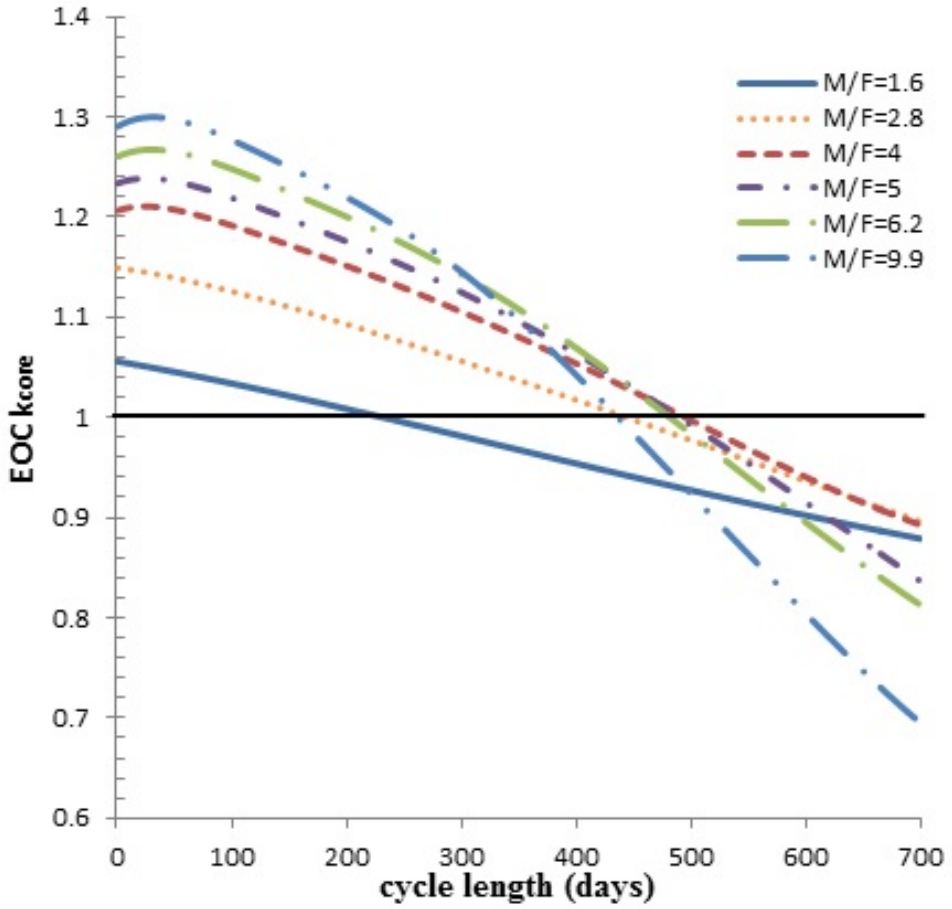

Figure 5.13: EOC k evolution in the reference PWR unit cell using 18% FIMA TWR fuel reconditioned using a melt-refining process for various moderator-to-fuel volume ratios as a function of the cycle lenght

Table 5.9: Maximum Discharge Burn-up for AIROX Treated Fuel for various Moderator-to-Fuel Volume Ratios

M/F	P/D	discharge burnup MWd/MT_{IHM}	Cycle length (days)
1.6	1.32	-	-
2.8	1.57	-	-
4.1	1.79	47,380	207
5.0	1.92	66,149	289
6.2	2.11	76,220	333

5.5.2 AIROX

Figure 5.14 shows the k_∞ evolution when using AIROX treated fuel for several moderator-to-fuel volume ratios. These k_∞ evolutions are of a parabolic shape; the relatively large initial increase in reactivity is due to the larger concentration of fission products in the AIROX processed fuel than in the melt-refined fuel. It is observed that in all M/F ratios examined above the reference value, k exceeds unity at a certain burnup range. This implies that for large enough M/F values a multi-batch core can be designed to have fuel batches with sufficient excess reactivity to compensate for the reactivity deficiency of the fresh fuel batch. Figure 5.15 shows the core average k for selected M/F ratios as a function of the cycle length for both BOC and EOC in a 5-batch core. These results were obtained by applying Equations (5.5) and (5.6) using polynomial fits to the curves of Figure 5.14. The maximum attainable burn-up can be graphically deduced from Figure 5.15 as the highest burn-up for which both EOC and BOC are > 1. It is observed that for M/F = 2.8 the BOC k_{core} is always < 1 implying that a critical reactor cannot be achieved for this M/F value. The vertical line in Figure 5.15 marks the longest cycle length for which the M/F = 5 core can be critical at BOC. Table 5.9 summarizes the maximum attainable cycle length and burnup for selected M/F ratios. It is observed that even with AIROX reconditioning the additional burnup B&B reactor used fuel can accumulate in an increased moderation PWR core exceeds the ~ 55 GWd/MT_{IHM} of contemporary enriched uranium fueled PWRs. This burn-up is, however, smaller that attainable using the melt-refining process.

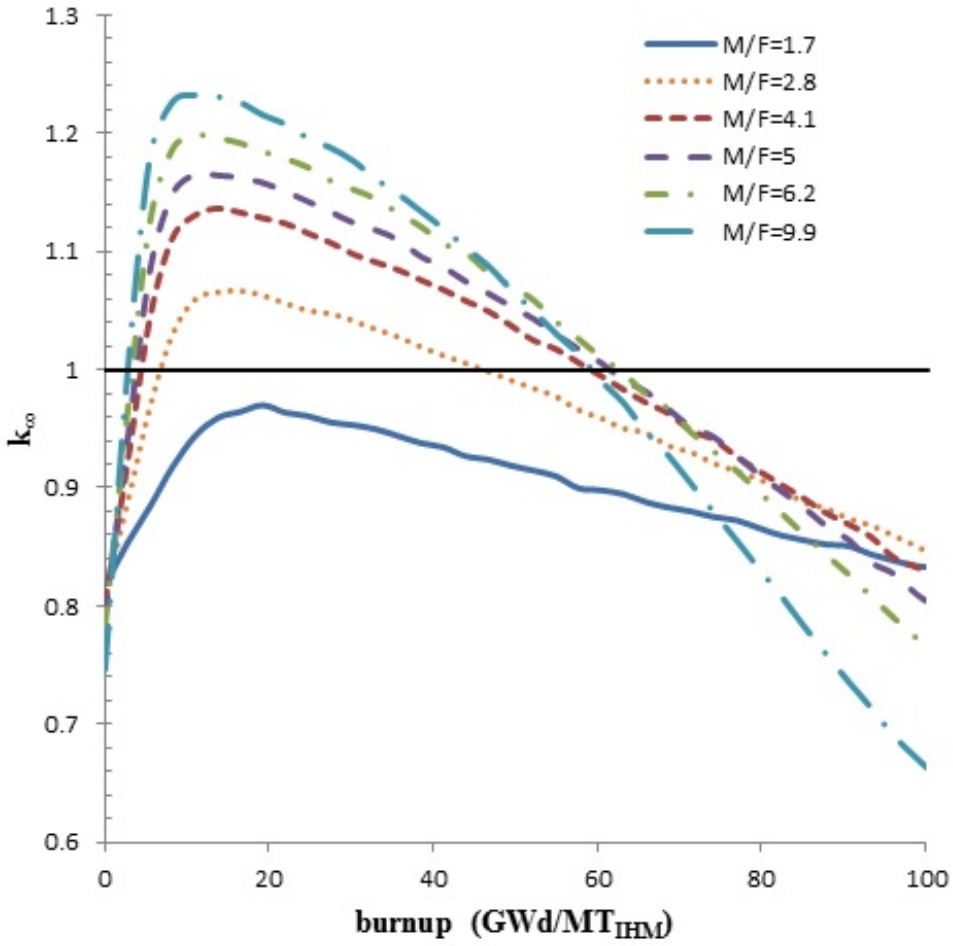

Figure 5.14: k_∞ evolution in the reference PWR unit cell using 18% FIMA TWR fuel reconditioned using AIROX process for various moderator-to-fuel ratios

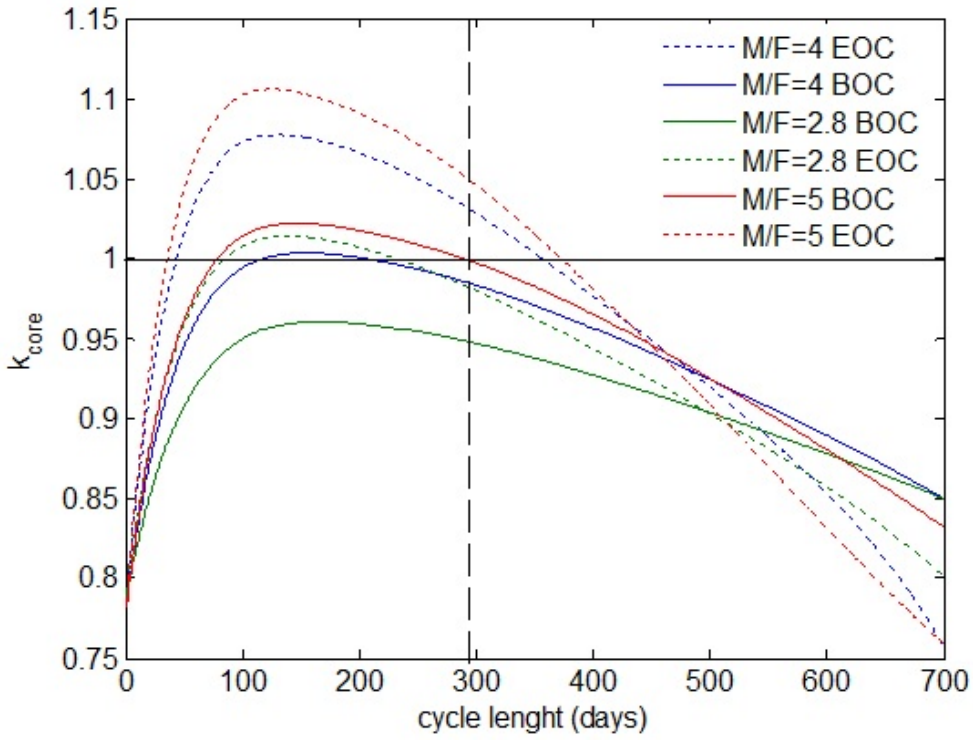

Figure 5.15: k_{core} at BOC and EOC as a function of cycle length in the reference PWR unit cell using 18% FIMA TWR fuel reconditioned using AIROX process for various moderator-to-fuel ratios. The vertical line indicates the maximum burn-up for M/F = 5.

5.6 Reactivity coefficients

To ensure safety, the PWR cores fed with discharged B&B fuel must have negative temperature coefficients of reactivity over the entire cycle. Of most concern is the coolant temperature reactivity coefficient; it is the focus of this section. As PWRs use soluble boron for excess reactivity control, the effect of soluble boron on the coolant temperature reactivity coefficients is accounted for. For melt-refined fuel, the maximum excess reactivity and, hence, maximum boron concentration, are at the beginning of cycle. However, with AIROX treated fuel the core excess reactivity peaks at the central part of the cycle. Figure 5.16 shows the k_{core} variation over a cycle calculated using Equation (5.3). The highest reactivity points are identified for each M/F examined. The coolant temperature reactivity coefficient of the melt-refining case is also calculated at the EOC, when there is no boron, but the fuel composition is significantly different compared to BOC.

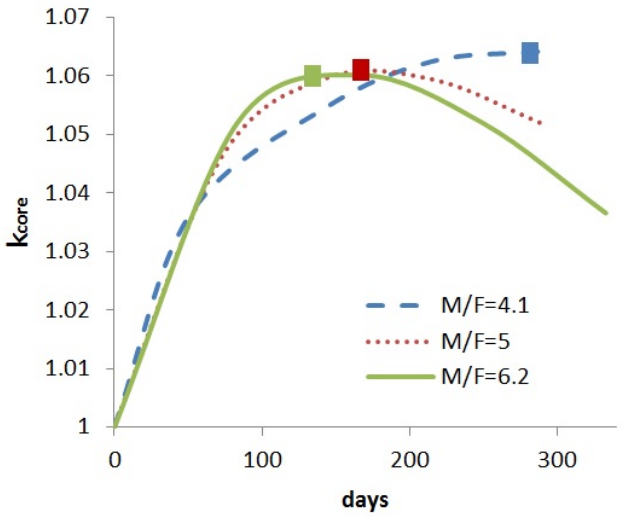

Figure 5.16: k_{core} evolution over a cycle for AIROX fuelled PWR for various M/F ratios. The highest reactivity points are identified with squares.

The coolant temperature reactivity coefficient at a given time in the cycle is deduced by simulating a unit cell the fuel composition of which is an average of the fuel composition in each of the five batches at the same time

in the cycle. Natural boron is added to the water at the amount required to compensate for the maximum excess reactivity - between 1100 ppm to 1490 ppm. The water density is varied over a range of 50 degrees from 0.68 g/cm3 (325 °C) to 0.76 g/cm3 (277 °C) considering 15 MPa pressure. Reactivity coefficients from a variation from state 1 to 2 is calculated as:

$$\alpha = \frac{k_1 - k_2}{k_1 k_2 \Delta T} \times 10000 \quad (\frac{pcm}{K}) \tag{5.7}$$

Figure 7 shows the reactivity coefficients inferred from these calculations. It is concluded that the permissible PWR design space for AIROX treated TWR fuel is $\sim 4 <$ M/F$<$5.4, while for melt-refined fuel it is $1.7 <$ M/F $<$ 4.5, by extrapolation from Figure 5.17. The maximum attainable burnups are about 70 GWd/MTIHM for AIROX and 105 GWd/MTIHM for melt-refined fuel. Both burnups are higher than the $\sim$ 55 GWd/MTU of typical enriched uranium fuelled PWR.

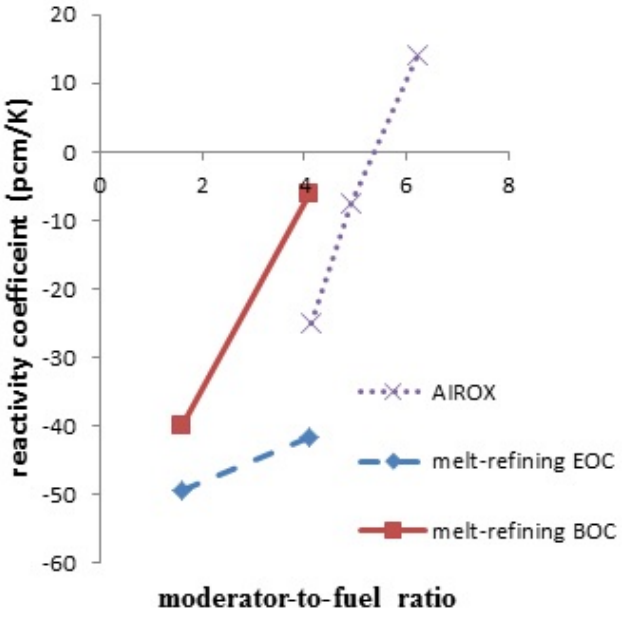

Figure 5.17: Coolant temperature reactivity coefficient for AIROX and melt-refining fuelled PWR cores for various M/F ratios.

5.7 Discharged Fuel Characteristics

Table 5.10 compares selected characteristics of the fuel discharged from PWRs for different feed fuel compositions and several M/F ratios. It is observed that the fissile Pu to total Pu ratio can decrease via additional irradiation in PWRs from 81% in the fuel discharged from the TWR core down to 38% for melt-refined fuel or 52% for AIROX treated fuel. Both values are smaller than the 68% of enriched uranium fueled PWR. The same applies to the total amount of plutonium discharged per unit of electricity generated by the fuel in the TWR and PWR cores 209 and 248 versus 281 kg/GW_eYr. Likewise for the total TRU discharged per unit of electricity generated. Table 5.10 compares the Figure Of Merit (FOM) for proliferation resistance, described in 3.6.

It is observed that for all the studied M/F ratios, except for the melt-refining M/F = 1.7 case, the FOM is negative; for certain designs even more negative than of the reference PWR. The additional irradiation step is therefore highly effective in making the final discharged fuel proliferation resistant.

Table 5.10: Summary of characteristics of TWR-PWR fuel cycle options

	TWR	PWR	melt-refining			AIROX	
M/F	-	1.6	1.6	2.8	4.1	4.1	5
burnup GWd/MT_{IHM}	171.0	55.0	49.5	94.8	105.6	47.4	66.1
Pu/HM	12.28%	1.54%	10.73%	7.27%	5.46%	9.45%	7.77%
Fiss. Pu/Pu	81.81%	67.93%	72.43%	52.87%	38.16%	64.45%	52.26%
Kg Pu/GWeY	597	281	360	209	148	309	248
Kg TRU/GWeY	608	312	369	221	161	317	258
FOM	0.90	-0.38	0.09	-0.57	-0.76	-0.29	-0.49

5.8 Conclusions

Based on this preliminary study it is concluded that it is feasible to operate PWRs with B&B used fuel that underwent a proliferation-resistant reconditioning using either the melt-refining or AIROX-like process. The additional burnup the TWR recycled fuel can achieve in the PWR is up to 70

GWd/MT_{IHM} for AIROX treated or 105 GWd/MT_{IHM} for ideal melt-refining treated fuel. The burnup reactivity swing is significantly smaller than of conventional PWR cores due to a combination of several phenomena: high initial concentration of fission products and fissile fuel, small relative reduction in the fissile fuel content with burnup, and depletion of certain fission products that function as burnable poisons. In order to achieve initial criticality of the PWR core that is loaded with AIROX treated B&B discharged fuel it will be necessary to add fissile fuel. The fissile plutonium fraction discharged from the PWR is smaller than in standard PWR used nuclear fuel, and so are the total amount of plutonium and of TRU per unit of electricity generated. The B&B fuel that underwent irradiation in PWR can be even more proliferation resistant than a standard PWR used nuclear fuel. However, due to the large water-to-fuel volume ratio required, these benefits may have to come on the expense of reduced PWR power density.

Chapter 6

Conclusions

6.1 Options evaluated

In this work, the fuel cycle of B&B reactors was studied, examining various options to maximize B&B fuel utilization. First, it was found in Chapter 3 that B&B reactors working at the minimum discharge burnup $\sim$ 18-20% produce a significant quantity of plutonium ($\sim$ 10%) in discharged fuel, of which $\sim$ 80% is fissile. Using limited separation reprocessing to bring the discharge burnup up to 55%, it was found that the fissile plutonium content can go down to 66% of total plutonium and the discharge plutonium has a 4-fold reduction.

Alternatives to high-burnup B&B reactors were studied with the goal of increasing fuel utilization. First, in Chapter 4 a second tier breed and burn reactor (2TB&B) working with double cladded fuel was designed. It was found that this reactor can bring fuel utilization up to 30% FIMA. Second, a Accelerator Driven Reactor (ADR) was studied, bringing fuel utilization up to 40% FIMA. Lastly, in Chapter 5 the possibility of recycling the spent fuel in PWRs was studied. It was found that it is possible to burn the B&B discharged fuel up to 105.6 GWd/MT$_{IHM}$ and 66.1 GWd/MT$_{IHM}$, for melt refining and AIROX, respectively. Table 6.1 gives a summary of the options studied in Chapter 4 and 5. For TWR AIROX and melt refining, the highest burnup case with negative reactivity coefficients has been chosen. It is observed that only the B&B-PWR fuel cycles are able to reduce the fraction of fissile plutonium to levels lower than PWR. It is also observed that all B&B options have a higher production of fissile Pu per GWeY. Only the

TWR melt refining cycle is able to bring fissile Pu production to essentially the same levels of PWR. Therefore when looking at reduction of plutonium content, an additional burnup step in a softer spectrum should be preferred.

Table 6.1: Comparison of selected fuel cycle characteristics of the 20%B&B and additional burnup steps. DU means depleted uranium; DC means double cladding.

Characteristic	PWR	20%B&B	TWR AIROX	TWR melt	2TB&B	ADR
fuel type	Enriched U	DU	DU+ AIROX	DU+ melt ref	DU+ DC	DU+ DC
U utilization (%)	0.6	20	25	29	30	40
Fis. Pu (Kg/GWeY)	143	388	248	148	235	153
Fis. Pu/Pu (%)	63.7	81.4	52.3	38.2	72.5	67.4
FOM	-0.32	0.77	-0.49	-0.76	0.31	0.16

The ingestion radiotoxicity, defined in Section 3.4, is plotted in Figure 6.1 for the fuel cycles analyzed in Chapter 4 and Chapter 5. Ingestion radiotoxicity and decay heat have been calculated with ORIGEN 2.2.

It is observed that the long term radiotoxicity of the fuel cycle with TWR discharged fuel that underwent an additional step in a PWR is higher than the initial B&B 20% radiotoxicity. This is due to the fact that minor actinides content increases in soft spectrum, though ^{239}Pu effectively decreases. It is also observed that the double cladding reactors, ADR and 2TB&B, yield a lower radiotoxicity than the 20%B&B. It is therefore preferable to choose a fast spectrum for additional burning rather than soft spectrum for radiotoxicity. However, for a reduction of the fraction of fissile Pu, the soft spectrum is more effective as can be noted from the summary Table 6.1.

Finally, Figure 6.2 reports the decay heat for the various fuel cycles. The same radiotoxicity observations can be made in regards of decay heat, as it follows substantially the same evolution of ingestion radiotoxicity.

In conclusions B&B reactors operating at the minimum burn-up have strong drawbacks in terms of discharged plutonium content and proliferation resistance. The addition of a further burnup step, is successful in utilizing the plutonium produced in the B&B reactors. This can be done with limited separation fuel cycles, but also with innovative strategies to reduce the plutonium content. Innovative strategies can involve a minimal recondition-

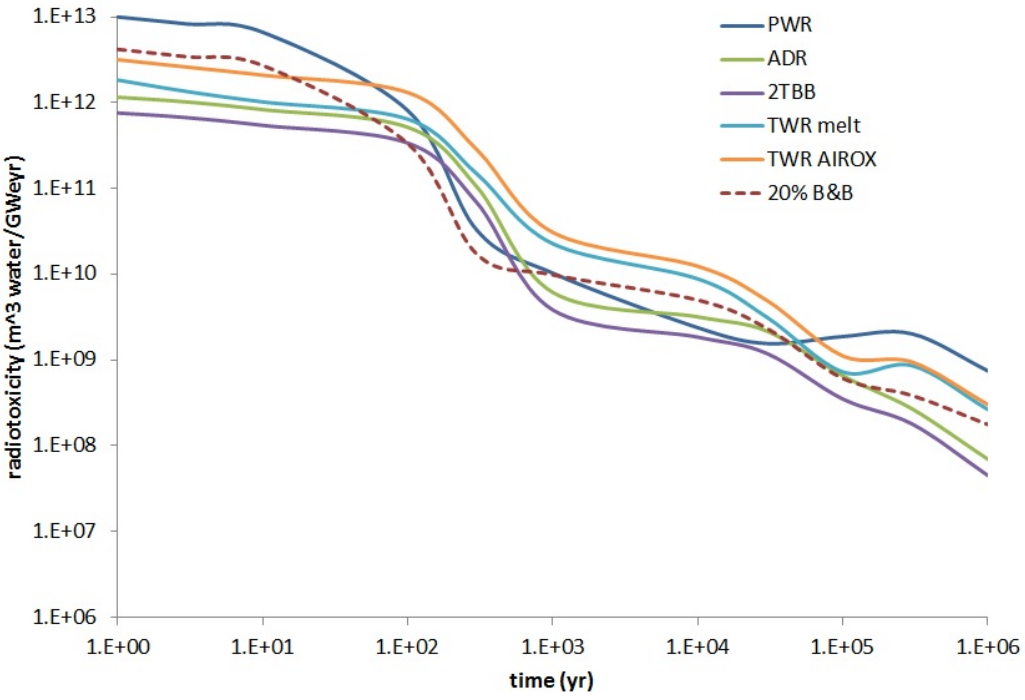

Figure 6.1: Ingestion Radiotoxicity for the various fuel cycle analyzed

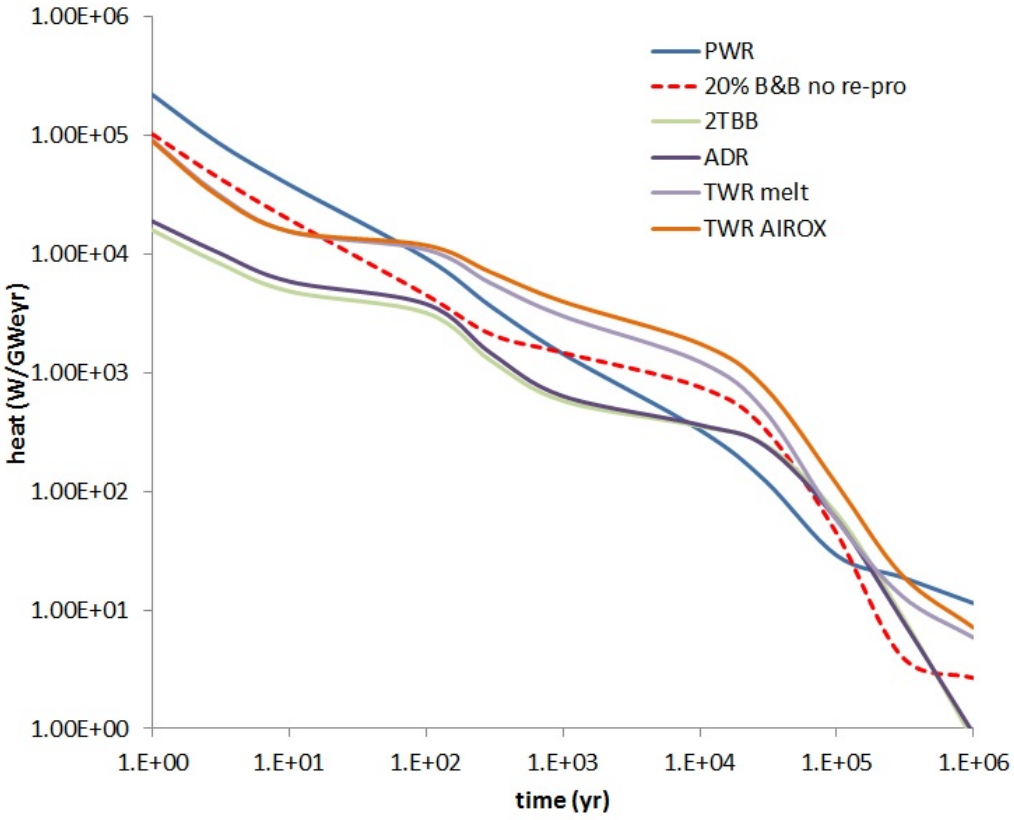

Figure 6.2: Decay Heat (W/GW_eYr) for the various fuel cycle analyzed

ing, double cladding, or a re-utilization of the fuel in PWR. These processes can utilize the fuel in a proliferation resistant fuel cycle. However, future studies are needed to assess the feasibility of these recycling processes such as double-cladding process and to assess the feasibility of AIROX and melt refining for oxide and metallic fuels.

Moreover, new design options still need to be explored. The double cladding process, which is a novel solution of this work, could be used in the same B&B reactor in place of melt-refining, designing a reactor that uses single and double clad assemblies. Moreover, the reduction of plutonium content in a soft spectrum could also be carried out in the same Breed and Burn reactor, with an additional blanket that uses a moderator such as graphite, producing a soft spectrum environment. Fuel could be discharged from the main B&B and then load into the soft spectrum blanket.

References

[1] U.S. Energy Information Administration. "International Energy Outlook 2013". *DOE/EIA-0484(2013)* (2013).

[2] International Energy Agency. "World Energy Outlook 2013" (2013).

[3] Intergovernmental Panel on Climate Change. "Climate Change 2014: Mitigation of Climate Change". *IPCC WGIII AR5* (2014).

[4] *Gen. IV International Forum - GIF overview www.gen-4.org.*

[5] L. Burris J.C. Hesson M. J. Feldman. "Description and proposed operation of the fuel cycle facility for the second experimental breeder reactor (EBR-II)". *ANL - 6605 Reactor Technology (TID-4500, 20th Ed.) AEC Research and Development Report* (1963).

[6] S. M. FEINBERG and E.P. KUNEGIN. *Proceedings of the International Conference on the Peaceful Uses for Atomic Energy* (1958), p. 447.

[7] W.T. LOH. "An evaluation of the fast-mixed spectrum reactor". *MA thesis. Massachussets Institute of Tecnnology,* (1980).

[8] Staffan A. Qvist. "Safety and core design of large liquid-metal cooled fast breeder reactors". *UC Berkeley Ph.D. Thesis* (2013).

[9] E. Teller et al. "Completely Automated Nuclear Power Reactors for Long-Term Operation: Ill. Enabling Technology for Large-Scale,Low-Risk Affordable Nuclear Electricity". *Lawrence Livermore National Laboratory* UCRL-JRNL-122708 (2003).

[10] R. Petroski. "Direct Use of Depleted Uranium As Fuel in a Traveling-Wave Reactor". *Transactions of the American Nuclear Society* 101 (2009), pp. 741–742.

[11] H. Sekimoto, K. Ryu, and Y. Yoshimura. "CANDLE: The new burnup strategy". *Nuclear Science and Engineering* 139.3 (2001), pp. 306–317.

[12] Tyler Ellis et al. "Traveling-Wave Reactors: A Truly Sustainable and Full-Scale Resource for Global Energy Needs". *Proceedings of ICAPP 10, San Diego, CA, USA, June 13-17, 2010* (2010).

[13] Florent Heidet and Ehud Greenspan. "PERFORMANCE OF LARGE BREED-AND-BURN CORE". *Nuclear Technology* 181.3 (2013), pp. 381–407.

[14] F. Heidet and E. Greenspan. "Neutron Balance Analysis for Sustainability of Breed-and-Burn Reactors". *Nuclear Science and Engineering* 171.1 (2012), pp. 13–31.

[15] M. J. Hackett and G. Povirk. "HT9 Development for the Traveling Wave Reactor, invited". *Transactions of the American Nuclear Society* 106 (2012), pp. 1133–1135.

[16] M. B. Toloczko, F. A. Garner, and C. R. Eiholzer. "IRRADIATION CREEP AND SWELLING OF THE US FUSION HEATS OF HT9-1MO AND 9CR-1MO TO 208-DPA AT SIMILAR-TO-400-DEGREES-C". *Journal of Nuclear Materials* 212 (1994), pp. 604–607.

[17] F. Heidet. "Maximum Fuel Utilization in Advanced Fast Reactors". *University of California, Berkeley, Department of Nuclear Engineering* (2010).

[18] Alan E. Waltar, Donald R. Todd, and Pavel Tsvetkov. "Fast Spectrum Reactors". *Springer Science* (2012).

[19] H. Sekimoto and A. Nagata. "Performance optimization of the CANDLE reactor for nuclear energy sustainability". *Energy Conversion and Management* 51.9 (2010), pp. 1788–1791.

[20] A. Nagata, N. Takaki, and H. Sekimoto. "A feasible core design of lead bismuth eutectic cooled CANDLE fast reactor". *Annals of Nuclear Energy* 36.5 (2009), pp. 562–566.

[21] A. Nagata and H. Sekimoto. "Effects of recladding in CANDLE reactor". *Bulletin of the Research Laboratory for Nuclear Reactors* 31.1-2 (2007), pp. 135–137.

[22] H. Sekimoto. "Application of candle burnup strategy for future nuclear energy utilization". *Progress in Nuclear Energy* 47.1-4 (2005), pp. 91–98.

[23] Hiroshi Sekimoto and Akito Nagata. ""CANDLE" burnup regime after LWR regime". *Progress in Nuclear Energy* 50.2-6 (2008), pp. 109–113.

[24] Z. Su'ud and H. Sekimoto. "The prospect of gas cooled fast reactors for long life reactors with natural uranium as fuel cycle input". *Annals of Nuclear Energy* 54 (2013), pp. 58–66.

[25] Charles Ahlfeld et al. "Conceptual Design of a 500 MWe Traveling Wave Demonstration Reactor Plant". *Proceedings of ICAPP 2011, Nice, France, May 2-5* (2011).

[26] PAVEL HEJZLAR et al. "TERRAPOWER, LLC TRAVELING WAVE REACTOR DEVELOPMENT PROGRAM OVERVIEW". *NUCLEAR ENGINEERING AND TECHNOLOGY* 45.6 (2013).

[27] Florent Heidet and Ehud Greenspan. "SUPERPRISM-SIZED BREED-AND-BURN SODIUM-COOLED CORE PERFORMANCE". *Nuclear Technology* 181.2 (2013), pp. 251–273.

[28] Florent Heidet and Ehud Greenspan. "Feasibility of lead cooled breed and burn reactors". *Progress in Nuclear Energy* 54.1 (2012), pp. 75–80.

[29] Ehud Greenspan and Florent Heidet. "Energy sustainability and economic stability with Breed and Burn reactors". *Progress in Nuclear Energy* 53.7 (2011), pp. 794–799.

[30] Ehud Greenspan. "A Phased Development of Breed-and-Burn Reactors for Enhanced Nuclear Energy Sustainability". *Sustainability* 4.10 (2012), pp. 2745–2764.

[31] A.E. Dubberley. "SuperPrism Oxide and Metal Fuel Core Designs". *Proceedings of ICONE 8, 8th Conference on Nuclear Engineering, April 2-6, 2000, Baltimore, MD USA* (2000).

[32] Allen E. Dubberley. "S-PRISM Fuel Cycle Study". *Proceedings of ICAPP 03, Crdoba, Spain, May 4-7, 2003* (2003).

[33] MCNP5. "MCNP5 MonteCarlo Code". *Los Alamos National Laboratory* (2008).

[34] Alan Croff. "ORIGEN 2.2 - Isotope Generation and Depletion Code." (2002).

[35] R.L. Moore. "MOCUP: MCNP-ORIGEN2 Coupled Utility Program". *INEL Editor* (1995).

[36] R. Petroski, B. Forget, and C. Forsberg. "USING THE NEUTRON EXCESS CONCEPT TO DETERMINE STARTING FUEL REQUIREMENTS FOR MINIMUM BURNUP BREED-AND-BURN REACTORS". *Nuclear Technology* 175.2 (2011), pp. 388–400.

[37] A. Hogenbirk. "An easy way to perform a radiation damage calculation in a complicated geometry". *Fusion Engineering and Design* 83.1012 (2008), pp. 1828–1831.

[38] D. Majumdar et al. "Recycling of Nuclear Spent Fuel with AIROX Processing". *U.S. Department of Energy DOE Idaho Field Office, DOE/ID-10423* (1992).

[39] K. Wang et al. "Benchmarking and Validation of MOCUP". *PHYSOR-2000, The 2000 ANS International Topical Meeting on Advances in Reactor Physics and Mathematics and Computation into the Next MillenniumPittsburgh, Pennsylvania, May 7-11,* (2000).

[40] S. Qvist, F. Heidet, and E. Greenspan. "Reactivity Feedbacks of the UCB Breed-and-burn Reactor". *Transactions of the American Nuclear Society* 104 (2011), pp. 857–8.

[41] E. A. Hoffman, W.S. Yang, and R.N. Hill. "Preliminary Core Design Studies for the Advanced Burner Reactor over a Wide Range of Conversion Ratios". *ANL-AFCI-177* (2006).

[42] Charles G. Bathke et al. "The Attractiveness of Materials in Advanced Nuclear Fuel Cycles for Various Proliferation and Theft Scenarios". *Proceedings of Global 2009, Paris, France, September 6-11* (2009).

[43] B. W. Sleaford et al. "NUCLEAR MATERIAL ATTRACTIVENESS: AN ASSESSMENT OF MATERIAL FROM PHWR'S IN A CLOSED THORIUM FUEL CYCLE". *LLNL-CONF-429545* (2010).

[44] C. G. Bathke et al. "AN ASSESSMENT OF THE PROLIFERATION RESISTANCE OF MATERIALS IN ADVANCED NUCLEAR FUEL CYCLES". *8th International Conference on Facility Operations Safeguards Interface, March 30 April 4, 2008, Portland* (2008).

[45] Kenneth D. Kok. "Nuclear Engineering Handbook" (2009).

[46] J.K. Fink and L Leibowitz. "Thermodynamic and Transport Properties of Sodium Liquid and Vapor". *Argonne National Laboratory* (1995).

[47] L. Leibowtiz and R.A Blomquist. "Thermal Conductivity and Thermal Expansion of Stainless Steel D9 and HT9". *International Journal of Thermophysics* 9.5 (1988).

[48] Bauer and Holland. "In pile measurements of thermal conductivity of irradiated metallic fuel". *Nuclear technology* 110 (1995).

[49] Yousry Gohar. "MEGAPIE Analytical Support Task: Characterization of Lead-Bismuth Eutectic and Sodium-Cooled Tungsten Target Materials for Accelerator Driven Systems". *Argonne National Laboratory, ANL/TD/02-02, ANL-AAA-053* (2002).

[50] YOUSRY GOHAR. "SPALLATION TARGET DESIGN FOR ACCELERATOR-DRIVEN SYSTEMS". *Applications of High Intensity Proton Accelerators*. 2009, pp. 285–294.

[51] Carissa Humrickhouse and Joshua Walter. "Melt Refining of Metallic Fast Reactor Fuel". *ICHEME Nuclear Fuel Cycle Conference, Manchester UK, 23-25 April.* (2012).

[52] Francesco Ganda and Ehud Greenspan. "Neutronic analysis of hydride fueled PWR cores". *Nuclear Engineering and Design* 239.8 (2009), pp. 1425–1441.

[53] M.J. Driscoll, T.J. Downar, and E.E. Pilat. "Linear Reactivity Model for Nuclear Fuel Management". *American Nuclear Sociery* ().